Matériaux pour la Géologie de la Suisse – Géophysique
publiés par le Service géologique national, swisstopo

Beiträge zur Geologie der Schweiz – Geophysik
herausgegeben von der Landesgeologie, swisstopo

2012

Seismic Atlas of the Swiss Molasse Basin

Text volume

ANNA SOMMARUGA, URS EICHENBERGER & FRANÇOIS MARILLIER

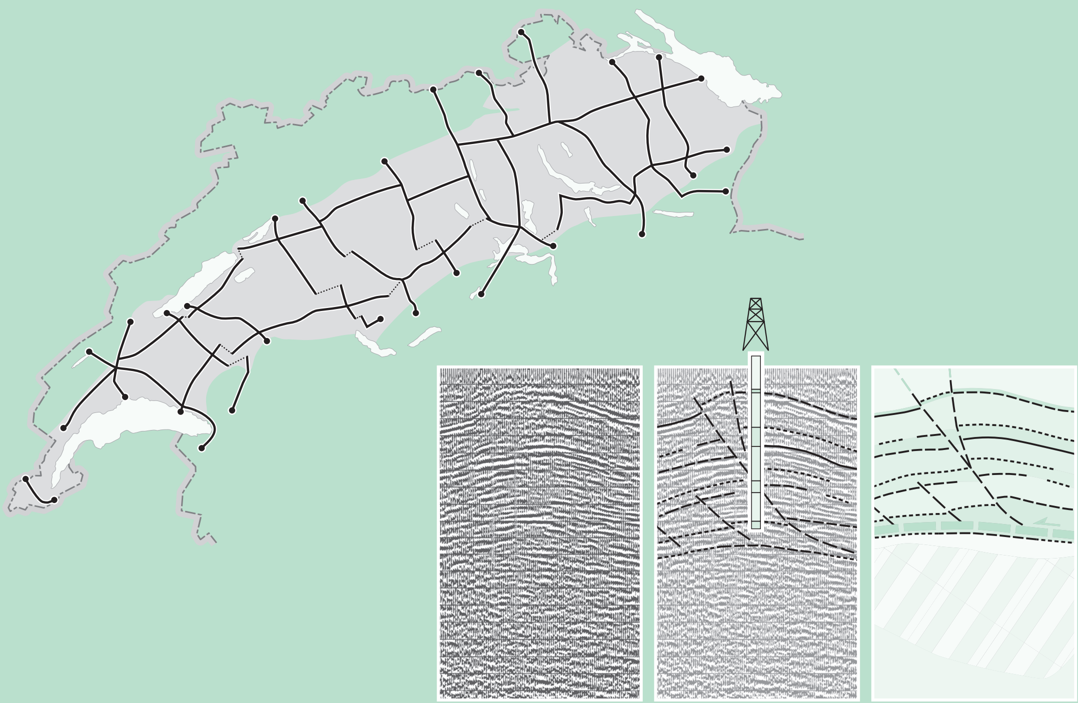

Schweizerische Eidgenossenschaft
Confédération suisse
Confederazione Svizzera
Confederaziun svizra

Swiss Confederation

Federal Office of Topography swisstopo

Matériaux pour la Géologie de la Suisse – Géophysique
publiés par le Service géologique national, swisstopo

Beiträge zur Geologie der Schweiz – Geophysik
herausgegeben von der Landesgeologie, swisstopo

2012

Seismic Atlas of the Swiss Molasse Basin

Text volume

With 37 figures and 9 tables

Authors:
ANNA SOMMARUGA, URS EICHENBERGER & FRANÇOIS MARILLIER

Edited by the Swiss Geophysical Commission
Editor: EDUARD KISSLING

GIS Contributor:
ROBIN ENGLER

Graphical design of enclosures:
ANDREAS BAUMELER

Published by the Federal Office of Topography swisstopo, Swiss Geological Survey
Coordinator: ANDREAS KÜHNI

Schweizerische Eidgenossenschaft
Confédération suisse
Confederazione Svizzera
Confederaziun svizra

Swiss Confederation

Federal Office of Topography swisstopo

Citation recommendation

SOMMARUGA, A., EICHENBERGER, U. and MARILLIER, F. (2012): Seismic Atlas of the Swiss Molasse Basin. Edited by the Swiss Geophysical Commission. – Matér. Géol. Suisse, Géophys. *44*.

Disclaimer

The authors alone are responsible for contents of text and graphics.

The user acknowledges that «The Seismic Atlas of the Swiss Molasse Basin» was developed partly with original geophysical and geological methods here applied for the first time and that the interpretation was often based on a very limited choice of kinds and quality of data. Although the authors have taken every reasonable effort to ensure that information contained on this Atlas is as accurate as possible, there is no warranty that the interpretation related to a definite point in the subsurface is accurate.

Publisher

© 2012, Federal Office of Topography swisstopo, CH-3084 Wabem, Switzerland. – All rights reserved. Except for personal non-commercial use, no portion of this document may be translated or reproduced by any means without prior written permission of the Federal Office of Topography.

The Federal Office of Topography swisstopo is a division of armasuisse.

ISSN 0253-1186
ISBN 978-3-302-40064-8

MIX
From responsible sources
FSC® C030149

Foreword of the editor

When some 40 years ago the Swiss Geophysical Commission (SGPK) was established by the Federal Government as a commission of the Swiss Academy of Sciences and was given the mandate to define, execute and coordinate the geophysical survey of Switzerland, endeavours like «The Seismic Atlas of the Swiss Molasse Basin» (SASMB) were far down the list of realizable projects. After completion of the basic geophysical maps in the mid 1990s, the SGPK initiated the SASMB project and asked Prof. Dr. F. Marillier (vice-president of SGPK) to act as head. A major reason for undertaking this large project was the growing awareness of the importance of the Molasse Basin subsurface for national, cantonal, and local planning. Crucial future-oriented projects for the extraction of deep water resources, exploration of geothermal energy, investigation of nuclear waste deposits, and assessment of the potential for carbon dioxide storage all require comprehensive knowledge of the Basin's subsurface structure and properties. Furthermore, the existence of a multitude of reflection seismic profiles reaching depths of 8 km or more was well known and the timely offer by private industry and public owners for selective usage of this wealth of information was much appreciated.

In all respects, this Seismic Atlas is the largest project ever executed by the SGPK and has consumed the majority of its funding and management resources over the past decade. In addition, the University of Lausanne and the Swiss Geological Survey contributed significantly to the benefit of the SASMB. Foremost, however, the SPGK is indebted to F. Marillier and his team who had the courage to begin, the expertise to execute, and the stamina to finish the Atlas. During the second half of the project, I often participated in discussions among the authors, and in retrospect I understand and fully appreciate how much the SASMB profited from the collaborative scientific sincerity and the personal engagements of Dr. A. Sommaruga and Dr. U. Eichenberger.

The SASMB is a regional Seismic Atlas uniformly compiled and jointly interpreted by geologists and geophysicists according to specifically defined principles. Thanks to the generous offer and support by specialists of swisstopo, the full information of the Atlas can be visualized in an extraordinarily attractive way, both in traditional print and in digital form (PDF files). I sincerely hope this Atlas will be widely used in a broad spectrum of applications.

July 2012
Prof. Dr. E. Kissling
President of the Swiss Geophysical Commission

Foreword of the project leader

The data gathered by various companies for hydrocarbon exploration in Switzerland over a time span of more than three decades comprised a wealth of information that needed to be compiled and synthesized to be turned into a valuable data set. The Seismic Atlas of the Swiss Molasse Basin is an attempt in this direction. It provides a new look into the deep structure of the basin, and it thus helps better understand the geology, not only of the Swiss Molasse Basin itself, but also of the Jura Mountains on its northern flank and the Alps on its southern flank. The internal structure of the Basin is far from being uniform. For example, the Atlas shows that the Tertiary and Mesozoic sedimentary strata vary considerably in thickness, dip, and strike directions. Also, folding and faulting of these sequences and the possible presence of (in places of very thick) Permo-Carboniferous sedimentary basins, appear more pervasive than generally assumed. The Atlas aims at presenting seismic data as well as their geological interpretation. Our hope is that, in addition to its many practical applications, it will be the basis of future scientific work that will build on its content and implications.

The present work is the result of a longterm project that has been supported by the Swiss Geophysical Commission since its inception. The members of the commission and its two successive presidents, Prof. Emile Klingelé and Prof. Eduard Kissling, were always supportive. Before the project started, the idea of synthesizing the numerous data gathered by the oil industry over the years in Switzerland had been in the air for some time, and I am indebted to several people who suggested this research subject to me, especially Prof. Peter Ziegler and Prof. Alan Green. At that time, of course, I had no idea about the challenging amount of work that it was going to imply, and that it would extend over more than a decade.

The content of the Atlas largely reflects the experience and in-depth knowledge of Dr. Anna Sommaruga and Dr. Urs Eichenberger as geologists and as seismic interpreters. But it also owes much to their deep involvement in all aspects of the project. Perhaps the most important and certainly the most fundamental one, was to secure access to the various data sets such as paper copies of seismic sections, shotpoint maps, and borehole data that would provide a reasonable coverage of the basin; some of this necessitated skilled negotiations. The major part of the data set was generously provided to us by SEAG, Nagra, and the Cantons of Vaud, Geneva and Fribourg. Although A. Sommaruga and U. Eichenberger were working only part time on this project, their commitment to it never failed. I wish here to thank them for their determination at overcoming all sorts of difficulties, for their enthusiasm and for always keeping a good sense of humour. In short, it was a real pleasure to work with both of them.

Dr. Robin Engler, who was simultaneously working on his thesis on a completely different subject (in Biology), did a tremendous job with the GIS database. Even when he flew to the other side of the world, he would continue to work for the project through remote access to our local computers. To him also I extend my sincere thanks for the excellent work he did and for his continuous willingness to help.

Another key person is Andreas Baumeler who, after several other draftspersons, drafted the enclosures and oversaw all final graphics. This necessitated many meetings and sending files back and forth, time after time, and A. Baumeler did this skilfully and patiently, yet never losing his critical judgment. All graphics in the Atlas bear his mark, and I wish to thank him for turning scientific results into such clear and beautiful displays.

Prof. Eduard Kissling is the Atlas' editor. This simple word, however, does not reflect the time, enthusiasm, scientific input and management efforts he put in the project. He helped us in decisive phases of the project, in particular at a time when its very realisation was put in question. Together with A. Sommaruga and U. Eichenberger, I wish to thank him sincerely for all this.

Since the initiation of the project in 1997, many others participated in the various tasks that this work required such as gathering data, georeferencing them, processing seismic data, drafting figures, digitizing interpreted seismic sections, storing computer files, reviewing parts of or the entire Atlas, etc. These people are mentioned in the Acknowledgements.

Thus the Seismic Atlas of the Swiss Molasse Basin is the result of a collective work of dedicated people. I am convinced that they participated in this endeavour, hoping as much as I do, that this work will benefit all those interested, one way or another, in the geology of Switzerland.

July 2012
Prof. Dr. F. Marillier

Table of content

List of figures, tables, appendices and enclosures

Figures

Tables

Appendices (digital files only, in pdf or xls-format)

Enclosures (in separate envelope and on CD-ROM)

List of acronyms and explanations of selected terms used in the Atlas

2D	Two-dimensional
3D	Three-dimensional
ahD	along hole depth (in a well)
amsl	above mean sea level
ArcGIS	Brand name of a GIS software developed by company ESRI
ArcMap	Brand name of a GIS software developed by company ESRI
ArcScene	Brand name of a GIS software developed by company ESRI
BEAGOil	Consortium Berne
BLP	Basel-Land Petrol Ldt.
CDP	Common Depth Point
CMP	Common Mid Point
DEM	Digital elevation model
DHM25	Digital Höhenmodel (Digital elevation model) with 25 m cell size
DP	Datum plane. The reference elevation used in a seismic survey.
FM	Folded Molasse
FREAG	Oil Consortium Fribourg
GE	Ground elevation
GIS	Geographic Information System
IeMa	Intra Early Malm
JBP	Jura-Bernois Petrol Ltd.
JSP	Jura Soleurois Pétrole Ltd.
JVP	Jura Vaudois Pétrole Ltd.
LEAG	Luzerner Erdöl AG
Nagra	Nationale Genossenschaft für die Lagerung radioaktiver Abfälle. National Cooperative for the Disposal of Radioactive Waste
NA	not available
NBMes	Near Base Mesozoic
NBTer	Near Base Tertiary
NTDo	Near Top Dogger
NTLi	Near Top Liassic
NTlMa	Near Top Late Malm
NTMuka	Near Top Early–Middle Triassic (Muschelkalk)
NTTr	Near Top Triassic
OMM	Upper marine Molasse (Obere Meereswassermolasse)
OSM	Upper fresh water Molasse (Obere Süsswassermolasse)
OWT	One-way traveltime
P-wave	Compression seismic wave
PM	Plateau Molasse
PROSEIS	now Interoil E&P Switzerland AG
PSBR	Petrosvibri Ltd. (Canton Vaud)
RP	Receiver point. Usually the location of a geophone group
SAdH	Société Anonyme des Hydrocarbures (Canton Vaud)
SAM	Subalpine Molasse
SEAG	Schweizerisches Erdöl AG (Aktiengesellschaft für schweizerisches Erdöl)
SEG	Society of Exploration Geophysicists
SEGY	A digital recording format for seismic data defined by the SEG
SLP	Seismic Location Point standing for either CDP, RP, SP, or VP. Not a standard term in seismic terminology
SMB	Swiss Molasse Basin
SP	Shotpoint
SR	Seismic reference
TGK	Tiefengas Konsortium
TD	Total depth reached by well (generic term)
tvD	Total vertical depth reached by well
TWT	Two-way traveltime
TZ-curve	A depth (Z) versus time (T) curve that is recorded in a well by vertical seismic profiling in a borehole.
UMM	Lower Marine Molasse (Untere Meereswassermolasse)
USM	Lower fresh water Molasse (Untere Süsswassermolasse)
VP	Vibration point
VSP	Vertical seismic profiling

Abstract

The Swiss Molasse Basin is situated between the Jura Mountains and the Alps and it stretches from Lake Geneva to Lake Constance. At the surface, it corresponds to the so-called Swiss Plateau where the majority of the Swiss population lives. Its structure at depth is poorly known because most of its constituting rocks are deeply buried. This Atlas of the Swiss Molasse Basin provides new insights into the basin deep structure at regional scale, based on a three-dimensional model, from the surface down to the base of the deepest sedimentary layers at depths down to 7 km.

This work is based on the interpretation of more than 4300 km of deep reflection seismic profiles and well data, most of which were collected by industry for the purpose of hydrocarbon exploration between 1960 and 1990. We assembled the data set by soliciting the archives of different private companies and public institutions in Switzerland. The interpretation of the seismic profiles, calibrated by more than 30 wells, made it possible to map eight seismic horizons that are near major geological boundaries.

The 3D geological model of the Swiss Molasse Basin, among other items, is represented by 15 transects based on 1284 km of seismic profiles. These profiles were subjected to a more in-depth interpretation that includes an estimate of the data quality and interpretation uncertainty. Among the transects, 13 are in the NW–SE basin-dip direction and 2 are in the SW–NE basin-strike direction. The 3D model is also represented by a series of maps providing regional information: maps of seismic horizons in two-way traveltime (TWT) and in depth, maps of vertical layer thickness between the horizons (Tertiary Molasse and Mesozoic layers) and velocity maps within each layer. Velocities were derived from well data. Moreover, maps of interpreted faults were put together for three major horizons. The Atlas also includes seismic location maps of existing deep seismic profiles in Switzerland, a compilation of well data.

Despite unevenly distributed data sets, we highlighted stratigraphical and structural differences between the western and the central to eastern parts of the Swiss Molasse Basin The western part of the basin contains thicker Mesozoic strata and in particular thicker Triassic evaporite beds. Cretaceous beds are only present west of a line that runs roughly between the towns of Biel and Thun. The majority of faults (normal, reverse or strike slip faults) affect Mesozoic strata in the west part of the basin. We found little evidence for long laterally extending faults, and en echelon fault patterns seem to dominate structural styles. In the westernmost part of the basin, structures in the Mesozoic sequence are characterized by NE–SW oriented anticlines and synclines of low amplitude with Middle–Early Triassic evaporite cores. The latter represent a detachment zone in the western Swiss Molasse Basin. Above the detachment, tear faults of variable length affect both Tertiary and Mesozoic strata. There is no clear evidence for faults extending into the crystalline basement in this part of the basin. The easternmost part of the Swiss Molasse Basin is dominated by extensional structures within the Mesozoic and Paleozoic units.

Normal and reverse faults are observed in the Tertiary units, several of them extending into the Mesozoic units. Tertiary sediments within the Plateau Molasse are folded independently from lower lying strata, requesting a detachment horizon near the base of the Tertiary unit or within shale beds of this unit. In the Subalpine Molasse, folds are related to thrust faults that can be followed all the way to the base of the Tertiary strata. Within the folded Plateau Molasse to the east of the Aar River, the Tertiary strata are displaced along thrusts and back-thrusts, representing a triangle zone.

Zones of seismic reflectivity observed in many places under the Mesozoic units suggest in many cases the presence of Permo-Carboniferous sediments. However, a direct connection between these zones and Permo-Carboniferous layers can only be established in few locations based on well control, and the geological meaning of their limits remains questionable.

Résumé

Le Bassin molassique suisse, situé entre les montagnes du Jura et la chaîne des Alpes, s'étend du Lac Léman au Lac de Constance. A la surface, il correspond à ce que l'on nomme communément le Plateau suisse, région où vit la majorité de la population suisse. Sa structure profonde est peu connue car la plupart des roches qui le constituent sont profondément enfouies. L'Atlas du Bassin molassique suisse présente un nouvel aperçu de la structure profonde du bassin à l'échelle régionale basé sur un modèle tridimensionnel, de la surface à la base des couches sédimentaires les plus profondes jusqu'à 7 km de profondeur.

Ce travail se fonde sur l'interprétation de plus de 4300 km de profils sismique réflexion profonde et sur des données de forages, la plupart recueillis pour l'exploration des hydrocarbures entre 1960 et 1990. Les données ont été rassemblées à partir d'archives appartenant à différentes compa-

gnies privées ou institutions publiques en Suisse. L'interprétation des profils sismiques, étalonnée grâce à plus de 30 forages, a permis de cartographier huit horizons sismiques situés au voisinage immédiat de discontinuités géologiques majeures.

Le modèle géologique 3D du Bassin molassique suisse est notamment constitué de 15 coupes transversales basées sur 1284 km de profils sismiques. Ces profils ont fait l'objet d'une interprétation plus approfondie qui inclut une estimation de la qualité et de la précision des données. Parmi les coupes transversales, 13 sont orientées selon la direction NO–SE du pendage du bassin et 2 selon la direction SO–NE de son extension principale. D'autre part, le modèle 3D est aussi représenté par une série de cartes qui fournissent des informations régionales: des cartes des horizons sismiques en temps double et en profondeur, des cartes des épaisseurs verticales des couches comprises entre les horizons (Molasse tertiaire et couches mésozoïques) et des cartes de vitesses de chacune de ces couches. Les vitesses ont été déterminées à partir des données de forages. De plus, des cartes des failles interprétées ont été établies pour trois horizons principaux. L'Atlas inclut également des plans de position des profils de sismique réflexion profonde existant en Suisse ainsi qu'une compilation des données de puits.

Des différences stratigraphiques et structurales entre les parties occidentales et les parties centrales et orientales du Bassin molassique suisse sont mises en évidence et ceci en dépit de la distribution inégale des données. La partie occidentale du bassin contient des strates mésozoïques plus épaisses, notamment en ce qui concerne les couches évaporitiques du Trias. Les couches du Crétacé ne sont présentes qu'à l'ouest d'une ligne reliant approximativement les villes de Bienne et de Thoune. De plus, la majorité des failles (normales, inverses ou de décrochements) perturbent la séquence mésozoïque dans la partie occidentale du bassin. Très peu d'observations attestent de l'existence de failles s'étendant sur de longues distances, et des systèmes de failles en échelon paraissent plutôt dominer le style structural. Dans la partie la plus occidentale du bassin, la séquence mésozoïque est caractérisée par des structures anticlinales et synclinales d'orientation NE–SO, de faible amplitude et comprenant des noyaux d'évaporites du Trias inférieur à moyen. Ces derniers représentent une zone de décollement dans la partie ouest du Bassin molassique suisse. Au-dessus de cette zone de décollement, des décrochements de longueur variable affectent aussi bien les strates tertiaires que mésozoïques. Dans cette partie du bassin, on n'observe pas le prolongement clair de failles jusque dans le socle cristallin. La partie la plus orientale du Basin molassique suisse est dominée par des structures en extension dans les unités mésozoïques et paléozoïques.

Des failles normales et inverses sont observées dans les unités tertiaires et plusieurs d'entre elles se prolongent dans les unités mésozoïques. Les sédiments tertiaires de la Molasse de Plateau sont plissés indépendamment des couches sous-jacentes ce qui implique l'existence d'un horizon de décollement près de la base de l'unité tertiaire ou dans les couches marneuses de cette unité. Dans la Molasse Subalpine, les plis sont liés à des chevauchements qui peuvent être suivis jusqu'à la base des strates tertiaires. Au sein de la Molasse de Plateau plissée, à l'est de la rivière Aar, les strates tertiaires sont déplacées par des chevauchements et des rétrochevauchements qui forment une zone de triangle.

Des zones de réflectivité sismique observées en de nombreux endroits sous les unités mésozoïques suggèrent la présence de sédiments permo-carbonifères. Toutefois, un lien direct entre ces zones et des couches permo-carbonifères n'a pu être établi qu'à quelques endroits seulement grâce à la présence de forages et la signification géologique de leurs limites demeure douteuse.

Zusammenfassung

Das schweizerische Molassebecken erstreckt sich von Jurasüdfuss bis an den Alpenrand und vom Genfersee bis an den Bodensee. Geografisch betrachtet entspricht diese Region dem Schweizer Mittelland, in dem der Grossteil der Bevölkerung lebt. Über die Geologie des Molassebeckens ist wenig bekannt. Dies ist hauptsächlich die schlechten Aufschlussverhältnisse zurückzuführen. Dieser Atlas gibt mit einem dreidimensionalen Modell einen neuen Einblick in die regionalen Strukturen der Sedimentgesteine zwischen der Oberfläche und einer Tiefe von 7 km.

Das Modell basiert auf der Interpretation von mehr als 4300 km seismischer Linien, welche zum grossen Teil durch die Ölindustrie in den Jahren 1960 bis 1990 aufgenommen wurden. Die Daten stammten aus Archiven öffentlicher Institutionen und der Privatindustrie.

Acht seismische Reflektoren in der Nähe von wichtigen geologischen Grenzen konnten mit Hilfe von Messungen aus mehr als 30 tiefen Bohrungen kalibriert werden.

15 regionale Profile (Transects) von insgesamt 1284 km Länge geben Einblick in das Modell. Entlang dieser Profile werden Angaben zur Unsicherheit sowie zur seismischen Qualität der Reflektoren gemacht. 13 Profile liegen quer zur Hauptachse des Beckens, 2 verlaufen parallel dazu. Eine Serie von Karten dokumentiert das Modell: Karten mit Reflexionszeiten der seismischen Horizonte, Karten mit seismischen Intervallgeschwindigkeiten zwischen den Horizonten und daraus errechneten Tiefen- und Intervallmächtigkeiten. Die Geschwindigkeitskarten sind aus den eher spärlichen Bohrlochmessungen interpoliert. Auf drei Horizonten wurden die Brüche angegeben, und für das ganze Becken wer-

den alle bekannten seismischen Linien ab 1960 sowie die wichtigsten Tiefbohrungen gezeigt.

Trotz der unterschiedlichen Datendichte werden stratigraphische und strukturelle Unterschiede zwischen dem westlichen und östlichen Molassebecken klar sichtbar. Im Westen sind das gesamte Mesozoikum und besonders die Evaporite der Trias mächtiger. Die Kreide ist nur westlich der Linie Biel–Thun erhalten.

Die Bruchdichte (normal, invertiert, transversal) ist im Mesozoikum des westlichen Beckens höher. Oft lösen sich die Bruchflächen lateral ab, und es gibt nur wenige Anzeichen für grosse, weitreichende einzelne Bruchflächen.

Im westlichsten Teil des Beckens sind die Strukturen durch SW–NE verlaufende Antiklinalen charakterisiert. Ihre Kerne sind mit triassischen Evaporiten gefüllt, in welchen auch der wichtigste regionale Abscherungshorizont liegt. Darüber sind das Mesozoikum und das Tertiär oft durch transversale Störungen (tear faults) verstellt, welche nicht bis in den Sockel zu reichen scheinen.

Der östliche Teil des schweizerischen Molassebeckens ist durch Extensionsbrüche im Mesozoikum und Paläozoikum charakterisiert.

Einige der Brüche (normal und invertiert) erfassen ebenfalls das Tertiär. Wo das Tertiär unabhängig vom Mesozoikum gefaltet ist, müssen interne Abscherungshorizonte bestehen; diese finden sich oft in der tonhaltigen Unteren Süsswassermolasse

In der subalpinen Molasse können Überschiebungen unter den alpinen Decken bis an die Basis des Tertiärs verfolgt werden. In der Faltenmolasse östlich der Aare sind die tertiären Schichten durch Überschiebungen und Rücküberschiebungen versetzt. Diese bilden eine Triangelzone.

Unter dem Mesozoikum können Zonen mit erhöhter seismischer Reflektivität beobachtet werden. Diese Zonen wurden ausgeschieden und als Permokarbon-Tröge interpretiert. Nur in wenigen Fällen konnte jedoch deren Existenz aber durch Bohrungen belegt weden. Damit bleibt die Bedeutung der Reflektoren fraglich.

1. Introduction

This Seismic Atlas presents a regional synthesis based on seismic data and dee p wells of the internal structure of the Swiss Molasse Basin (SMB) down to a depth of about 7 km. The Atlas is based on the geological interpretation of seismic profiles representing more than a third of all profiles acquired in Switzerland and about half of the total number of kilometres of seismic data. We used deep wells to calibrate the seismic data. For this seismic Atlas, the industry contributed confidential data, enabling us to present a seismic and geological regional model of the SMB. This work gives public access to regional information and offers a link between the public, scientific research, and more practical aspects of geology with national importance. The latter include commercial hydrocarbon exploration, discussion on storage of nuclear waste or CO_2 sequestration, better understanding of large-scale groundwater circulation to access new water sources, increased knowledge of heat-flow distribution for a better usage of geothermal energy, and more certain estimation of seismic hazard around main urban and industrial sites in Switzerland. However, the study presented here aims at providing a regional model, and it does not claim to be accurate at local scale.

The SMB is the western – central part of the large northern Alpine foredeep basin that stretches along the long axis of the Alps (see Figure 1.1). In Switzerland it is commonly named «Plateau Suisse» in French and «Schweizer Mittelland» in German. The architecture of the SMB is not as well understood as the neighbouring Alps or Jura Mountains. The SMB provides few outcrop exposures that would allow insight into shallow structural elements; the knowledge of surface structures has improved in the last decade with the publication of several geological maps at 1:25 000 scale by the Swiss Geological Survey (swisstopo). The deep structure of the SMB has been investigated mainly between the 60 s and 90 s by reflection seismic profiles, covering more than 11 500 km and by more than 40 wells deeper than 1 km, that have been acquired by companies or institutions, mainly for hydrocarbon exploration and for reconnaissance of sites for nuclear waste repositories. Few local studies based on these seismic surveys have been published, and most of the data and results are not public

1.1 Objectives of this work

The objective of this seismic Atlas is to present, at a regional scale, a 3D geological model of the SMB. Cenozoic, Mesozoic and pre-Mesozoic geological units were investigated using seismic and well data. Together these data form the best tool to image sub-horizontal lithological boundaries within the uppermost kilometres of the Earth's crust. The study concentrated seismic horizons between the base of the Cenozoic unit (Tertiary sediments) and the base of the Mesozoic layers in the SMB (within the Cenozoic unit the available data are not sufficient enough to build a reli-

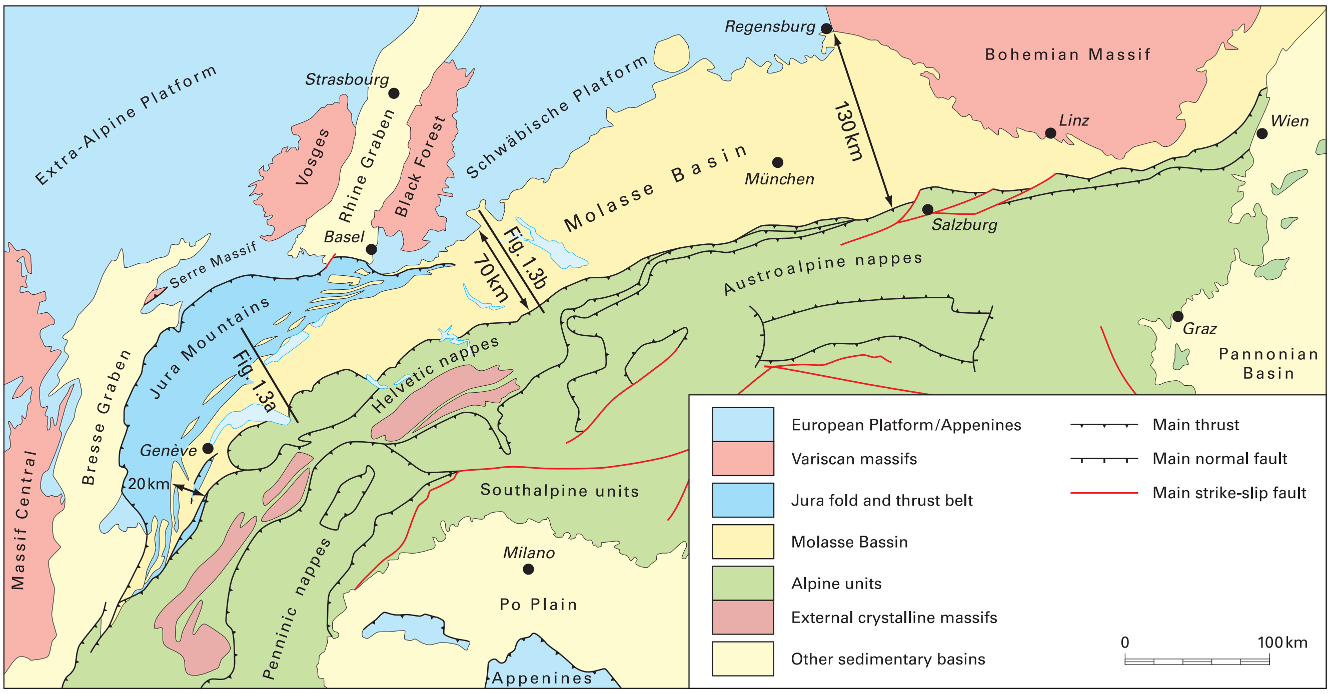

Fig. 1.1: Location of the Molasse Basin with respect to the Alps to the south and to the Jura and the Schwäbische Platform to the north. Modified from PFIFFNER 2009.

able model). The model consists of depth-converted surfaces that are not linked in space. The space between the surfaces is defined as a homogeneous layer. The fault information is not correlated in 3D.

Other objectives of this work were to provide regional information within the Swiss Molasse Basin on:

- lateral changes in thrust fault geometry within Tertiary layers of the Folded Molasse and the Subalpine Molasse,
- geometry of folds and faults within Mesozoic strata,
- lateral extension of Cretaceous beds and Triassic layers,
- possible extension of Paleozoic sediments based on reflective zones along transects through the SMB and
- lateral variations within the SMB from west to east.

Our regional compilation does not address the local scale. Obviously, in our regional Atlas there are missing «local data» that are crucial for industrial applications as well as for geological hypothese s. These should be considered together with the local surface geology for getting higher local precision than our regional model provides.

1.2 Outline of text and enclosures

The text is organized into six chapters providing information on methodology and results. The remainder of chapter 1 summarizes the content of the Atlas and the geological setting of the Swiss Molasse Basin. Chapter 2 deals with the database consisting of subsurface data (seismic reflection profiles and well data) and surface data (and tectonic geological maps). Chapter 3 presents the methodology used to establish a subsurface 3D model of the SMB from the available data. Chapter 4 describes the geological interpretation of fifteen seismic transects within the SMB. Chapter 5 presents a 3D geological model based on two-way traveltime, velocity, depth and thickness, and fault maps. The transects and maps described in chapters 4 and 5 provide the basis for the geological discussion and conclusions of chapter 6.

The Atlas includes twenty-four large enclosure plates:

- a compilation map of existing reflection seismic profiles and deep wells in Switzerland; the seismic profiles interpreted in this work and their owner are specifically indicated (Enclosure 1),
- a compilation map showing the detailed location of individual seismic profiles in Switzerland (Enclosure 2),
- a series of 15 transects (13 dip and 2 along strike) across the Swiss Molasse Basin based on the interpretation of composite seismic profiles, deep wells and surface geological data (Enclosures 3 – 15),
- a well penetration chart with compilation of deep well data with indications of seismic travel-times and interval velocities between stratigraphic boundaries (Encl. 16),
- a series of key maps for eight interpreted horizons and units: two-way traveltime maps (Enclosure 17), velocity maps (Enclosure 18), depth maps (Enclosure 19), vertical thickness maps (Enclosure 20), and selected depth maps with interpreted faults (Enclosure 21) and
- a compilation of depth-converted transects presenting from, west to east, the lateral variations of structures in the Swiss Molasse Basin (Enclosure 22).

1.3 Geological setting

1.3.1 General overview

The Molasse Basin sensu lato is a flexural foreland basin that developed in front of the Alpine mountain range (Homewood 1986, Sinclair et al. 1991, Schlunegger et al. 2007). On the map, the Basin extends over more than 700 km from Chambéry, north of Grenoble (France) in the Southwest to Linz (Austria) in the Northeast, encompassing French, Swiss, German and Austrian territories (see Figure 1.1). The basin runs parallel to the Alpine front and widens progressively to the east from less than 20 km southwest of Geneva to 170 km in Austria. The southern border of the basin is hidden under the Alpine nappes, whereas the northern border is an erosional limit of the Tertiary sediments. To the west, between Chambéry (France) and the Lägeren (north of Zürich), the present day northern extension of the basin is a natural erosional limit against the fold-train of the Jura Mountains. In Germany, the northern limit runs south of the Tabular Jura (Schwäbische Platform). Whereas the Molasse Basin corresponds to an Oligo – Miocene Alpine foredeep, other Tertiary basins such as the Rhine- and the Bresse Grabens to the north and to the west respectively are associated with the Oligocene West-European rift system. The southern limit of the Molasse Basin corresponds to the Alpine front represented by the northern limit of the External crystalline massifs in the Alps.

The part of the Molasse Basin addressed in this seismic Atlas extends from Geneva to Lake Constance. Its limits are defined by the Swiss boundary and not by geological limits (see Figure 1.2). This area is commonly called the Swiss Molasse Basin (SMB). The SMB occupies the western part of the Molasse Basin; it extends over 300 km and widens from west to east from 30 km to 70 km. It consists of mildly folded and faulted Mesozoic and Cenozoic beds (see Figure 1.3). In the central and eastern part of the SMB there are deformation zones and detachment horizons mainly within the Tertiary sequence, whereas in the western part of the SMB, most of the Mesozoic and Tertiary cover is detached from its pre-Mesozoic basement along a décollement horizon.

The main units of the Swiss Molasse Basin can be summarized from bottom to top as follows (see Figure1.4):

(1) Crystalline basement of Precambrian to Paleozoic age that dips gently by a few degrees from the foreland (Massif Central, Vosges, Black Forest, Bohemian Massif; see Figure 1.1) towards the Alpine mountain range.
(2) Late Carboniferous and Permian clastics that accumulated in grabens and sag basins of mostly unknown location in the Paleozoic European basement. These sediments are regarded by many authors as a syn-rift series associated to a late expression of Variscan tectonics (Trümpy 1980, Ziegler 1982). The crystalline basement and Permo-

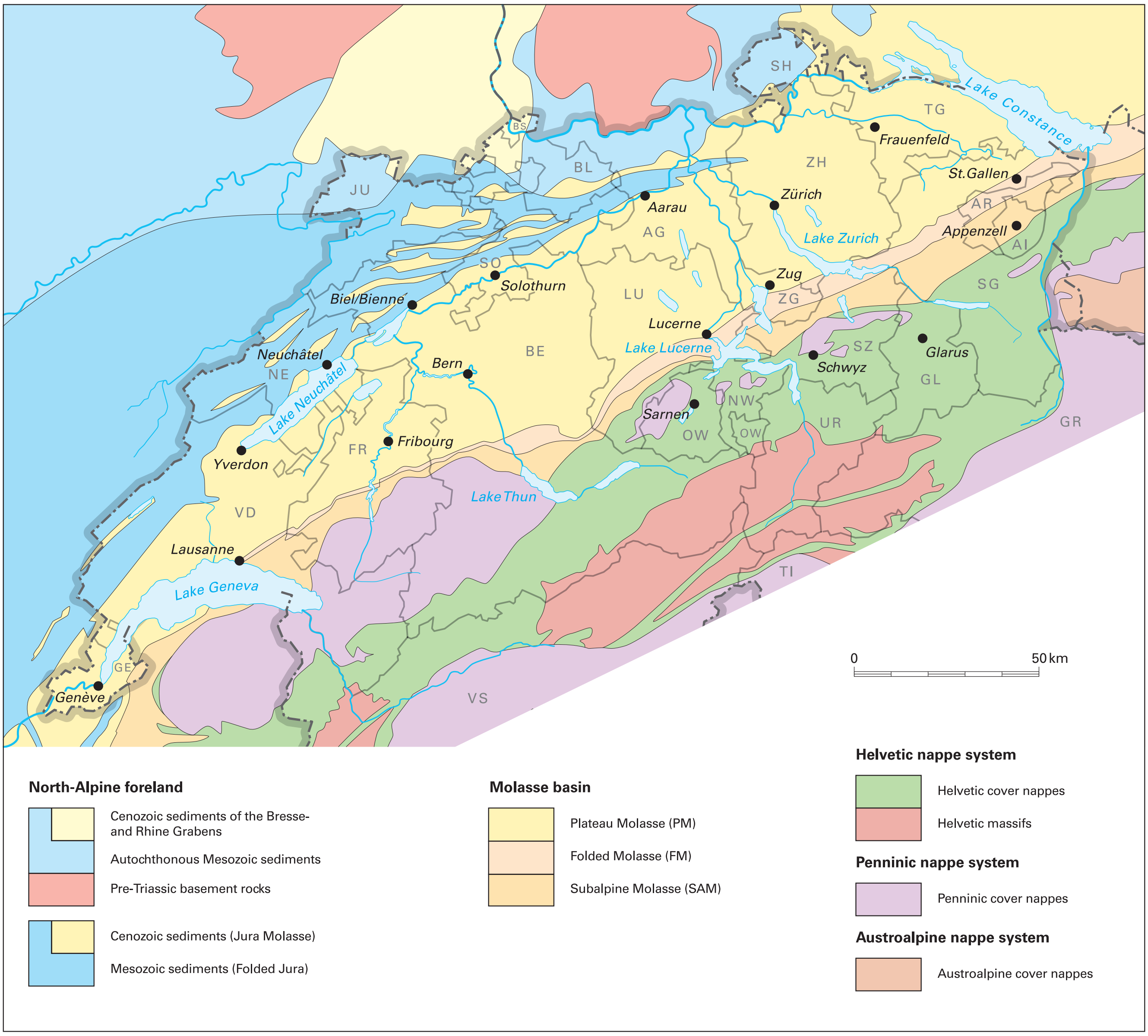

Fig. 1.2: Main tectonic units of the Swiss Molasse Basin and surrounding areas. In light grey abbreviations of the Swiss Cantons together with their boundaries. Towns mentioned in this atlas are indicated with black dots.

Carboniferous sediments are nowhere exposed in the Molasse Basin. They reach the surface at the basin margins in the Vosges and Black Forest Massifs and in synclines and graben structures of the External Crystalline Massifs to the south (Aiguilles Rouges- and Mont-Blanc-, Aar- and Gotthard Massifs; see Figure 1.1), as well as in Alpine nappes (e.g. Helvetic Glarus nappe) and in some small isolated outcrops along the north-western external border of the Jura Mountains (Serre Massif). Permo-Carboniferous sediments were, however, penetrated by several drillholes reported in this atlas.

(3) Middle Triassic to Late Cretaceous shallow-marine sediments represent carbonate-ramp and shale-platform deposits with a total thickness between 400 m and 2500 m (Wildi et al. 1991, Loup 1992). These sediments are separated from the pre-Mesozoic basement by a major post-Variscan erosional unconformity (see Figure 1.3). They are deposited in a rim-basin environment near the southern, passive margin of Europe. They spread over the future Jura area, the Swiss Moalsse Basin, the autochthonous-, parautochtonous- and Helvetic domains. Considerable thickness changes (e.g. at Dogger and Liassic levels) may be related to subsidence variations between the continental sag-basins and the periodically less stable southern European shelf.

(4) Tertiary clastic layers of Oligocene (Rupelian stage) to Late Miocene (Tortonian stage; Figure 1.5 a) age (Berger et al. 2005 a, 2005 b) are deposited above a pronounced foreland unconformity (see Figure 1.4). These sediments form a wedge with thickness increasing from north to south. The foreland unconformity can be traced from the external Jura southward into the most internal Hel-

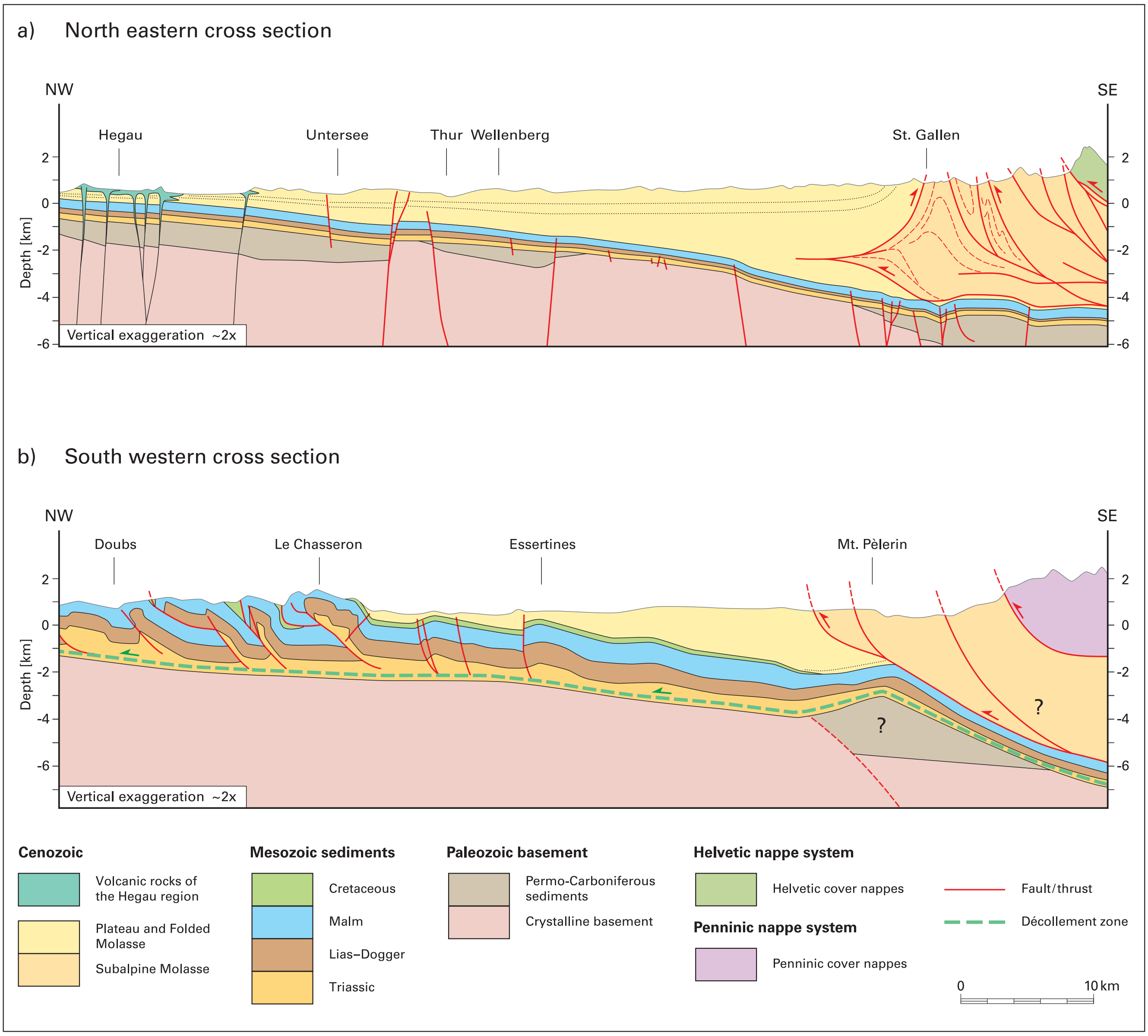

Fig. 1.3: a) Cross-section of the northeastern Swiss Molasse Basin (modified from NAEF et al. 1995 and NAGRA 2008). b) Cross-section of the southwestern basin (modified from SOMMARUGA, 1999 and from CHEVALIER et al, 2010). Profile locations see Figure 1.1.

vetic domain (BOYER & ELLIOTT 1982, HERB 1988). This unconformity marks the flexural response of the European plate to Alpine loading (HOMEWOOD et al. 1989).

(5) The southern rim of the SMB is tectonically complicated. Molasse type sediments are interfering with Flysch type deposits. The continuity between the Helvetic realm and the Molasse parts of the foreland basin has been obscured and partly destroyed by incorporation into the advancing deformation belt. Tectonic activity started in the internal parts and progressively advanced towards the northwest, including Penninic, Helvetic and Subalpine Molasse thrust systems (PFIFFNER 1986 and 2009, BURKHARD 1988; see Figure 1.4). With the advent of Jura folding, starting in the Late Serravallian (12 Ma), the entire western Molasse Basin was incorporated into the Alpine thrust system and was displaced by up to 30 km to the northwest (BUXTORF 1907, LAUBSCHER 1965, LAUBSCHER 1992, MUGNIER & MÉNARD 1986, GUELLEC et al. 1990). No Tertiary sediments younger than uppermost Serravallian are observed in the Molasse Basin (RAHN & SELBEKK 2007). This indicates that the north-western Alpine foredeep has been bypassed and cannibalized since the Early Tortonian (8 Ma). Accordingly, the present-day Swiss Molasse Basin is an erosional remnant of a much larger foreland basin in an advanced stage of its evolution (SCHLUNEGGER & MOSAR 2010). An important step in unravelling the foreland basin's history is the restoration of the initial position of the various involved and surrounding tectonic elements (BOYER & ELLIOTT 1982, HOMEWOOD et al. 1986, PFIFFNER 1986, BURKHARD 1988, BURKHARD 1990, BURKHARD & SOMMARUGA 1998, AFFOLTER & GRATIER 2004).

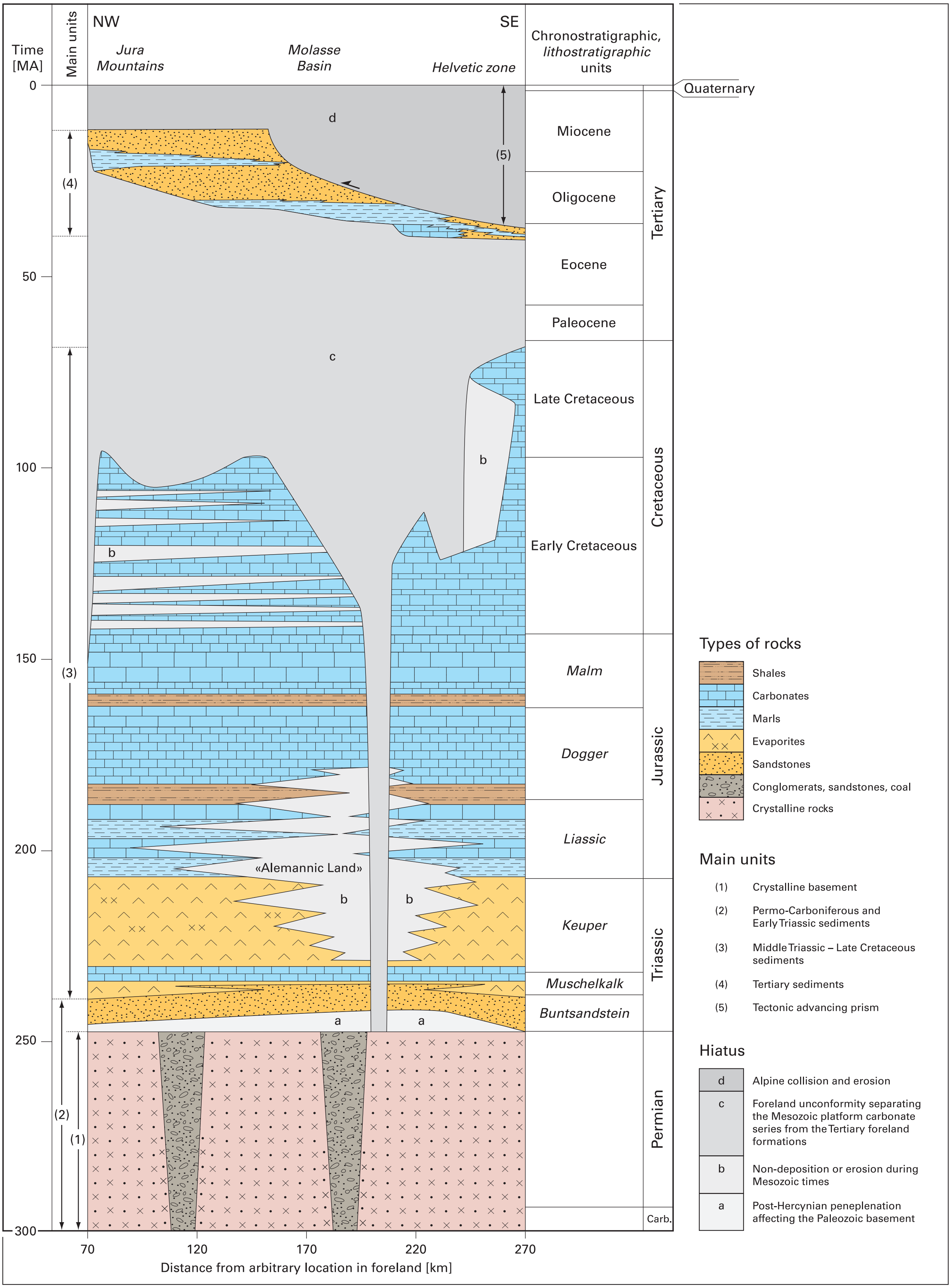

Fig. 1.4: Schematic stratigraphic time section summarizing the most important Paleozoic, Mesozoic and Cenozoic lithostratigraphic units in the Swiss Molasse Basin. The horizontal axis, measured from an arbitrary location in the foreland, is a restoration of the different paleogeographic domains. Units 1 to 5 are described in the text. Modified from SOMMARUGA (1999).

1.3.2 Tectonic units

At the Tertiary level, the Swiss Molasse Basin can structurally be subdivided into four units: the Jura Molasse, the Plateau Molasse, the Subalpine Molasse and in between the latter two, the Folded Molasse (Trümpy 1980, Homewood et al. 1989, Hofmann 1957, Tectonic map of Switzerland, Swisstopo 2005b; see Figure 1.2).

Jura Molasse (JM)

The Jura Molasse represents the remnants of the Molasse Basin that has been passively involved in the Jura folding and thrusting. Due to uplift and erosion, only isolated patches of Molasse sediments are preserved within major synclines of the internal Jura (see Figure 1.2).

Plateau Molasse (PM)

The Plateau Molasse, representing the major part of the Molasse Basin shows distinct structural styles between the western and eastern parts. In the western Swiss part, the structures consist of broad anticlines oriented NE–SW and tear faults trending N–S, NW–SE and WNW–ESE (Fig. 1.2). The northern limit of the PM corresponds to an erosional limit along the most internal folds of the Jura Mountain belt. In eastern Switzerland and Bavaria, outcrops show an onlapping Tertiary wedge in the Tabular Jura of the Franconian and Schwäbische Platform (Bachmann et al. 1987). The only known deformation, which is also visible on seismic data, is characterized by small normal faults oriented WSW–ENE, parallel to the basin and affecting the Mesozoic and Cenozoic strata (Bachmann et al. 1982, Diebold and Noack 1997, Lüschen et al. 2004, Pfiffner 2009, Ibele 2011).

Folded Molasse (FM)

The deformed realm that follows the thrusts of the Subalpine Molasse on the northern side is called Folded Molasse. It occurs from the Penninic Prealps in the west to the Rhine River in the east, and it is rather large in the area north of the town of Thun and east of the city of St. Gallen (see Figure 1.2). The structural style is dominated by both, small and larger-scale folds with close to vertical axial planes, that are often sheared (Habicht 1945, Hofmann 1955, 1956).

Subalpine Molasse (SAM)

The Subalpine Molasse reaches the surface only in a narrow zone of variable width (10–20 km), in front of the Helvetic nappes and the Penninic cover nappes. This zone is characterized by a stack of internally deformed steeply inclined thrust sheets of Tertiary sediments that flatten out at depth. In some areas, they are clearly detached along a décollement zone within the Lower Freshwater Molasse («Grisigen Marls», Trümpy 1980). The southern limit of this zone corresponds to the Paleogene Flysch–Molasse transition into autochthonous Flysch series. This transition has been tectonically overprinted by the progressing Oligocene Alpine front, and it has later been buried beneath the Alpine nappes stack. The northern limit of the Subalpine Molasse is a structural transition zone characterized by north-west pointing thrusts. From Lake Thun to southern Germany and Austria, it becomes a complex triangle zone with backthrusts and a duplex core (see Figures 1.1, 1.2 and 1.3; Bachmann et al. 1982, Vollmayr & Wendt 1987, Müller et al. 1988, Vollmayr 1992, Pfiffner 2009).

Many authors consider the western part of the basin to be detached from its crystalline or Permo-Carboniferous substratum (Buxtorf 1907, Laubscher 1965, Allen et al. 1986, Homewood 1986, Vann et al. 1986, Boyer & Elliot, 1982, Burkhard 1990, Sommaruga 1997, Bonnet et al. 2007). According to them, the change in structural style along the strike of the Molasse Basin is related to the presence of this décollement zone situated in the Triassic evaporites. This concept is commonly known as the «Fernschub hypothesis» or distant push (Buxtorf 1907, Laubscher 1961, Laubscher 2008). This hypothesis is, however, disputed by some, who argue that faults disrupting the Mesozoic sequences extend into the crystalline basement and thus invalidate the detachment hypothesis at least locally (Pavoni 1961, Wegmann 1963, Ziegler 1982, Gorin et al. 1993, Pfiffner 2006). In the western area, the Swiss Molasse Basin is considered to be a wedge-top basin according to Willet & Schlunegger (2010).

In the western area, thick evaporite horizons in Triassic strata are present beneath the Jura and the western Swiss Molasse Basin (Rigassi 1977, Sommaruga 1997). Following the «Fernschub hypothesis», the Alpine deformation propagated from south to north into the Jura fold belt and an intra-Triassic detachment horizon must have operated during the development of the thin-skinned Jura fold-and-thrust belt up to Canton Aargau, whereas east of the Lägeren (see Figure 1.2), there is as yet no evidence for an extended décollement zone beneath the Tertiary sediments. East of the Lindau-1 well, the presence of a décollement zone is improbable. Triassic beds onlap basement to the North-East (Bohemian Massif) and evaporitic series become progressively thinner in the same direction. In the eastern Molasse Basin (Germany), Jurassic strata unconformably lie directly on crystalline basement (Bachmann et al. 1987). The generally small-scale synthetic and antithetic normal faults in areas east of the Jura fold-and-thrust belt in Bavaria and Austria are considered as having formed during the Oligocene–Early Miocene flexural subsidence of the Molasse Basin. Such syn-flexural faulting reflects tension in the upper part of the lithosphere whilst its lower part is in compression (Ziegler & Dèzes 2007). For a specific discussion on the Molasse internal deformation, refer to Burkhard (1990), Pfiffner (2009) and Ibele (2011).

1.3.3 Lithostratigraphic subdivision

Quaternary

In the Swiss Molasse Basin, Quaternary sediments are generally very thin, their thickness ranging from a few meters to several hundreds of meters in narrow, overdeepened paleo-valleys that are remnant of glacial and glacial runoff activity (e.g. Jordan 2010). They are heterogeneous clastics ranging from coarse grain tills to fine grain fluvial and lacustrine sands. Because Quaternary sediments are very thin relative to the deeper parts of the basin, they do not significantly contribute to a regional model of the SMB. In this Atlas, they were included in a Cenozoic unit that is largely dominated by the thick Tertiary sequence.

Tertiary

The Tertiary stratigraphy of the Molasse Basin has been reviewed by Homewood (1974), Homewood et al. (1989) and Keller (1990). For correlations on a European scale see Berger (1992) and for the paleogeographic distribution of the units see Berger et al. (2005a). Figure 1.5 relates the traditional nomenclature to more modern usage. Tertiary sediments are almost entirely derived from the rising Alps, with only a minor influx from the Bohemian Massif to the northwest and from the Black Forest and Vosges in the Jura Mountains. Stratigraphic subdivisions within the often oxidized and bare series are mainly based on micro mammals, charophyta, ostracoda and the occurrence of heavy minerals or ash layers (Engesser et al. 1984).

Four lithostratigraphic groups are distinguished in the Tertiary Molasse Basin (Matter et al. 1980, Sinclair et al. 1991) from bottom to top (see Figure 1.5).

Lower Marine Molasse «Untere Meeresmolasse» (UMM)

The rapid deepening of the basin, starting at the Eocen–Oligocene boundary, led to the accumulation of Flysch series in the area of the present day Subalpine Molasse and the Helvetic nappes. Main turbidite fans were located in front of the Rhône valley, near Thun, Canton Bern and near Altdorf, Canton Uri. The Lower Marine Molasse (UMM) is topped by a regressive series deposited in a narrow, wave dominated seaway that disappeared from west to east (Valruz Formation or Grisigen Mergel).

Lower Freshwater Molasse «Untere Süsswassermolasse» (USM)

At least seven gravel fans were active in late Oligocene times at the southern margin of the Swiss Molasse basin, accumulating coarse gravel in steep proximal positions. This is the case for «Nagelfluh» (poudingues) beds (e.g. the Mt Pèlerin near Vevey or the Rigi Mountain near Lucerne), whereas meandering river sandstones accumulated in adjacent low gradient flood plains. Coal swamps and small lakes led to the formation of the «Molasse à Charbon» and «Molasse Grise de Lausanne» in the western basin in Chattian time (Büchi & Schlanke 1977, Fasel 1984). In the late Lower Freshwater Molasse (USM), drainage directions turned from the radial sediment distribution of individual fans to regional longitudinal transport in the basin towards the east.

a)

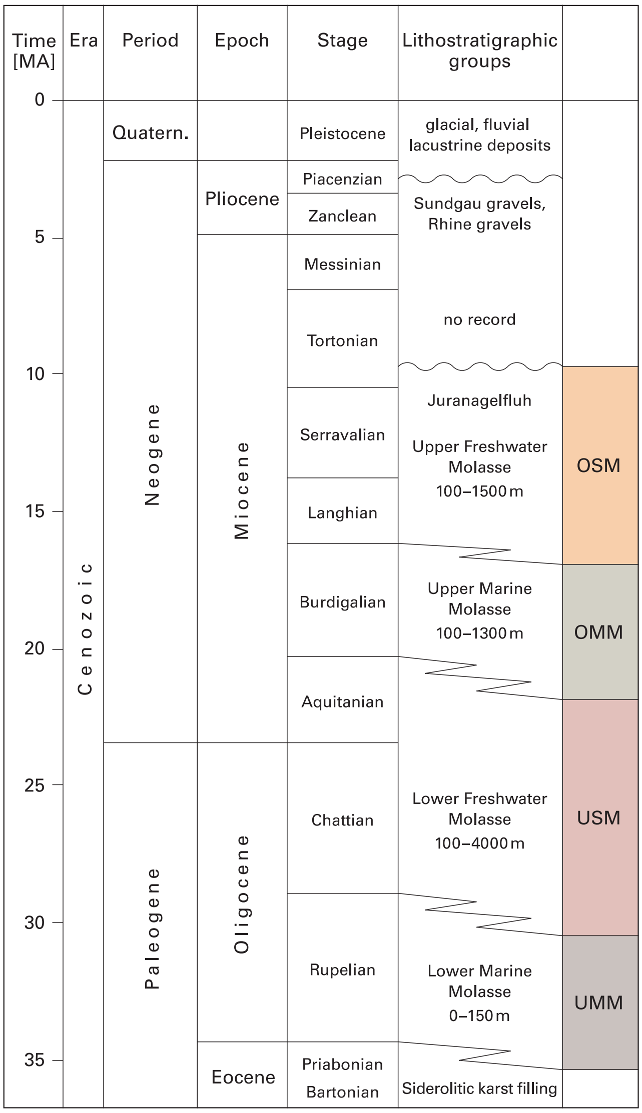

b)

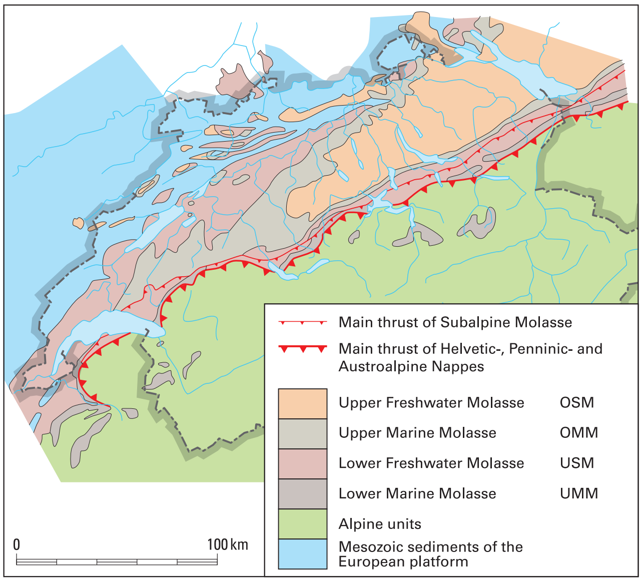

Fig. 1.5: a) Lithostratigraphic groups of the Tertiary units. Modified from Berger (2011). b) Distribution of Molasse outcrops in the Swiss Molasse Basin. Modified from Matzenauer (2007).

Upper Marine Molasse, «Obere Meeresmolasse» (OMM)

A shallow marine seaway linked the Rhône Basin with the Vienna Basin from the Aquitanian–Burdigalian boundary until early middle Miocene times (see Figure 1.5). The coarse clastics in the basal, proximal fan delta facies are interpreted as erosion products of the main emplacement movements of the Helvetic nappes (ALLEN et al. 1986). The marine facies include deeper basin parts up to 100 m water depth (coquina beds) as well as shallow shell bars with subareal cementation. The Upper Marine Molasse sandstone facies is widespread in Switzerland (see Figure 1.5 b) and there are many constructions with this rock, such as the «Tribunal Fédéral» in Lausanne, the Cathedral St-Nicolas in Fribourg, the «Bundeshaus» in Bern, the «Lowendenkmal» in Lucerne and the monastery of Einsiedeln.

Upper Freshwater Molasse, «Obere Süsswassermolasse» (OSM)

From early middle to late middle Miocene times, renewed continental sedimentation led to the accumulation of a prism with a thickness of up to 1500 m near the Alps and some 100 m to the north. From the deposition centres, where coarse gravel sandstones form cones such as the Napf Mountain near Lucerne, streams veered to the SW with a drainage direction parallel to the basin. Thin coal seems were deposited in more distal parts (e.g. in the Jura Mountains).

Mesozoic

While Tertiary sediments present mostly facies and thickness changes from south to north, the greatest variations of Mesozoic layers are parallel to the SW–NE axis of the Swiss Molasse Basin. The thickness of the Mesozoic unit varies from more than 3 km in the western part to 800 m in the eastern part of the SMB. During Mesozoic time, the Molasse Basin realm was part of the Alpine Tethys passive margin, and it mainly comprises alternating limestones and marls. These rocks are buried beneath the Tertiary wedge sediments within the SMB. Limestones of Middle and Late Jurassic age crop out all along the Jura Mountains anticlines, whereas Cretaceous age limestones form the synclines of the eastern Jura Mountains. Triassic beds consist of shallow marine carbonates and marls including dolomites and evaporites mainly in the western and central regions.

Pre-Mesozoic

Pre-Mesozoic units consist of Permian and Carboniferous sediments and of Precambrian crystalline basement with some Ordovician to Carboniferous intrusive rocks. They are nowhere exposed in the Swiss Molasse Basin or in the neighboring Jura Mountains. The crystalline basement is known from few drillholes beneath the SMB. The Paleozoic layers consist of Permo-Carboniferous troughs first discovered by Nagra (National Cooperative for the Disposal of Radioactive Waste) seismic and well investigations in northern Switzerland (DIEBOLD et al. 1991). Other hidden troughs are suspected beneath the Swiss Molasse Basin (LEU 2008).

1.4 Previous regional and local seismic studies

In the SMB, seismic profiles were mainly acquired for hydrocarbon exploration and for the reconnaissance of sites for nuclear waste repositories. Many of these data are confidential, and the analysis of the SMB as a whole therefore long remained the privilege of oil companies (ZIEGLER 1992, LAHUSEN 1992, LAHUSEN & WYSS 1995). Local seismic studies, however, have contributed to the understanding of the SMB in specific areas. Some of them are available in public archives or are published in scientific journals, but many of them are in unpublished data or reports.

Published studies

Eastern and western traverses of the Swiss Molasse Basin were presented in the NRP20 study that contains both refraction and reflection seismic data. It provides tectonic interpretations that include the SMB based on selected seismic profiles (PFIFFNER et al. 1997).

In the western Swiss Molasse Basin, several studies, mainly conducted at Universities, present interpretations of seismic profiles in the Geneva Basin (SIGNER 1992, SIGNER & GORIN 1995), in Canton Vaud, (GORIN et al. 1993, SOMMARUGA 1997, GORIN et al. 2003), in Canton Fribourg (GORIN et al 1995, STRUNCK 2001, MOSAR et al. 2011, SOMMARUGA et al. 2011). In the latter canton, studies by private companies planning the replacement of nuclear power stations were recently published (RESUN 2008).

In the central Swiss Molasse Basin, no regional work has been published, but few local studies exist (ERARD 1999, VOLLMAYR 1992, SCHLUNEGGER et al. 1993). In the eastern and northern SMB, regional seismic interpretations were presented essentially by Nagra (see next paragraph), and some local studies were published (STÄUBLE & PFIFFNER 1991, KEMPF 1998, KEMPF & PFIFFNER 2004).

A large body of regional seismic studies has been published by Nagra. For the last three decades, this institution has been looking for undisturbed, low permeability rock volumes down to a depth of 900 m throughout Switzerland. In northern Switzerland, it first focussed on the shallow basement, and drilling revealed complex structures and alteration patterns. Three 2D seismic surveys (1982, 1983 and 1984) shed new light into the eastern Jura fold belt and adjacent parts of the northern Swiss Molasse Basin (SPRECHER & MÜLLER 1986, DIEBOLD 1987, DIEBOLD & NAEF 1990, DIEBOLD et al. 1991). Nagra also reprocessed many older seismic profiles, and in 1991 it acquired a 2D survey to investigate potential storage sites in shaly Dogger and Malm units (NAEF et al. 1995). The Benken survey remains the only 3D land survey in the whole basin for a decade (BIRKHÄUSER et al. 2001, MARCHANT et al. 2005). More recently the Nagra report NTB 08-04 presented a re-interpretation of data from various seismic campaigns.

Seismic surveys within the Jura Mountains also help us to understand the link between the Jura fold-and-thrust belt structures and the SMB (SOMMARUGA 1997, 1999, PFIFFNER et al. 1997, DIEBOLD et al. 1991, TURRINI et al. 2009).

Several authors undertook compilation studies in the basin for the purpose of geothermal modelling (BAUJARD et al. 2007), for seismic hazard analysis of nuclear power plants (BURKHARD & GRUNTHAL 2009, SCHMID & SLEJKO 2009), and for CO_2 sequestration (CHEVALIER et al. 2010).

Unpublished work

Nagra produced many unpublished internal reports. It mandated several 2D seismic interpretation studies that combined their own profiles with industry profiles covering the area from the eastern Swiss border to the east of Canton Vaud (MEIER 1994a, MEIER 1994b, ROTH et al. 2008, MEIER 2010, MOSAR et al. 2008). Several oil companies (Shell, Elf Aquitaine, BEB) have produced internal reports on exploration in the SMB. They often include well data, seismic profiles, shotpoint maps and seismic horizon maps that we used for our interpretation (see chapter 2). A more recent evaluation of the oil and gas potential of Switzerland based on public well data, seismic profiles, and basin modelling results, has been compiled by Geoform Ltd (GREBER et al. 2004). It includes an interpretation of the public seismic profiles available at swisstopo (see chapter 2). Seismic interpretations of the westernmost basin have also been published by workers of the University of Geneva (GORIN 1989, GORIN 1992, PAOLACCI & GORIN 2001).

2. Database

2.1 Inventory of available data

In addition to the 2D seismic reflection data, we compiled other data for this work such as seismic location maps (so-called «shotpoint maps»), maps of already interpreted seismic horizons, well data, geological and geophysical reports, geological maps, as well as published literature dealing with the geology or tectonic models of the Swiss Molasse Basin (SMB). Oil companies, the Swiss National Research Foundation, water supply industries, thermal heat producers, waste disposal and electricity companies, cantonal offices and others were involved in the acquisition of seismic profiles and / or well drilling. Most of these data are not part of a countrywide database and Switzerland has no federal laws regulating access to them; each canton has its own regulation. The data are therefore dispersed in public and private archives through the country.

Table 2.1 summarizes the compiled data while details are provided in Appendices 2.1 (geological maps), 2.2 (seismic profiles), 2.3 (seismic location maps), and 2.4 (well data). Ownership of interpreted seismic profiles and used wells are also shown in Enclosure 1 and their detailed locations are shown in Enclosure 2. Some seismic profiles have changed ownership after acquisition; Enclosure 1 indicates ownership that existed at the time we obtained the data.

Publicly available geological and geophysical data are stored in the archives of the Geological Information Centre of the Swiss Geological Survey (swisstopo). About 1000 km of seismic data (few in digital format, mostly on paper) and 7 wells became public following an agreement reached in November 1994 between the Swiss Ministry of Energy and the SEAG company (Aktiengesellschaft für schweizerisches Erdöl). The Canton of Vaud has a unique legislation in Switzerland that imposes seismic and well data to become public 10 years after acquisition. In that case, documents are deposited at the Musée de Géologie located at the University of Lausanne. Publicly accessible 2D seismic profiles total 15 % of the total seismic data ever acquired in Switzerland (see Enclosure 1). Seismic data were also obtained from Canton Fribourg and Canton Geneva. Digital geological maps were made available by swisstopo for the duration of the project.

Non-public data were obtained through contracts or agreements specially negotiated for this work with institutions or private companies. One such agreement was signed by SEAG that holds the rights of the majority of seismic and well data in Switzerland (LAHUSEN, 1992), and the Swiss Academy of Sciences (legally representing the Swiss Geophysical Commission). An agreement with Nagra provided access to its seismic data and internal reports that cover the SMB. Through this agreement, we could exchange digital files of interpreted data. Another agreement with Celtique Energie Ltd gave us access to their digital database in Canton Vaud. The FREAG company (Fribourg Erdöl AG) gave us access to its seismic paper sections.

2.2 Seismic profiles

2.2.1 Seismic profiles in Switzerland and interpreted profiles in this Atlas

The coordinates and complementary data of 833 seismic profiles corresponding to a total length of 11 579 km were introduced in our GIS database (see Figure 2.1, Enclosures 1 and 2 and Appendix 2.2). This represents almost the total reflection seismic data collected in Switzerland since the 1960s. While the western part of the Swiss Molasse Basin and north eastern Switzerland are densely covered, seismic

Table 2.1: *Data types and their sources used in the Atlas for interpretation. Most seismic data are in the form of paper records and their corresponding location maps. For some lines, seismic interpretation results such as TWT or depth maps were also available. Well data include paper copies of geological and geophysical records. Some additional data were also introduced in the project GIS data base, such as the location of seismic profiles that were not interpreted.*

Type of data	Source of data	Additional information
Seismic data	SEAG	Number of interpreted profiles: 66 (1446 km)
Seismic data	swisstopo, Swiss Geological Survey, Geological Information Centre	Number of interpreted profiles: 49 (1047 km)
Seismic data	Canton VD, Musée de géologie, Lausanne	Number of interpreted profiles: 69 (823 km). Survey names: SADH, PSBR, VD
Seismic data	Canton Fribourg, Direction de l'Aménagement, de l'Environnement et des Constructions	Number of interpreted profiles: 41 (535 km). Survey names: FRS, FRN
Seismic data	Nagra	Number of interpreted profiles: 13 (293 km). Survey names: S84, U82, U83, U84, U91
Seismic data	FREAG	Number of interpreted profiles: 5 (69 km). Survey name: FREAG
Seismic data	Canton Bern, Bergregalarchiv, BVE Direktion	Number of interpreted profiles: 7 (61 km)
Seismic data	Canton Geneva, Services Industriels de Genève	Number of interpreted profiles: 6 (45 km). Survey name: SIG
Seismic data	Canton Geneva, Service Cantonal de Géologie	Number of interpreted profiles: 7 (37 km). Survey name: GG
Seismic interpretation maps	Interoil Exploration & Production ASA (former PROSEIS)	Digital format
Seismic interpretation report	Canton VD, Musée de Géologie, Lausanne	Reports from oil companies in Canton Vaud
Seismic interpretation report	GEOFORM	Seismic interpretation in the Swiss Molasse Basin
Seismic location maps	Various	See Appendix 2.3
Geological maps; 1:25 000	swisstopo, Swiss Geological Survey, Geological Information Centre	Scans and vector files. See Appendix 2.1
Geological and Tectonic Maps of Switzerland; 1:500 000 (SWISSTOPO, 2005a, 2005b)	swisstopo, Swiss Geological Survey, Geological Information Centre	Digital version
Geological map of the central and northern part of Switzerland; 1:100 000 (ISLER et al. 1984)	Nagra	Paper version
Regional tectonic sketches; 1:200 000	Extracted from the 1:25 000 geological maps. swisstopo, Swiss Geological Survey, Geological Information Centre	The tectonic sketches were compiled into one map and georeferenced at scale 1:100 000
Well data	SEAG (11 wells), swisstopo (7 wells), Nagra (6 wells) and others	The data for some of these wells have been published (see Appendix 2.5)

surveys in the central and eastern parts of the SMB show wider profile spacing. In this work, 263 seismic profiles corresponding to a total of 4357 km were interpreted from which 1284 km were used for a more in-depth interpretation and displayed in the transects. The interpreted profiles correspond to about one third of all profiles in Switzerland (SMB and other areas) and about 50% of the existing profiles located in the study area (SMB only). Our seismic interpretation covers the SMB from west to east, from Canton Geneva to Lake Constance (see Figure 2.2).

Our seismic profile selection was essentially guided by two criteria, data availability and regional coverage of the basin. While we wanted to include most public profiles, confidential profiles were selected based on their quality and on their location. As a consequence, the seismic profile grid is much tighter in the western SMB because of the larger number public profiles. This led to a somewhat uneven distribution of the interpreted data, and has some influence on the regional maps (in TWT, depth, and vertical unit thickness) that we calculated from this data set (chapter 3).

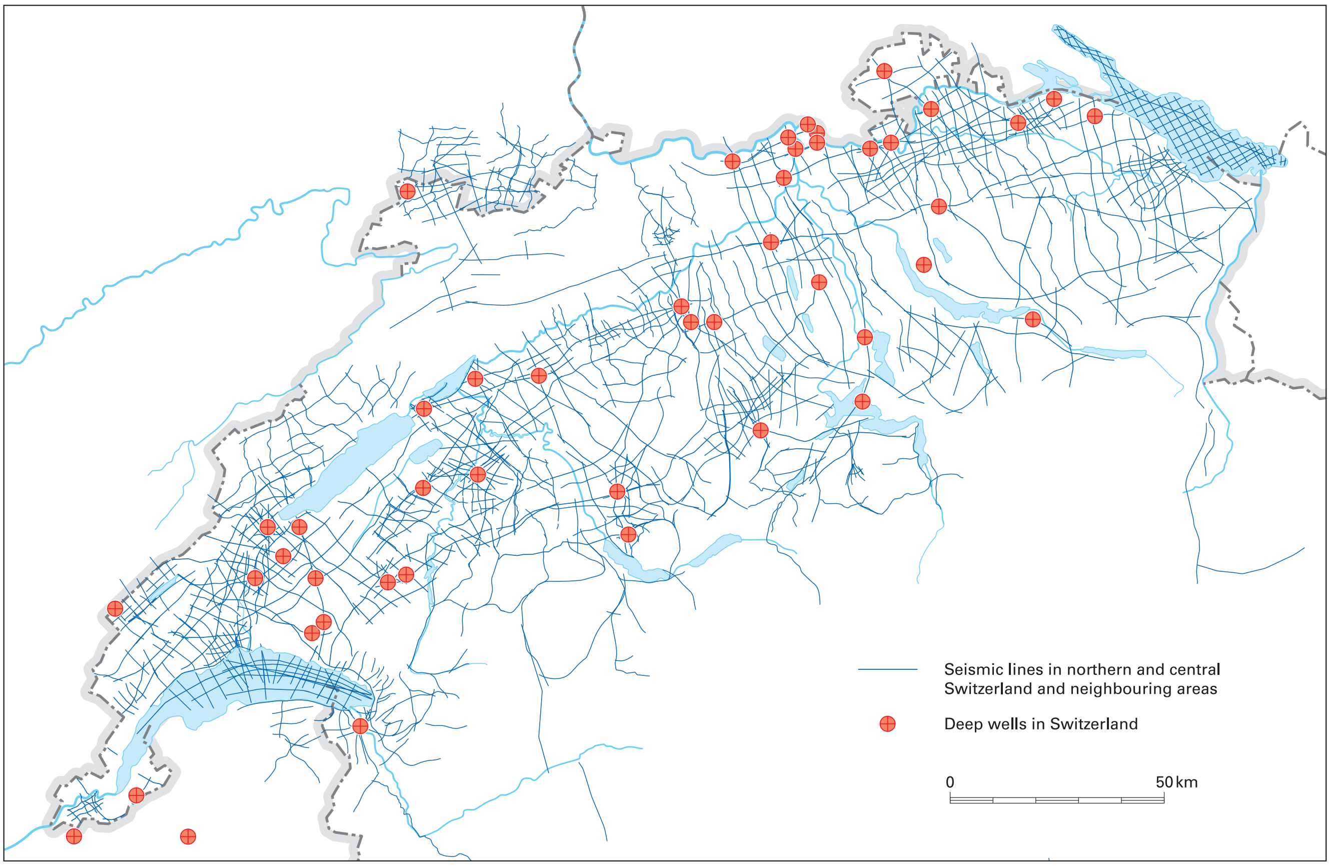

Fig. 2.1: Distribution of seismic lines and of most deep wells drilled in the Swiss Molasse Basin.

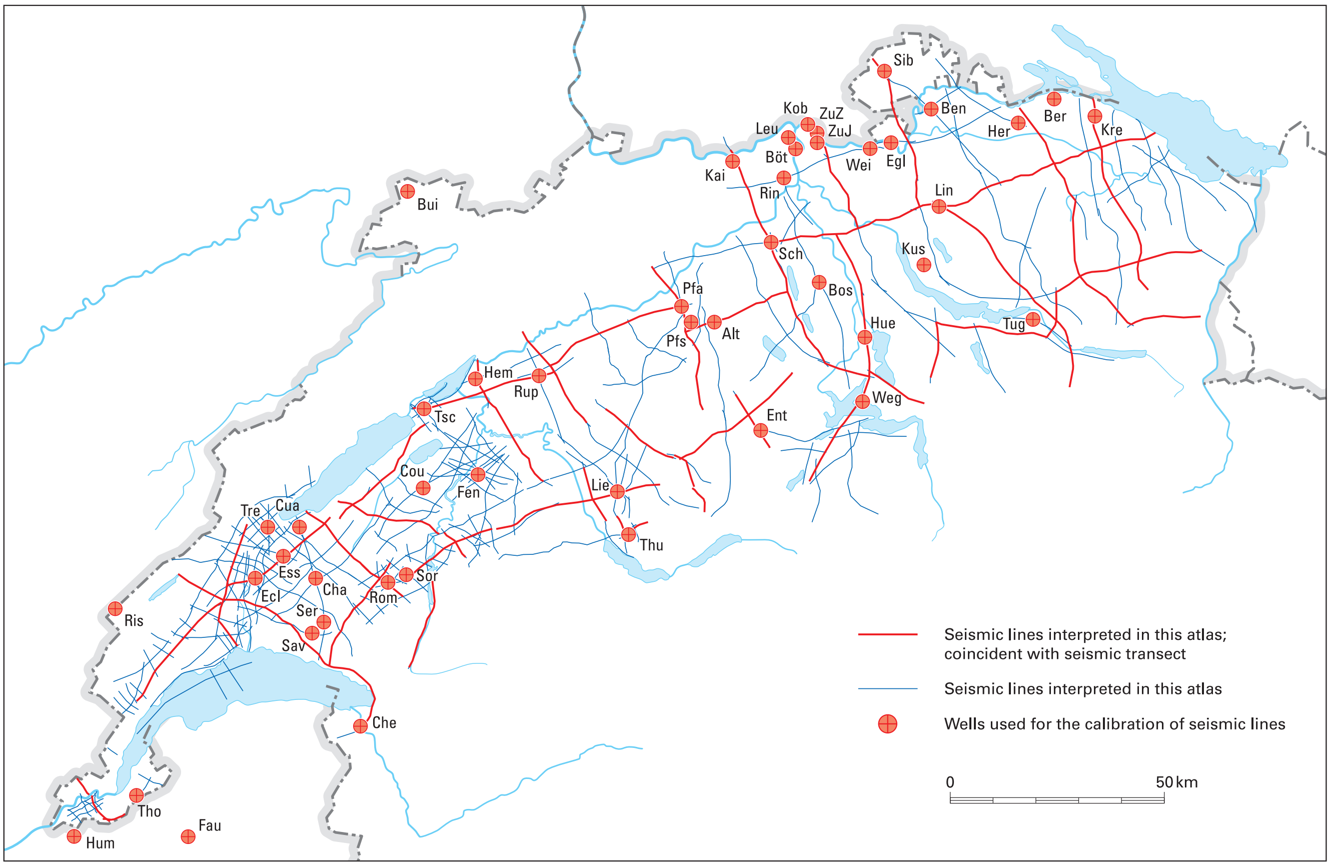

Fig. 2.2: Distribution of the interpreted seismic lines and wells used in this work. For the meaning of well abbreviations see Enclosure 1.

2.2.2 Seismic location maps

Enclosure 2 shows the detailed location of the seismic profiles with their Seismic Location Points (SLP). We define an SLP as a generic term for any type of point used in seismic reflection to locate seismic profiles. An SLP can be any of the following: Common Depth Point (CDP), Common Mid Point (CMP), Receiver Point (RP), Shotpoint (SP) or Vibration Point (VP). Appendix 2.2 indicates which SLP type was used for each seismic profile. Geco-Prakla compiled a seismic location map for Nagra in 1997, and this map was later handed over to Proseis AG (now Interoil E & P Switzerland AG). We used the digital map provided to us through the agreement with Nagra as a starting point for our GIS database. A number of regional and local location maps at different scales and elaborated by different companies were subsequently introduced into the database (see Appendix 2.3).

The GIS seismic database of the seismic profile coordinates was constructed as follows:

1. Existing vector data obtained from different sources were merged.
2. Location maps on paper (Appendix 2.3) were scanned, georeferenced and finally merged together as a single file. The locations maps were compared with the pre-existing data. Whenever a seismic profile of the newly introduced maps was found to differ from the pre-existing database, the entire seismic profile was digitized from the georeferenced map.
3. For each seismic profile, the start and end SLPs were read from the georeferenced maps. For profiles interpreted in this Atlas, all these SLPs in the database were checked with SLPs indicated on top of the paper seismic sections and corrected if necessary.
4. Intermediate SLPs along seismic profiles to be interpreted were then generated using an automated routine that distributed them at equal intervals along the section of the seismic profile.

We discuss the precision of the SLPs obtained by this procedure in paragraph 2.4.2. In Enclosure 2, SLP numbers of the interpreted seismic profiles are indicated every 100^th^ value and every 20^th^ SLP is indicated by a dot. Along uninterpreted profiles, only the first and the last SLP (when available) of the profile are given. During data interpretation, the SLP map (Enclosure 2) was used to locate intersections of seismic profiles and to tie observed reflections to surface geology; it was also later used in the computation of the different grids and contour maps.

2.2.3 Seismic surveys, datum plane, acquisition and processing parameters

The seismic data compiled for this project are heterogeneous for a number of reasons. Seismic surveys in Switzerland comprise a variety of acquisition campaigns carried out as part of exploration investigations that took place between 1957 and 1994. Onshore acquisition started with dynamite and 12 channel recording and it ended in more recent years with sophisticated Vibroseis© or dynamite campaigns. Only 2D seismic profiles were used in this work; the 3D survey shot by Nagra in Zürich Weinland in 1996 (Birkhäuser et al. 2001) was only consulted for calibration of the 2D data.

On lakes, only few exploration seismic profiles (for example, the VD77 survey of Lake Geneva) were used in this project either because of their poor quality or because they were not available at the time we compiled the data. Shallow, high-resolution surveys on Swiss lakes, although they sometimes add interesting new information on fault position and shallow sedimentary features, were not integrated in this study because they only rarely image the base of the Tertiary unit. Also, it is generally difficult to establish connections between reflections observed on such high-resolution data and on oil-industry type data because of their inherently differing acquisition characteristics.

Because surface topography varies in the SMB, the elevation reference levels or datum planes (DP) of the different seismic surveys range from 300 m amsl in Canton Geneva up to 700 m amsl in the foothills of the Alps and in the eastern part of the basin (see Figure 2.3). The data needed therefore to be adjusted to the same DP (see paragraph 3.2.4).

Acquisition and processing parameters play an important role in the resulting seismic profile. In general, the aim of hydrocarbon exploration in the SMB was to image strata near the base of the Mesozoic units (main seals) and the shallow Palaeozoic basement at depths of 1000 m to 4000 m. Parameters were therefore geared to these targets. However, they changed considerably depending on survey and year of acquisition (see a summary of acquisitions parameters in Appendix 2.4). Field reports of the individual surveys were generally not consulted in this project (mostly for lack of availability), with the exception of the profiles that were reprocessed at the Institute of Geophysics, University of Lausanne (see paragraph 2.2.5).

In general, the parameters used by the different processing companies vary from survey to survey; some profiles were reprocessed at a later stage using again different parameters. In the normal case, migrated profiles, if available, were used for the interpretation. In cases where both stacked and migrated profiles were available, the two profile types were taken into account. Clearly, differences in acquisition and processing parameters add to uncertainties in the geological interpretation (see paragraph 2.4.5 and paragraph 3.6).

2.2.4 Seismic display

The display of seismic 2D profiles normally follows the SEG (Society Exploration Geophysicists) standards. Most of the profiles shot in the SMB show a normal SEG polarity on their display, meaning that a positive impedance contrast (hard kick) is shown as a black loop to the right. This information is normally stated in the seismic profile legend. This convention was respected in our horizon picks. In some old surveys, no polarity information could be found, but we decided not to systematically investigate possible polarity inversions mainly for the lack of reliable data. The interpretation work was based on the technical information on ac-

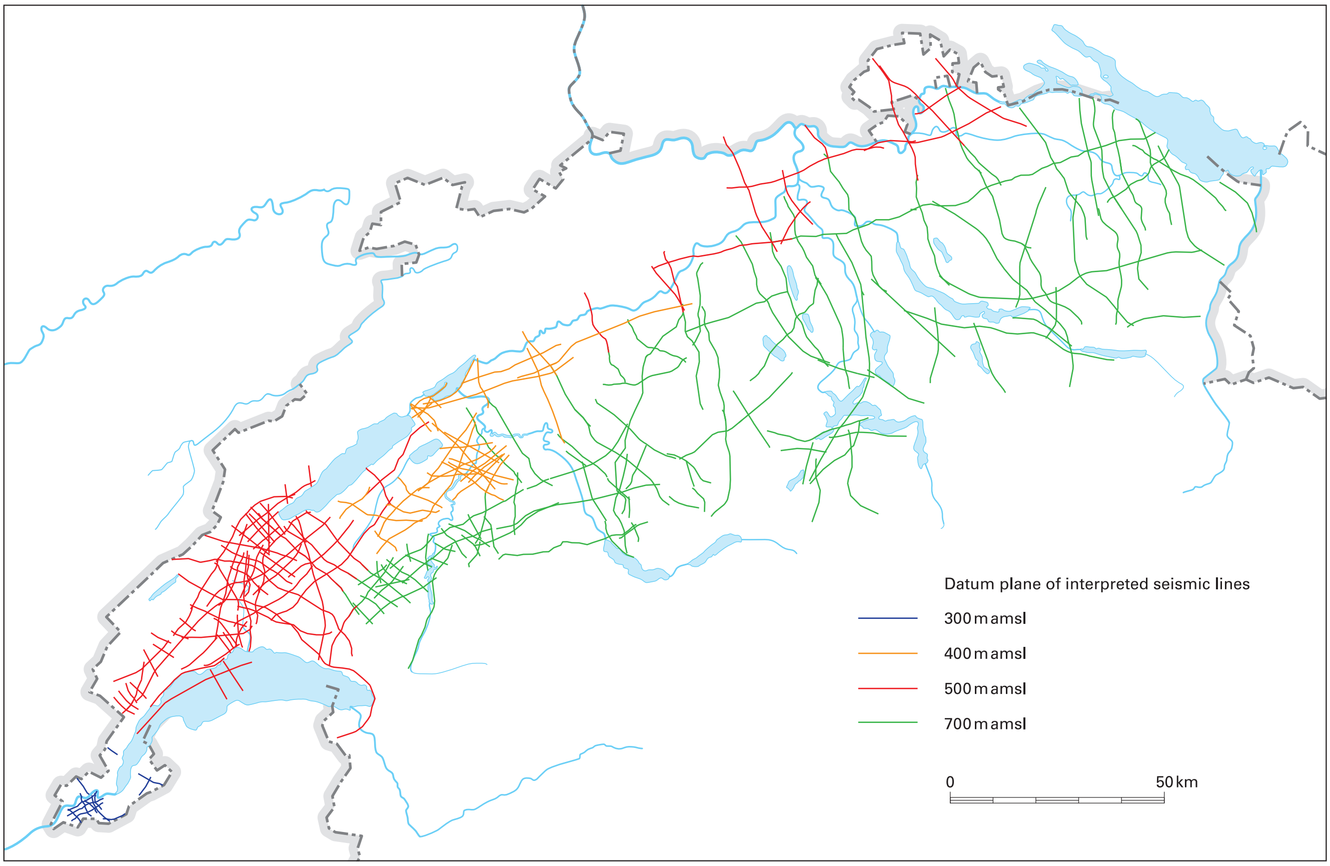

Fig. 2.3: Datum plane of the interpreted seismic lines in the Swiss Molasse Basin.

quisition and processing as stated in the legend of the paper sections. The recorded frequencies normally range from 15 Hz to 60 Hz; higher frequencies and therefore a higher resolution is available in the Nagra profiles postdating 1986.

2.2.5 Reprocessing of seismic data

The aim of our reprocessing was threefold. Firstly, to improve the general appearance and interpretability of the seismic profiles. Secondly, to homogenize the visual appearance of the seismic profiles across the entire SMB and thus to facilitate their geological interpretation at regional scale. Finally, processing attempted to better image deep reflectors at the base of the Mesozoic sequence and deeper (e.g. in Permo-Carboniferous basins) because we assumed that the original processing did not focus on these targets.

When our work started (in 2001) we considered only the digital data that were publicly available through swisstopo for reprocessing (52 profiles). From this data set, only 14 profiles were found to be adequate assuming reasonable efforts to recover shot and geophone locations as well as the necessary information for static corrections. For some profiles, this information was simply not available and in other cases the old data tapes had so deteriorated that they could not be read any more. The reprocessed profiles were all acquired in the 1980s (see Figure 2.4).

The reprocessing sequence is shown in Figure 2.5, and results are briefly described below. Details can be found in the internal report of Odello (2004). In comparison to conventional processing, particular attention was given to noise reduction and to deep reflector imaging. Parts of some profiles had to be harmonized where dynamite and vibroseis sources alternated along the same profile. Routines, such as FX filtering, were used that were not available at the time of original processing. Finally, migrated and un-migrated stack sections of each profile were produced.

The reprocessing results can be summarized as follows (see Figure 2.6). In general, our reprocessing enhanced signal to noise ratio and reflector continuity of deep reflectors, while high-frequency reflections in the uppermost parts of the section were in some instances lost. Reflections at the base of the Mesozoic sequence and below are better defined. The reprocessed sections all have the same DP of 500 m amsl, and because the seismic profiles were reprocessed with the same parameters, they enable a better comparison of seismic facies in different parts of the Swiss Molasse Basin.

The obtained results are useful for regional interpretation of the base of the Tertiary sequence and, more importantly, the base of the Mesozoic units (Profiles SADH8401, SADH8405 and LEAG / SEAG8307). Some deep reflections below the Mesozoic units indicate the presence of either Permo-Carboniferous basins or reflections within crys-

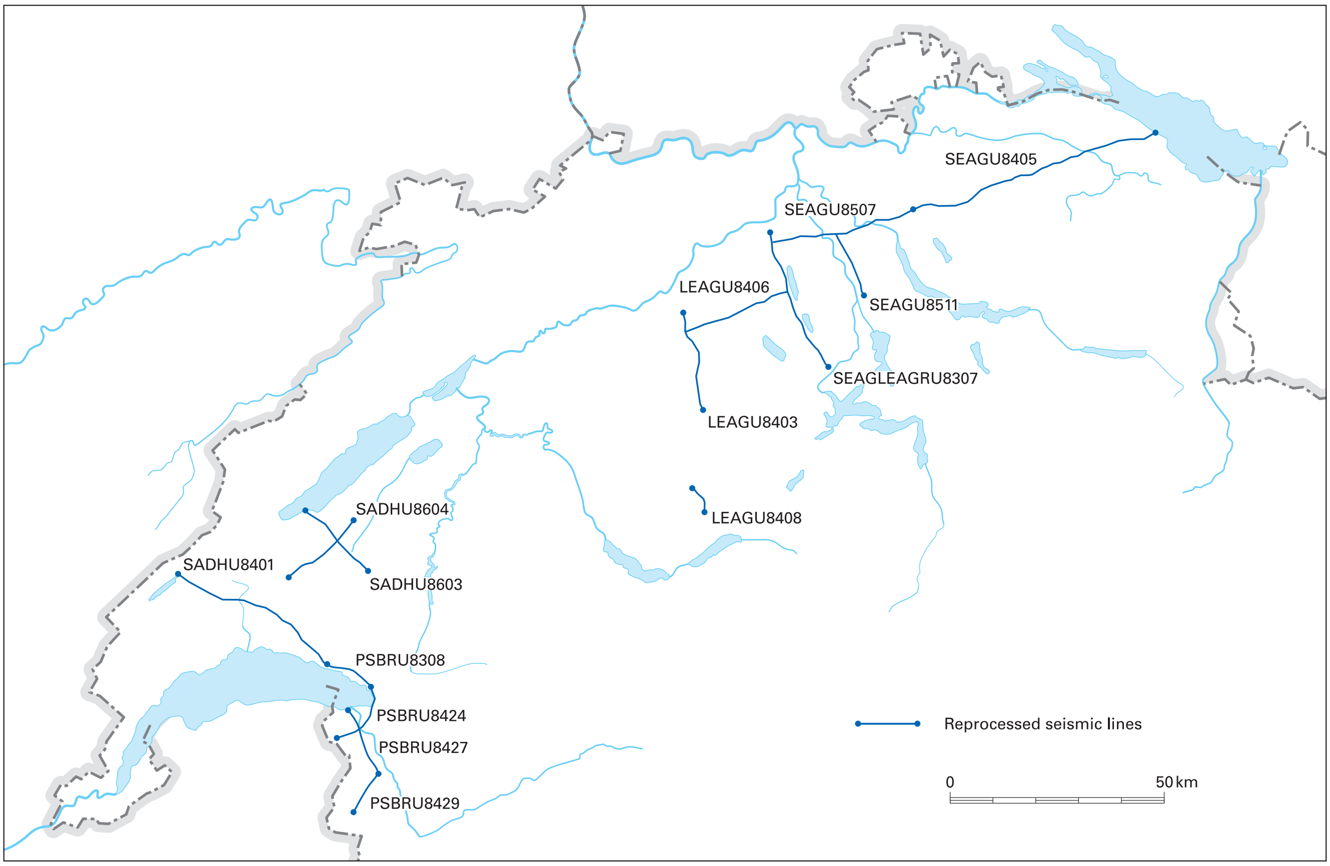

Fig. 2.4: Seismic lines reprocessed at the Institute of Geophysics, University of Lausanne. An example of a reprocessed seismic profile (SADHU 8401) is shown in Figure 2.6.

talline basement. The continuous character of such events is more apparent in the reprocessed profile (see Figure 2.6). In addition, this work provides a better feel for what may be expected from future data reprocessing in the SMB with the objective of enhancing deeper parts of the sections. It also illustrates the problems one may encounter in reprocessing data in the SMB, in particular when it comes to retrieve old seismic data and its complementary information.

Because CDP numbering was modified during reprocessing, new CDP numbers no longer corresponded to the original ones. To avoid confusion only the CDP numbers of the original sections are shown in Enclosure 2.

2.3 Wells

To control the basin stratigraphy, we used the data from 43 deep wells, i.e. most of wells available in Switzerland. The wells are not ideally distributed throughout the Swiss Molasse Basin; in the Subalpine Molasse area and in the eastern SMB there are only a few wells (Figure 2.1 and Enclosures 1 and 2). This unequal spatial distribution leaves large areas without stratigraphic control. Seismic data were calibrated to the wells using the existing information on well stratigraphy and by calculating velocities within stratigraphic units from TZ-curves (see paragraph 3.3, for more details). Although well data have been published in scientific papers more often than seismic profiles in the Swiss Molasse Basin, they are not always useful for calibrating seismic horizons because velocity data are often missing.

The well data used in this project are shown in Appendix 2.5, and the well locations are indicated in Figures 2.1 and 2.2 as well as in Enclosures 1 and 2. There are more deep wells in Switzerland than the ones we used, namely the ones drilled by Nagra into the crystalline basement of northern Switzerland. In that area, we used only the most relevant ones for stratigraphic calibration on the SMB side.

The wells drilled from 1961 onwards for oil and gas exploration or for nuclear waste storage provide the best data for calibration, as they were designed to test deep structures and to calibrate reflection seismic profiles. Seismic traveltimes through the different stratigraphic units were measured, which enabled velocity determination. In some cases, vertical seismic profiles were shot and synthetic seismograms calculated (see paragraph 3.2.2). Some geothermal wells reach deep into the Tertiary sequence, like Weggis-1 (1993) or include important data on the Mesozoic stratigraphic sequence, such as Thônex-1 (Jenny et al. 1995). Unfortunately, not all of these reports provided data with which we could calculate velocities.

Seismic velocities in the different stratigraphic units were calculated from available TZ-curves or, in absence of TZ-curves or where resolution was insufficient, they were estimated from general velocity trends in the SMB (see paragraph 3.3). Existing synthetic seismograms were exploited, such as the recent ones from Nagra and the ones from the Essertines-1 and Thun-1 wells. Some other geophysical logging curves were consulted, but only for control purpose. For complete references on each well, see Appendix 2.5.

2.4 Data quality

The general data quality is discussed in the following paragraphs. Quantitative uncertainty estimates will be presented in chapter 3 (see paragraph 3.6.2) building on the features presented here.

2.4.1 Quality of seismic section display

In general, the seismic profiles in Switzerland acquired between 1960 and 1980 poorly image the subsurface. The main reasons for this poor quality are the presence of heterogeneities in the near surface layers combined with inappropriate acquisition parameters, insufficient near-surface corrections and incomplete processing sequences. The profiles shot and processed by Nagra in the 1980s and 1990s provide the best seismic images.

To appraise the data quality of the interpreted seismic profiles, we defined three quality types of seismic-profile display. This quality rating, obviously subjective, is determined by the seismic interpreter who evaluates the geological interpretability of a paper section (see Figure 2.7):

- Quality type 1, the best, shows reflections with good lateral continuity and stratigraphic reflections with specific characteristics that are easily followed throughout the entire profile. This quality type includes only 4 profiles with a total of 92 km (or 2 % of the total 4357 km of interpreted seismic profiles).
- Quality type 2 characterizes profiles with moderate to good lateral continuity; correlation of reflections is not easily followed across the entire profile. This quality type includes the majority of the interpreted profiles, i.e. 190 profiles for 3458 km of data (i.e. 80 % of the total interpreted profile length).
- Quality type 3, the lowest, is defined by reflections with low to poor lateral continuity (interrupted by so-called «transparent» areas) and by reflections from stratigraphic discontinuities that are difficult to recognize. It contains 69 profiles for 808 km (18 % of the total interpreted profile length).

Although there are other more objective ways of qualifying seismic profiles, this rating provides some estimate of the general quality of the data across the Swiss Molasse Basin (see Figure 2.8). These quality estimates of a seismic-profile display as a whole are not to be confused with the seismic quality classes defined for the interpretation of the transect seismic profiles (chapter 3). In the latter, the quality of each individual seismic reflection and fault is assessed.

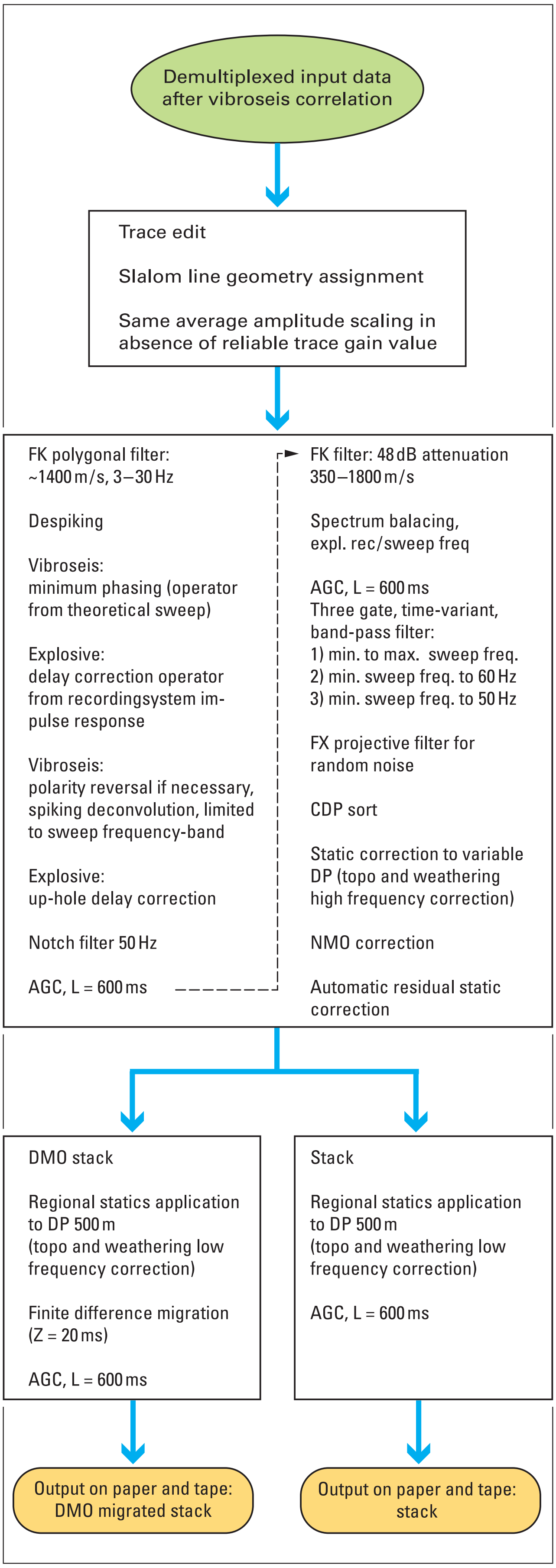

Fig. 2.5: Reprocessing sequence for seismic profiles (see Figure 2.4) in the Swiss Molasse Basin (ODELLO, 2004). For more details see text.

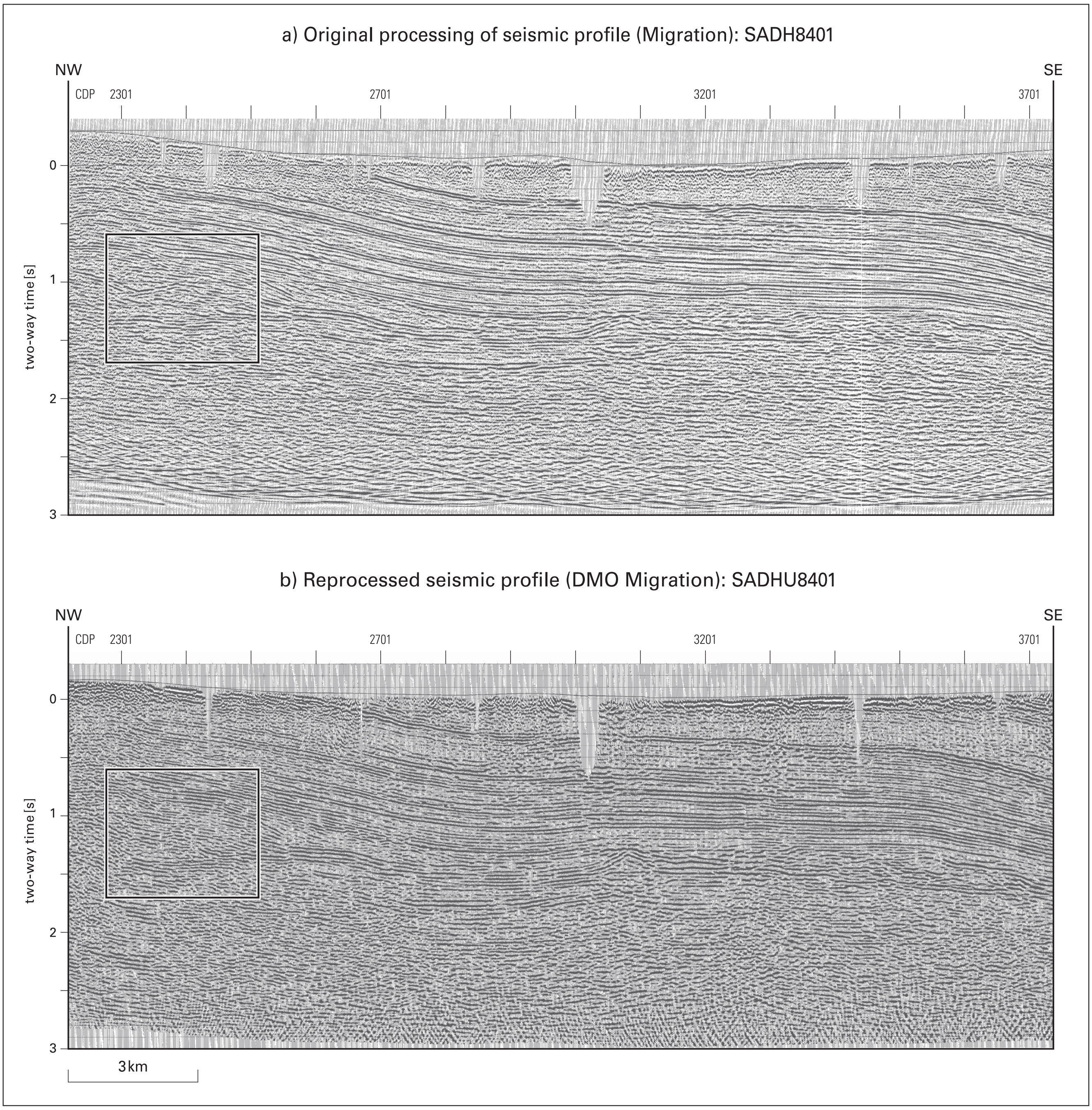

Fig. 2.6: Example of seismic reprocessing. a) Portion of profile SADH8401 as originally processed. b) Same seismic profile reprocessed at the Institute of Geophysics, University of Lausanne. In general, reprocessing enhanced signal-to-noise ratio and provided better reflector continuity. In the indicated square, a problem with conflicting dips apparent in the original section is resolved in the reprocessed version. For location of the seismic profile see Figure 2.4. (CDP: common depth point)

2.4.2 Precision of seismic profile location

The precision of the seismic profile coordinates depend on the quality of the original data (in digital form or on paper). Seismic profiles for which no original location maps were available correspond to the least precise, profiles reprocessed at the Institute of Geophysics (UNIL) and Nagra profiles represent the best case because their coordinates were directly obtained from field tapes or from the CDP locations calculated during reprocessing. When digitized from paper maps the precision of seismic profile coordinates rely on the original accuracy of the map, on the map scale, and on the line thickness of the map drawing. Precision estimates range from a few meters, in the best case, to more than 150 m in the worst case. Based on the quality of these estimates we defined a specific precision code and attributed this to each seismic profile in the database (see Appendix 2.2).

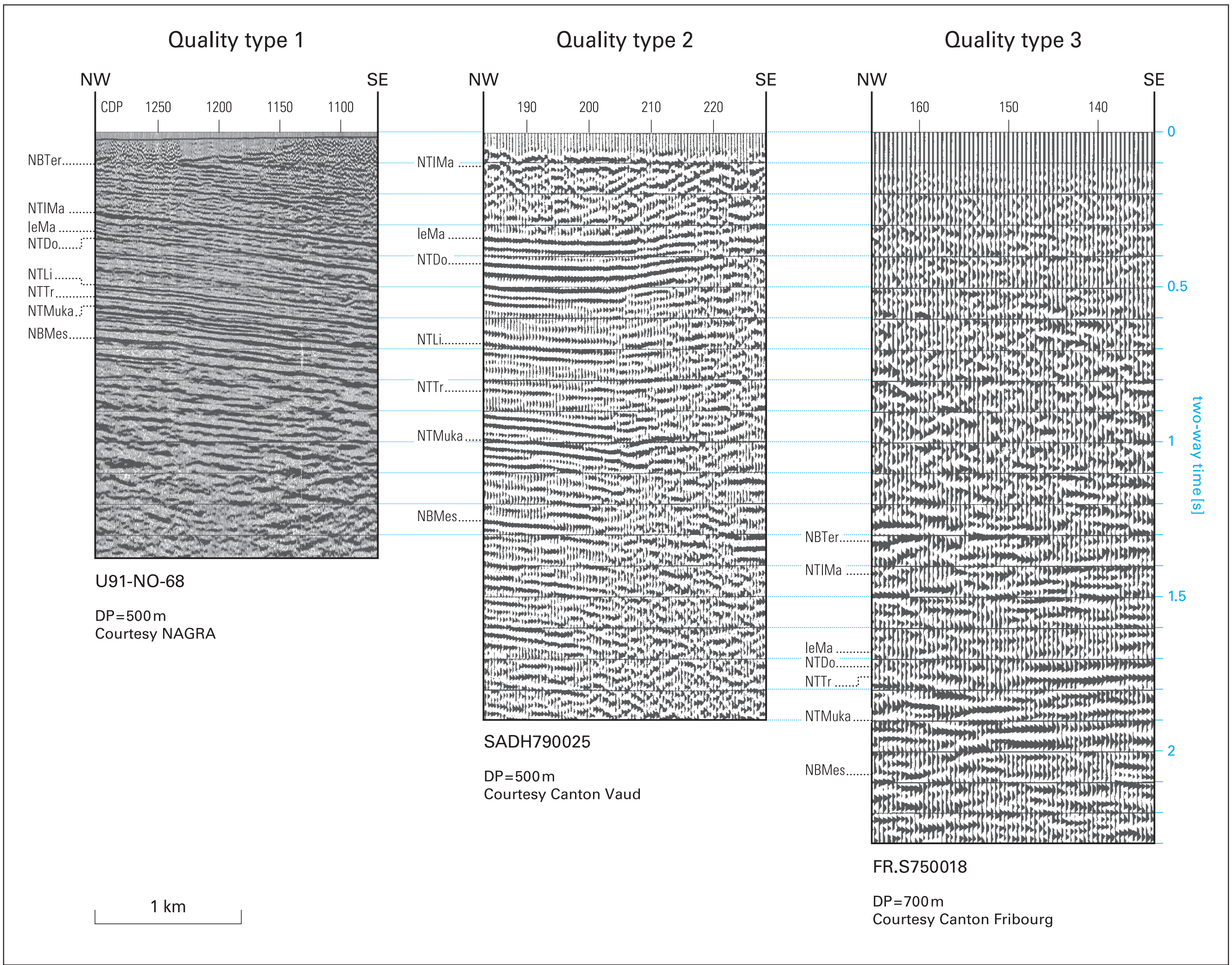

Fig. 2.7: Examples of the three quality types defined according to the display characteristics of the seismic profiles (see text for quality type definition). The distribution of the different quality types in the Swiss Molasse Basin is shown in Figure 2.8.

2.4.3 Quality of the well stratigraphy and of the well velocity surveys

Well-data quality relies on completeness of the different data and their recording. More recent techniques are likely to provide better stratigraphic determinations, and different companies may have had different ways to interpret the data. In this study, we used both stratigraphic and velocity data.

The stratigraphic interpretation of well data is usually based on micropalaeontology and lithostratigraphy derived from cuttings, geophysical logs, and later detailed lab analysis. Cutting-derived boundaries are precise to the order of several meters. Geophysical log locations may also be off by more than one meter. Location surveys allow for a calculation of the true vertical depth in the well. We usually assumed an uncertainty of several decimetres.

P-wave velocity measurements along a well must be corrected for various effects such as non-linear ray paths, borehole deviation from the vertical, low-velocity layers in the near surface (such as soil and unconsolidated sediments). Downhole geophones were often positioned at the major stratigraphic boundaries as they were known at the time of the survey. These are not necessarily the depths of major impedance contrasts that contribute most strongly to the reflection seismic image of a near-by 2D profile. In general, the scale of stratigraphic resolution in a well, a few decimetres or even centimetres, cannot be compared to the vertical resolution of a seismic image that can be as large as several tens of meters.

2.4.4 Accuracy of geological maps

Swiss geological maps are the best sources to understand the surface and regional geological settings of the Swiss Molasse Basin. However, some maps present fault patterns derived from seismic data that are interpolated along large distances between scarce data points unconfirmed by other data. This is in particular the case for the 1:500 000 tectonic map of Switzerland (Swisstopo, 2005 b)

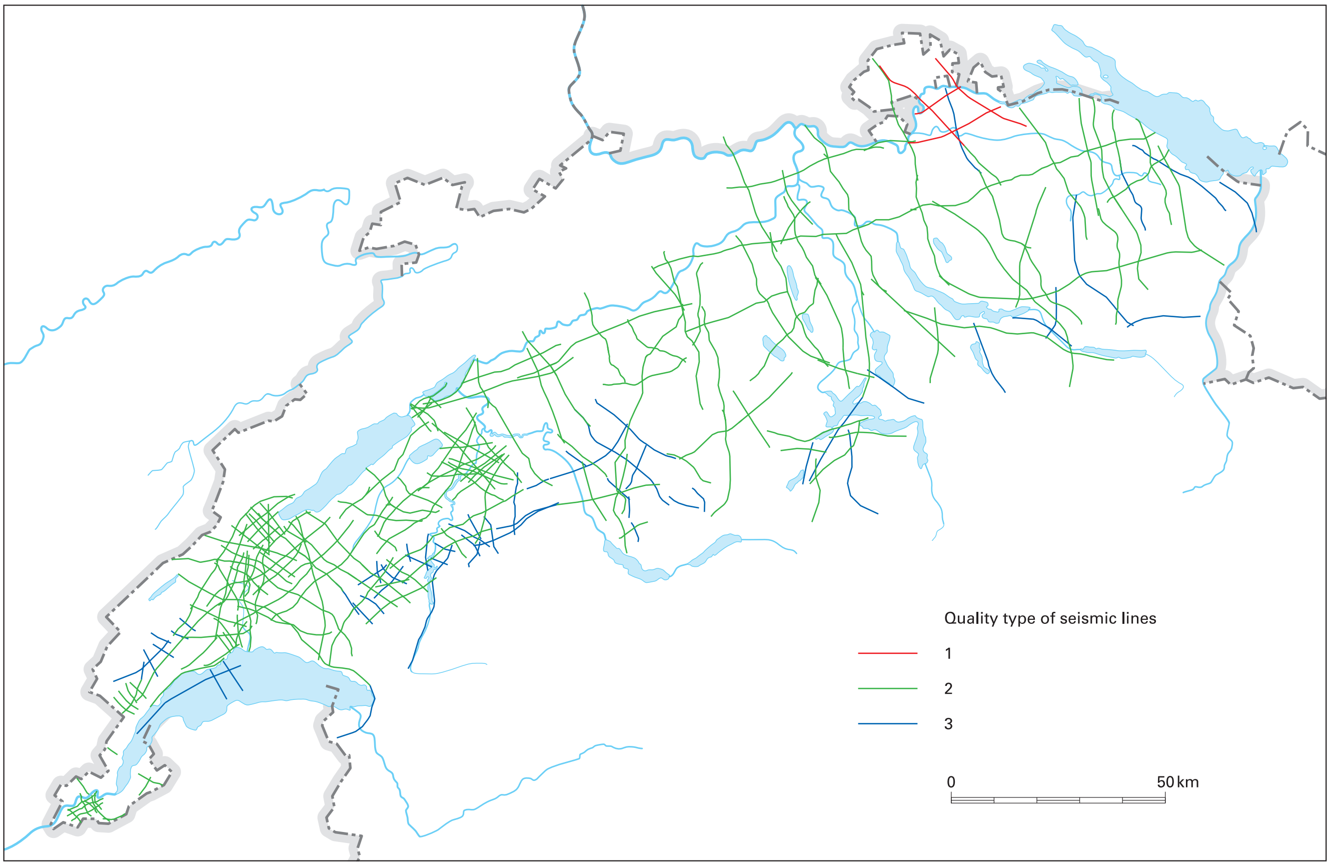

Fig. 2.8: Distribution of quality types of the interpreted profiles in the SMB. See example of quality types in Figure 2.7.

that includes some data derived from seismic profiles or wells in its legend. On the other hand, 1:25 000 geological maps can include information with a precision of a few meters or tens of meters. Features of that size cannot be resolved by the seismic data used in this work.

2.4.5 Accuracy of seismic data

Seismic reflections are images of variations of the physical rock properties and thus they are expressions of the heterogeneous character of a volume of rock. Their locations in two-way traveltimes (TWT) depend on many data features and on corrections applied to them, such as the signal-frequency content, seismic datum plane (DP) and mistie corrections of the profile, and processing parameters, just to name a few. Moreover, the interpretation of a 2D seismic profile assumes that the observed reflections originate from variations of the rock properties that are located in the plane of the profile. However, this is not always true, particularly in the case of complex 3D geological settings.

Vertical resolution of seismic waves depends on their frequency content and on the velocity of the rocks through which they travel. It is generally accepted that details smaller than a quarter of a wavelength cannot be resolved. For example, the best vertical resolution of seismic waves with a dominant frequency of 50 Hz and travelling through rocks that have a velocity of 5000 ms^{-1} is 25 m; for waves with the same velocity but a dominant frequency of 25 Hz the best vertical resolution becomes as large as 50 m.

In contrast to well data, seismic data do not provide information at single points. Rather the seismic signal recorded at a surface point is the superposition of signals reflected from a region (the Fresnel Zone), the deeper the reflector, the larger its Fresnel Zone. Hence, the size of the Fresnel Zone provides an estimate for the horizontal resolution of the seismic technique. For example, for seismic waves with a dominant frequency (f) of 50 Hz travelling at a velocity (v) of 2500 ms^{-1} and reflected at a depth (z) of 1000 m, the diameter (D) of the Fresnel Zone is 316 m ($D = (2vz/f)^{1/2}$). At a depth of 2000 m, waves with the same frequency content and travelling at 4000 ms^{-1} the diameter of the Fresnel zone becomes 566 m. Furthermore, a considerable amount of uncertainty in seismic interpretation results from image distortion effects that may only partly be corrected by 3D migration. In this study, no 3D migration was applied, and only a few profiles could be obtained in 2D migrated form.

Our uncertainty estimates of the interpreted seismic reflections used in this work take the above considerations into account (see paragraph 3.6), and they also include the fact that our seismic database is a collection of seismic profiles from various surveys that differ from each other in many respects.

3. Methodology to establish a subsurface structural model from seismic reflection and well data

3.1 Introduction

3.1.1 General work flow (methodology)

The general scheme followed in this work is illustrated in Figure 3.1. It is based on the input data set described in chapter 2, with seismic profiles and well data as principal data sets. In addition, we used geological and tectonic maps to further constrain the seismic interpretation. The data that can be spatially located were georeferenced and stored in a GIS database. For example, the seismic location map can be superimposed on the geological maps to establish links between the interpreted seismic reflections and surface geology.

Seismic interpretation focussed on eight major seismic reflections (or seismic horizons) across the entire seismic data set in the Swiss Molasse Basin (SMB). These horizons correspond to, or are located near major discontinuities between stratigraphic units and the link between them was constrained by the well data. We identified faults that offset the seismic horizons. These interpreted features were digitized and georeferenced.

Once included in the GIS database, the digitized seismic horizons were adjusted to the same Datum Plane or reference elevation (DP) of 500 m amsl. At the intersections of seismic profiles, differences in two-way traveltime (TWT) or mis-ties between seismic horizons that correspond to the same discontinuity were subjected to a minimizing procedure. All mis-ties could not be reduced to zero, and the average remaining mis-tie value contributes to the total uncertainty of the TWT position of the interpreted reflections. We estimated sources of error in the interpretation process, in addition to mis-ties, in terms of relative and absolute errors. Uncertainties in depths were calculated by converting uncertainties in TWT to depths using seismic velocities.

To convert seismic TWT to depths, seismic velocities must be known. We obtained velocities from well data within each of the eight stratigraphic units between the interpreted seismic horizons. Velocities were interpolated between well locations and extrapolated across the entire area where seismic data were available. A velocity map was computed for each interval between two seismic horizons.

TWT values along seismic profiles were interpolated to construct continuous TWT maps of the interpreted seismic horizons, and these maps were converted to depth using the velocity maps. Finally, vertical thickness maps were derived by taking the difference between depth maps. The TWT and depth maps (see Enclosures 17 to 19 and 21) were computed for the eight interpreted horizons and vertical thickness maps for the eight stratigraphic units.

To provide insight into the entire SMB, we constructed 13 dip- and 2 strike vertical sections of the basin. Each section, hereinafter called transect, is based on a series of seismic profiles. Each transect includes the non-interpreted seismic profiles, the same data with superimposed seismic interpretation and a depth-converted seismic interpretation. We attributed quality classes to the interpreted reflections and faults within the Cenozoic and Mesozoic units. In the pre-Mesozoic unit, only the quality of the seismic reflectivity is assessed. Seismic reflectivity within this unit may be attributed to Permo-Carboniferous sediments, but it is by no means evidence for their presence. The above steps are described in more details below.

3.1.2 Georeferencing of the data sets

The GIS database includes, but is not limited to: digital geological- and tectonic maps (see Figure 3.2), a digital elevation model (DHM25 from swisstopo), coordinates of the seismic location points and wells, digitized seismic horizons and faults (see Figure 3.3), surface grids of the calculated horizons in TWT and in depth, and surface grids of interval velocities and vertical layer-thicknesses. We developed tools for the ArcGIS software to assist procedures, such as checking the digitized data, extracting TWT values along digitized seismic horizons, geo-referencing TWT data, and minimising computations of seismic mis-ties and decimation of data points along seismic profiles.

3.2 Interpretation of seismic profiles

3.2.1 Selection and interpretation of eight seismic horizons across the Swiss Molasse Basin

To carry out a regional study throughout the entire SMB we selected seismic horizons according to several criteria. First, we identified a set of stratigraphic units representative of the basin fill from well data. The limits of the units had to represent main system boundaries and they had to be spread more or less equally over the Cenozoic and Mesozoic stratigraphy. Secondly, we selected the limits of these units such that they correspond to clear reflections across the entire SMB. This criterion, however, turned out to be difficult to achieve everywhere. Especially in the Cenozoic units, seismic reflections could not be followed over long distances, and a systematic interpretation of Cenozoic horizons was therefore not carried out. The situation was found to be better in the Mesozoic units, although for some stratigraphic boundaries no reflections were found to correspond exactly and seismic horizons had to be selected above or below the boundaries. Thirdly, we based the final selection of seismic horizons on seismic profiles in the western part of the SMB because there the Mesozoic sequence is thickest and stratigraphically most complete. The selected horizons are listed in Table 3.1 where they are compared to those interpreted in the SMB by other authors. Their stratigraphic position is also shown on the well penetration chart (see Enclosure 16). The detailed seismic characteristics and nature of the interpreted horizons are described in chapter 4.

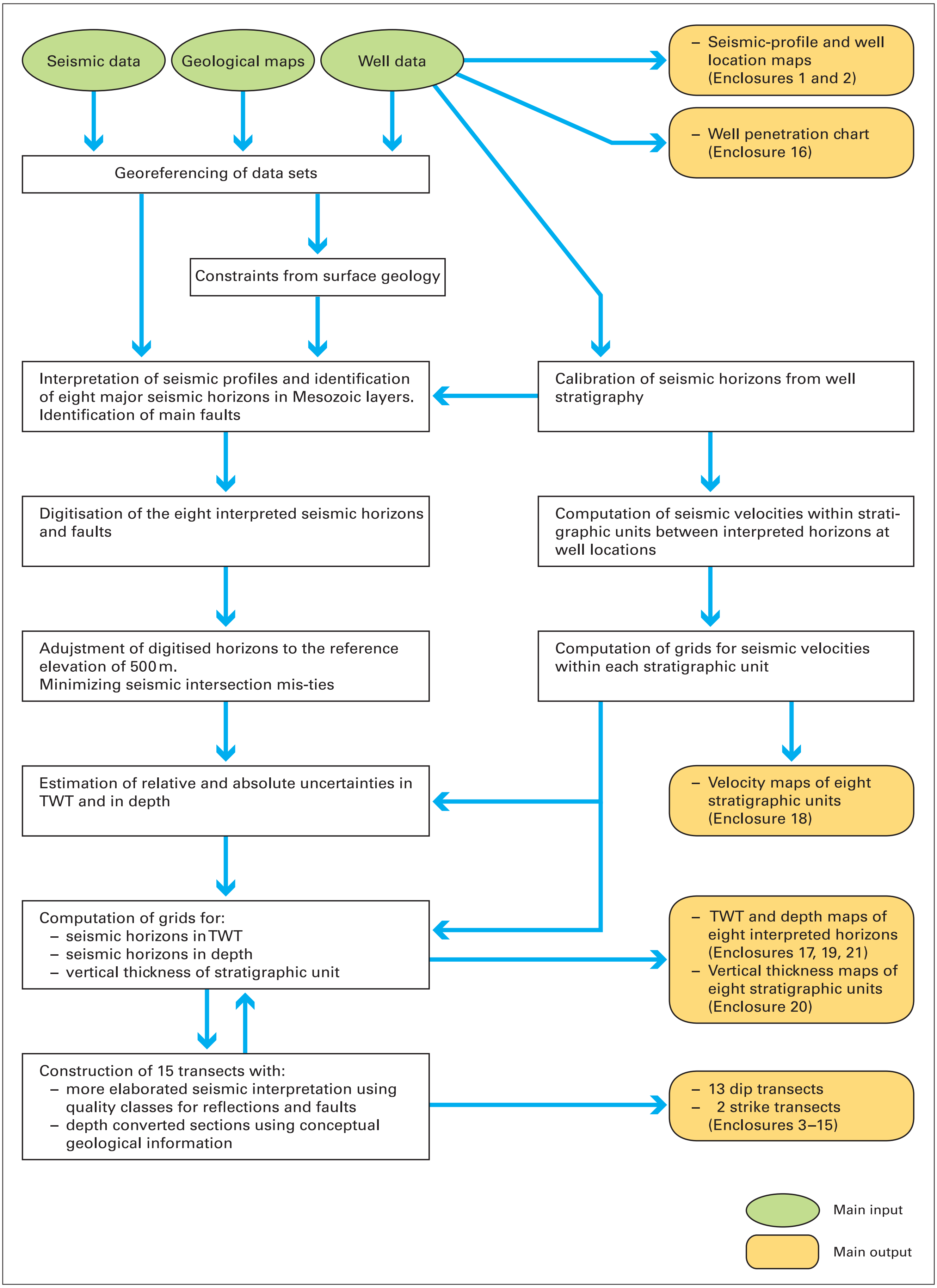

Fig. 3.1: Flow chart of main working steps (see text).

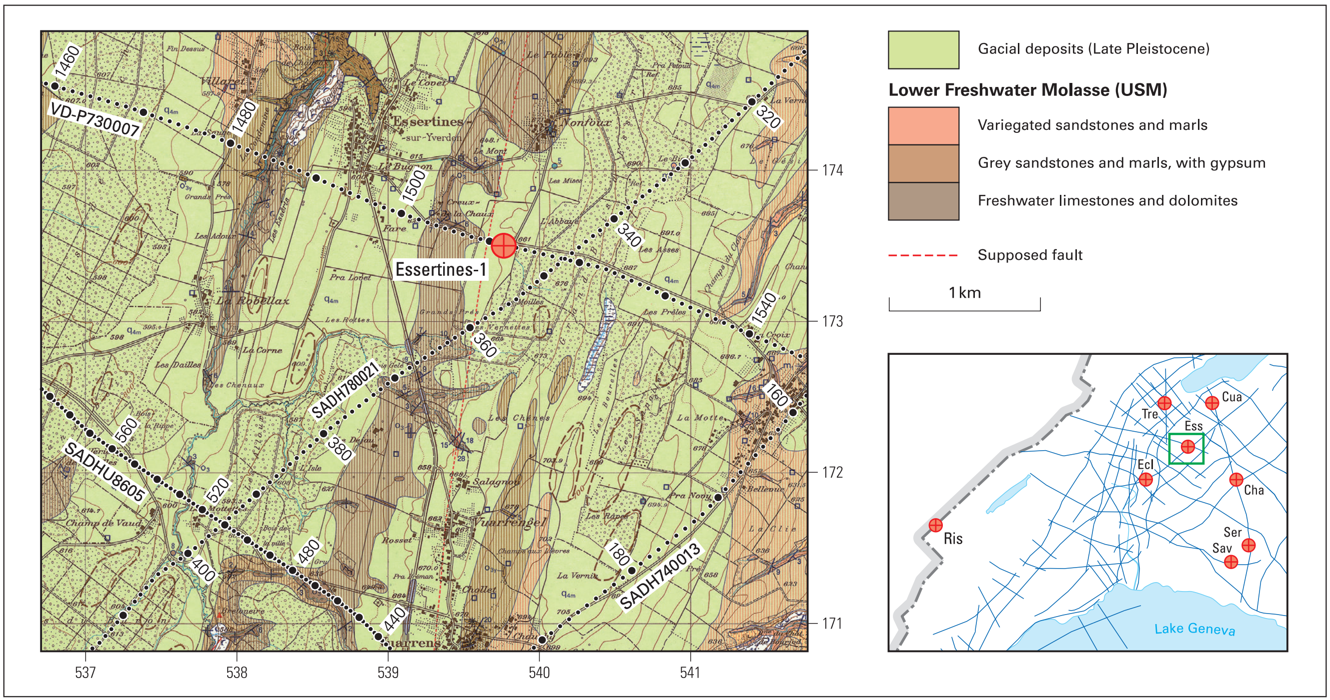

Fig. 3.2: Example of georeferenced seismic profiles and a well superimposed on a geological map (Map 1203, Yverdon-les-Bains). Black dots indicate seismic location points (SLP) along seismic profiles. The location of the Essertines-1 well is indicated by a green square in the right inset. Geological surface structures and formation boundaries along the seismic profiles were transferred from this map to paper copies of the seismic sections for interpretation, using the SLPs.

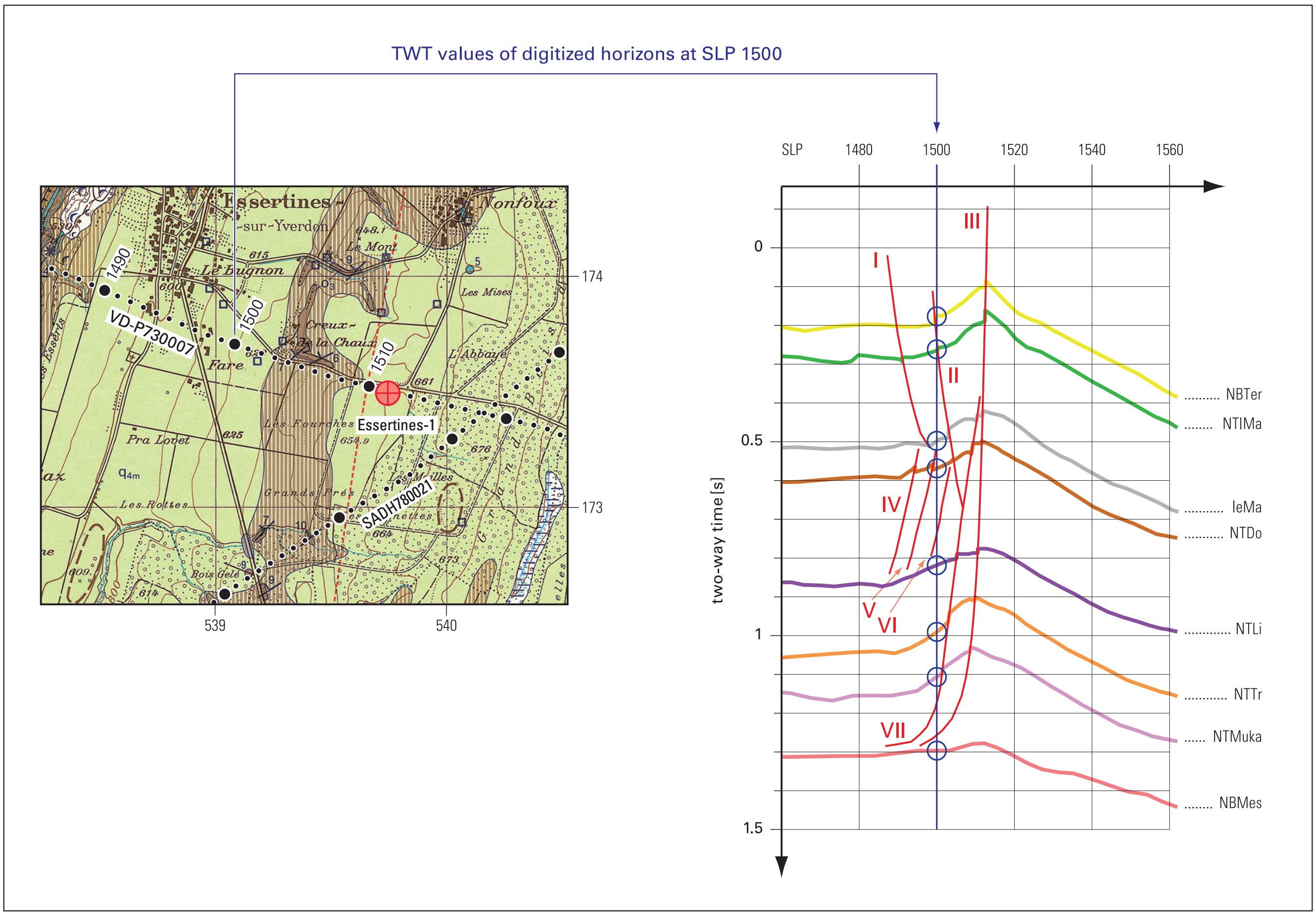

Fig. 3.3: Example of georeferenced data along an interpreted seismic profile. To each SLP correspond the TWT values of digitized horizons and faults, when defined. Additionally, each horizon and each fault segment (I to VII, red lines) has its own identification in the GIS data base.

Table 3.1: *Name conventions for seismic horizons interpreted in this work and for some selected reports that cover important parts of the Swiss Molasse Basin.*

This work (abbreviation and name convention)		Sommaruga (1997)		Leu (2002)	Naef & Diebold (1990) and Nagra (2008)
NBTer	Near Base Tertiary	A	Top Cretaceous or Base Tertiary	Top Cretaceous	Base Teriary, Top Malm
NTlMa	Near Top late Malm	B	Top Upper Malm	Top Malm	
IeMa	Intra Early Malm	C	Top Lower Malm «Argovien»	–	Intra Malm
NTDo	Near Top Dogger	D	Top Dogger	Base Malm	Base Malm
NTLi	Near Top Liassic	F	Top Liassic	Top Lias	Top Liassic, Base Opalinuston
NTTr	Near Top Triassic	G	Top Triassic Unit 1	Top Keuper	–
NTMuka	Near Top Muschelkalk	H	Top Triassic Unit 2	Top Muschelkalk	Top Hauptmuschelkalk
NBMes	Near Base Mesozoic	I	Top Basement	Base Mesozoic	Top Permian, Base Mesozoic

The geological interpretation of the seismic profiles was carried out according to the following steps:

1) Identification of seismic horizons by comparing boundaries between stratigraphic units observed in wells (see paragraph 3.2.2). This is possible for seismic profiles that run in the vicinity of a well with data that can be converted to TWT (i.e. velocities must be available). This assumes that geology (as far as it is known) can be extrapolated from the well to the seismic profile.
2) Interpretation of connecting seismic profiles by juxtaposing paper copies at their intersections and following the horizons from well locations into non-calibrated parts of the basin from one profile to the next.
3) Relevant geological surface features, such as faults, stratigraphic dips and unit limits were written down on top of the seismic profiles. This made it possible to establish connections between observed reflections and surface geology, the quality of which depends on how close the reflections are to the surface.
4) Faults were identified between disrupted seismic reflections. Offset of seismic reflections are good fault indicators. Alternatively, regions that are seismically transparent or that contain totally incoherent reflections may also indicate the presence of fault zones.
5) While interpreting the seismic data, care was exercised to avoid wrong interpretation of features that did not correspond to geological features such as multiple reflections or processing artefacts.
6) Once the interpretation was found consistent for an array of intersecting seismic profiles, key interpreted elements were digitized (see paragraph 3.2.3).

The interpretation of the seismic profiles displayed on the strike and dip transects followed additional interpretation criteria that involved the quality of the seismic data (see paragraph 3.5). Only a few seismic profiles were available to us in digital form (e.g. the reprocessed profiles see paragraph 2.2.5), so the interpretation was mostly done on paper copies.

3.2.2 Calibration of seismic profiles with well data

To calibrate seismic horizons, we used the following well data: ground elevation at well location, well track geometry, stratigraphic interpretation, velocity measurements within the well, geophysical logs and synthetic seismic profiles (see Figure 3.4). Complete data sets were not available for each well, and only few contained synthetic seismograms (we did not calculate synthetic seismograms in this work and only used published ones).

The depths of the stratigraphic limits were converted into TWT and compared with the observed TWT of the seismic reflections. The TWT conversion made use of the time-depth curves, or TZ-curves, obtained in wells by measuring the direct traveltime, or one-way time (OWT), of seismic waves generated at the surface and recorded at different depths within the well (see Figure 3.5).

The total depth (TD) of a well is measured from a level that was later converted to ground elevation (GE). The total depth of a well can be simply measured along the hole (this is the along hole depth or ahD), i.e. the total drilled length. However, because wells are rarely perfectly vertical, the ahD can be converted to true vertical depth (tvD) only where a directional survey was carried out. In old wells, this was gene-

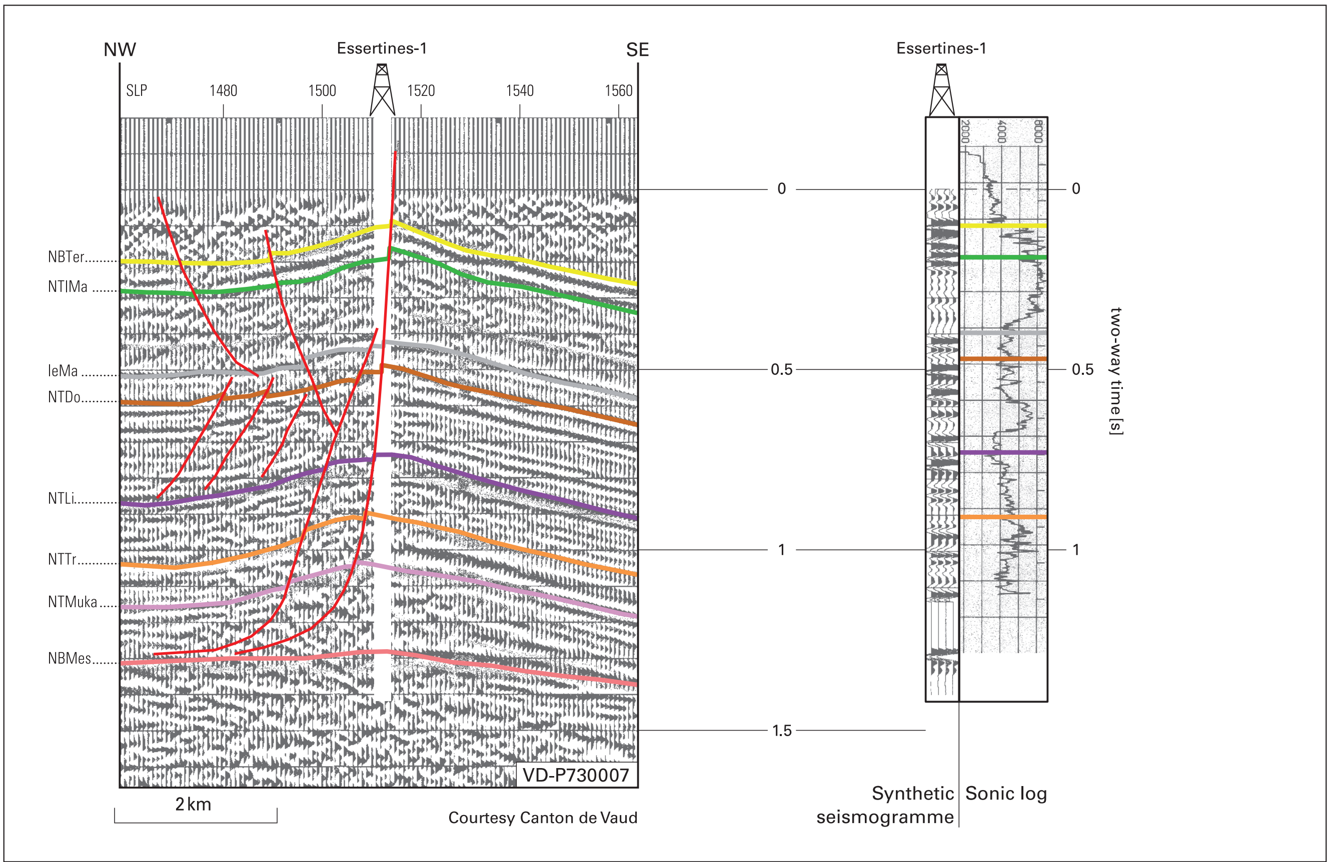

Fig. 3.4: Example of a seismic profile calibrated with the Essertines-1 well. The seismic profile is compared to a synthetic seismic profile and a sonic log (showing instantaneous rock velocities between 2000 ms^{-1} and 6000 ms^{-1} on the right). The synthetic seismic profile was calculated from 0 s in TWT; the earlier start of this sonic log corresponds to measures at shallower depths in the well. Only six of the eight seismic horizons interpreted in this study are identified on the sonic log. No seismic quality of reflection and fault classes are shown. The location of the seismic profile (courtesy: Musée Cantonal de Géologie, Canton Vaud) is shown in Figure 3.2.

rally not the case, and only the ahD is known. In Switzerland, most wells were drilled «vertically» without directional survey, and if lateral deviations have occurred the published depth may be off by 10 m or even more.

We applied the following procedure to identify seismic reflections that correspond to stratigraphic boundaries in wells:

1) Plot the stratigraphic boundary depths onto the depth axis of the TZ-curve measured in the well, and read off the corresponding one-way traveltime (OWT) values. Extract the OWT value corresponding to the limits of the interpreted stratigraphic units.
2) Adjust the time baseline of the TZ-curve to the datum plane of the seismic profile. This is calculated differently following the position of the zero-depth level of the TZ-curve (0_{TZ}) above or below the DP of the seismic profile (Figure 3.6). Convert the OWT to TWT's (these are the TWT values displayed along the well columns in Encl. 16). In Figure 3.6, an example calculation is shown for a DP of 500 m amsl. For seismic profiles with a different DP, computations were done relative to the DP of the profile.
3) Plot the well stratigraphy in TWT on the seismic profile at the well location (same scale as the seismic profile; 1 sec = 10 cm).
4) Compare the nature of stratigraphic unit with the seismic facies on the profile.
5) Select the best reflection candidate on the seismic profile close to the stratigraphic boundary of the well.

With industry data, discrepancies between seismically derived horizons and stratigraphic boundaries in wells are often accommodated by smoothing out missmatches by locally shifting horizons around the well until they fit the well data. In this process, horizons may be moved relative to each other and / or the entire seismic profile may be inclined. This means that the time proportions between individual horizons and the recorded context of the seismic profile are lost. In the present work, we opted for a more rigorous approach that treats seismic data consistently throughout the entire basin by adjusting the interpreted seismic horizons and the well stratigraphy separately to the 500 m DP (see paragraph 3.2.4), without moving horizons relative to each other nor allowing rotation of a whole seismic profile.

The fit between seismic reflections, well stratigraphy in TWT and the interpreted horizons of individual wells is discussed in chapter 4. Seismic horizon calibration for each well is shown in Appendix 2.5. Uncertainties in calibrating seismic profiles with well data are discussed in paragraph 3.6.

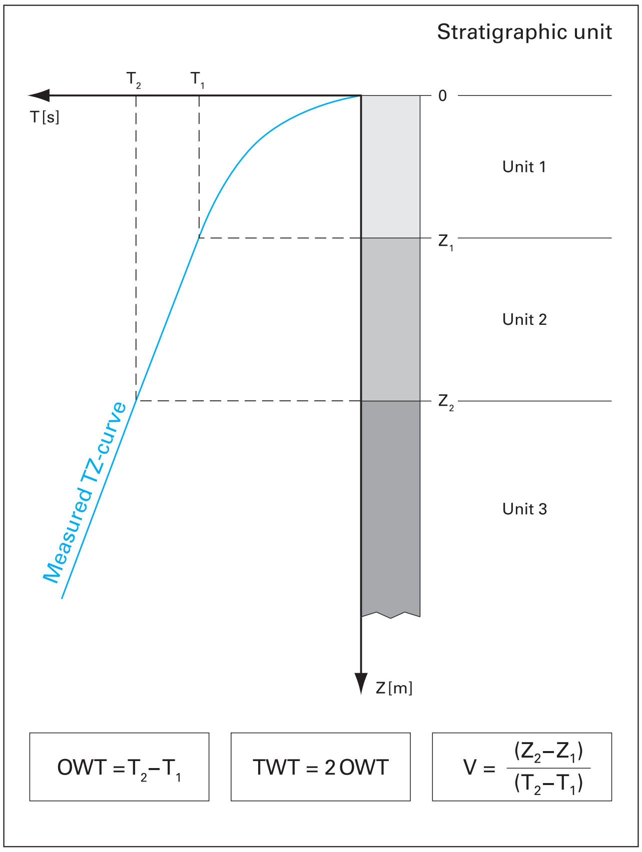

Fig. 3.5: Determination of two-way traveltimes (TWT) and velocities within stratigraphic units from a time-depth (TZ) curve measured in a well. In this example, the TWT within unit 2 between depths Z_2 and Z_1 is derived from the difference $T_2 - T_1$ (One-way travel time, OWT). The velocity (V) within a unit is calculated from the depth difference divided by the time difference. Note that in actual practice, the TZ-curve is measured at discontinuous depths that do not always correspond to unit boundaries.

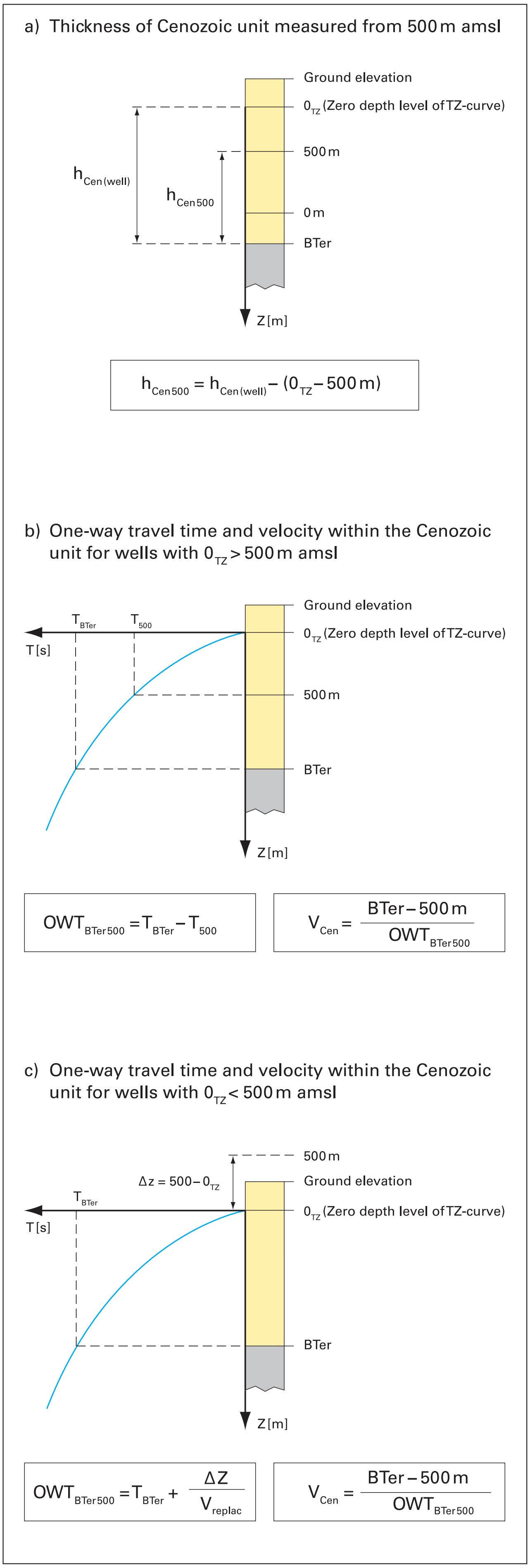

Fig. 3.6: a) Thickness determination of the Cenozoic unit measured within a well from 500 m amsl. b) One-way traveltime (OWT) and velocity computation from the TZ-curve in a well for the Cenozoic unit relative to 500 m amsl. If the 0-level of the TZ-curve (0_{TZ}) is located above 500 m amsl, the OWT to Base Tertiary ($OWT_{BTer500}$) is the difference between T_{BTer} measured across the Cenozoic unit and the OWT to 500 m amsl (T_{500}). c) If the 0-level of the TZ-curve located below 500 m amsl, the OWT to Base Tertiary (T_{BTer}) is added to the traveltime between 500 m amsl and 0_{TZ}. This traveltime is calculated using a replacement velocity V_{replac} over the distance DZ. V_{replac} is the velocity used for static corrections during processing of the profile nearest to the well or some other estimated value if the latter is not available. The velocity within the Cenozoic unit is calculated using the corrected OWT to Base Tertiary.

3.2.3 Digitization and georeferencing of the interpreted seismic profiles

The horizons, faults and thrusts interpreted on paper copies were transferred to transparent paper in order to clearly indicate the features to be digitized. Digitizing was carried out by digitizing each feature by hand on a digitizing table. The density of digitized points was increased in regions of steep seismic horizon topography (e.g. across faults), and it was reduced in regions of smooth topography. The digitized elements were stored in the GIS database as vector objects with the X coordinate (in meters) providing the point location along the seismic profile and the Y coordinate providing the TWT value (in seconds) at this location (see Figure 3.3). To reduce the number of points in later calculations and to obtain a more homogenous point density, data points were decimated just before data interpolation (see Figure 3.7).

3.2.4 Adjusting seismic data to the DP of 500 m amsl

We first adjusted seismic data with different DPs (300 m, 400 m and 700 m) to 500 m amsl in the GIS database. The required time adjustments were estimated with two different techniques depending on whether or not seismic profiles had intersections with interconnected profiles belonging to the majority of the data set in the Swiss Moalsse Basin.

1) For seismic profiles belonging to the interconnected data set, the TWT shift between two profiles of different DPs was obtained by shifting one time scale relative to the other until a series of identical reflections in the two profiles aligned. The time shifts were measured relative to profiles that had a DP of 500 m amsl. Alignment of all seismic reflections between two profiles was not always perfect and some mis-ties remained (see next paragraph). An average TWT shift was thus determined for each seismic survey (see Table 3.2).
2) For profiles that had no connection to the rest of the data set, the time shift necessary to adjust them to 500 m amsl was evaluated with another technique. The elevation difference between the local DP and 500 m amsl was converted to TWT using a seismic replacement velocity. The replacement velocity was derived from nearby well data or from velocities used for static corrections during processing. This was in particular the case for the surveys of Canton Geneva (DP = 300 m amsl) that are not seismically tied to other surveys in the SMB. Although this method could have been used for all seismic surveys throughout the basin, we felt that correct replacement velocities were not adequately available.

3.2.5 Correction of mis-ties between the interpreted seismic horizons

Adjusting the seismic profiles to the same DP does not completely eliminate TWT offsets between the interpreted seismic reflections of corresponding horizons (the so-called mis-ties, see Figure 3.8). This can also be the case between seismic profiles with the same registered DP. Mis-ties can be caused by a number of reasons such as differences in fre-

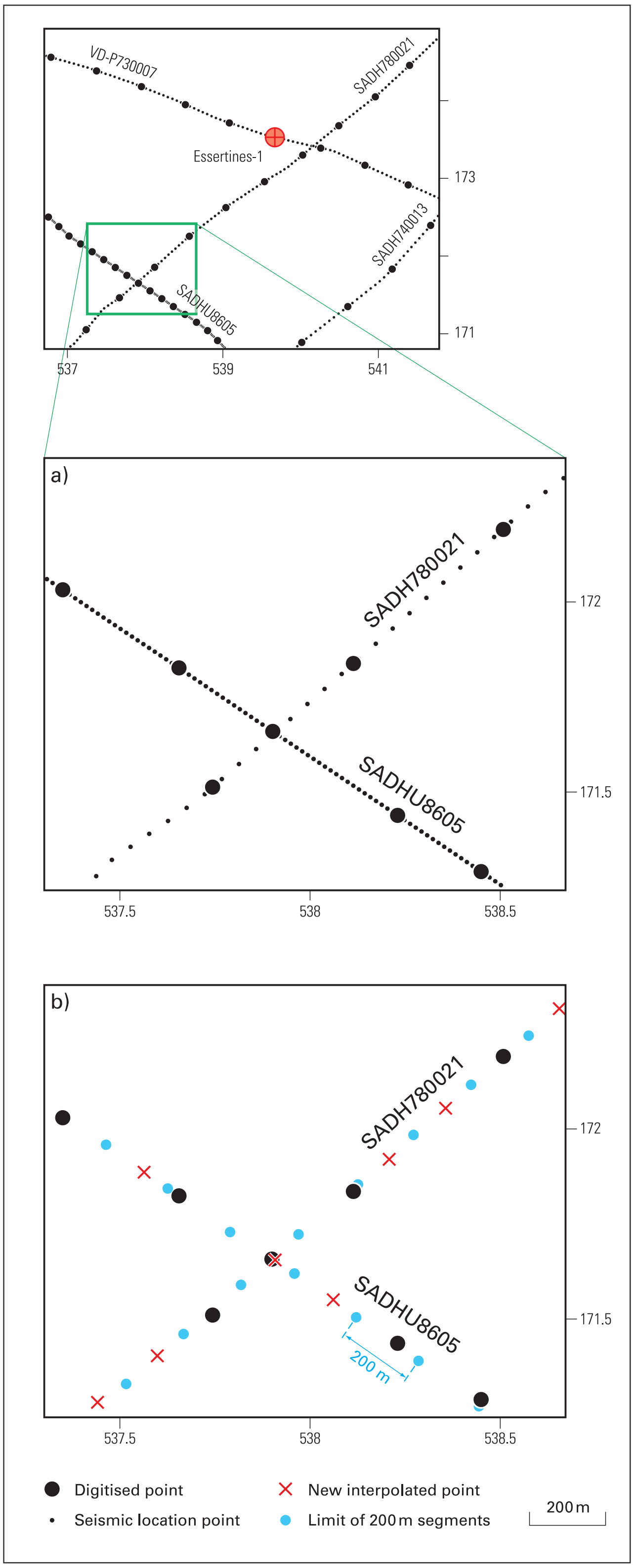

Fig. 3.7: Procedure to homogenise seismic horizon datapoints along profiles in the vicinity of the Essertines-1 well. a) Initial situation: along each profile two series of datapoints coexist in the GIS data base: the irregularly spaced digitised points (large dots) and the regularly spaced seismic location points (SLPs, small dots). b) To reduce the number of data points, the seismic profiles were subdivided into series of 200 m segments. If a 200 m segment included some digitised points, these points were held back. In segments that did not include any digitised point, a new data point was interpolated in the middle of the segment between two nearest digitized points. Finally, all original SLPs were removed. Swiss coordinates are indicated at bottom right sides.

Table 3.2: *Original datum planes of the seismic lines in the SMB and average TWT shifts necessary to adjust them to 500 m amsl (project DP). A positive TWT shift indicates that the shift value had to be added to the TWT of the seismic reflections.*

Seismic survey	Original DP [m amsl]	TWT shift [ms]
BEAG	700	-140
BEAGBE.N (Bern Nord, 1974–1977)	400	+70
BEAGBE.N (Bern Nord, 1978–1985)	700	-140
BEAGBE.S (Bern Sud)	700	-140
FREAG (FR.N, 1974)	400	+80
FR.N (Fribourg Nord, 1981–1985)	400	+80
FR.S (Fribourg Sud)	700	-180
GG and SIG (Genève)	300	+114
LEAG (Luzern)	700	-140
Nagra (1982–84, 1991)	500	0
SADH, PSBR, VD-P, 72-N (Vaud)	500	0
SEAG (East Switzerland)	700	-140
SOTN (Solothurn)	500	0
SEAGLEAG	700	-140

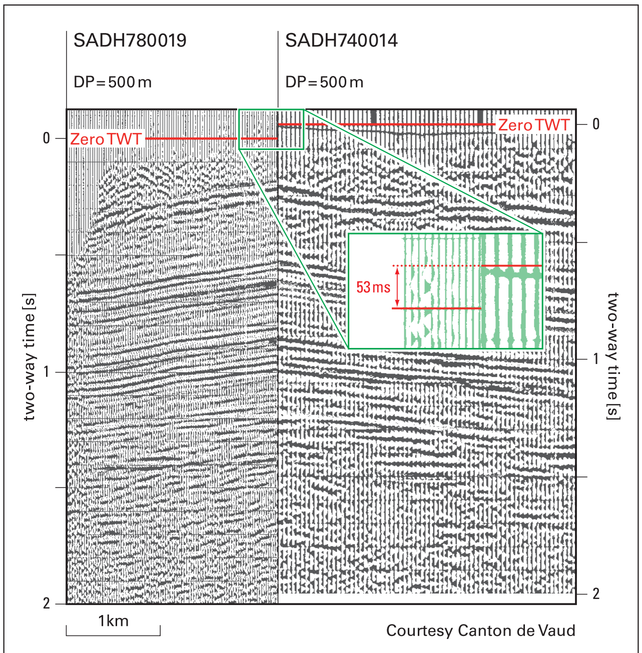

Fig. 3.8: Example of mis-ties between two intersecting seismic profiles. Although both profiles have the same DP of 500 m amsl, an offset of 53 ms is observed between the two zero-time lines (Zero TWT) when profiles are shifted to make corresponding reflections of the two profiles coincide.

quency content and in processing parameters, polarity reversals, 3D effects of dipping reflections, and the combined use of migrated and non-migrated profiles. For the computation of 2D maps, mis-ties must be reduced as much as possible to avoid interpolation problems. In general however, mis-ties cannot be totally eliminated, and a minimisation procedure was carried out in the GIS database by taking all intersections of digitized horizons into account.

Mis-tie values at each seismic profile intersection were averaged over the eight interpreted horizons providing a single average mis-tie value. The mis-tie minimizing process implied shifting all interpreted horizons of a seismic profile simultaneously by the same amount. Interpreted horizons were not shifted individually, nor were they rotated; thus the original relationship between horizons was not altered. Mis-tie corrections were done independently from the ties with wells. We computed mis-ties for profiles that do not intersect but come close to each other (in general less than 500 m).

In a first step, seismic profiles belonging to transects (see paragraph 3.5) were selected as references in the mis-tie calculations because they form a network of interconnected profiles with particularly reliable interpretation, they span the entire Swiss Molasse Basin and most of them are calibrated with wells. The transects thus provided a reference network relative to which all other seismic profiles in the basin were adjusted. They are hereafter referred to as «priority-1 profiles» (see Figure 3.9). Mis-ties among the transect profiles were minimized following a manual procedure in which individual profiles were subjected to small shift (for more details see Appendix 3.1). During subsequent mis-tie corrections these profiles were not shifted any more.

In a second step, seismic profiles not belonging to transects were allocated priorities depending on how they were connected to priority-1 profiles. Profiles intersecting priority-1 profiles were ranked as priority-2, profiles intersecting priority-2 profiles were ranked as priority-3, and so on (see Figure 3.9). A script was developed to automatically apply the following mis-tie minimization process to all profiles in the network. First, each priority-2 profile was individually shifted to the level of the intersecting priority-1 profile. Wherever a priority-2 profile intersected more than one priority-1 profile, it was adjusted until the average mis-tie between all its intersections with priority-1 profiles reaches a minimum (this is equivalent to minimizing the mis-tie sum of squares). The same process was then applied to adjust priority-3 profiles to priority-2 profiles, and so on. Because this automatic procedure occasionally introduced some important mis-ties between seismic profiles of the same priority level, some manual adjustments were made by overriding the priority of seismic profiles. The number of cases for which such adjustments were necessary was, however, minimal and the associated time shifts remained small (for more details see Appendix 3.1). A few profiles not connected to any other one (priority-0 profiles in Figure 3.9) were adjusted manually, after the mis-tie calculations, to the level of the nearest interconnected profiles. Figure 3.10 shows the distribution of mis-tie values before and after mis-tie corrections. A list of time shifts applied to each seismic profile is included in Appendix 3.2.

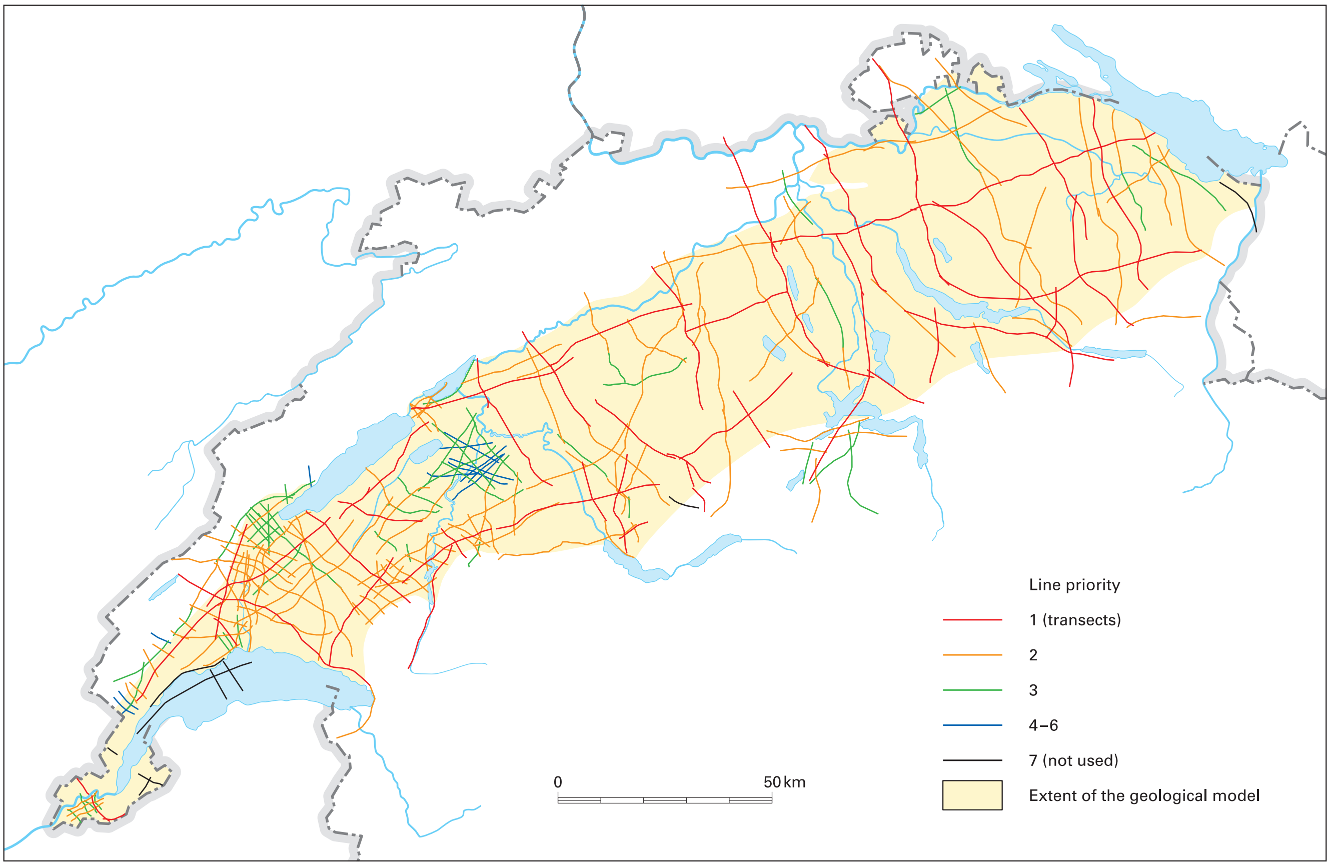

Fig. 3.9: Distribution of the priority levels of the interpreted seismic profiles used in the mis-tie calculation procedure. Seismic profiles compiled in the transects are by definition priority-1 profiles. Seismic profiles not belonging to transects were given priorities depending on how they were connected to priority-1 profiles. Profiles intersecting priority-1 profiles were ranked as priority-2, profiles intersecting priority-2 profiles were ranked priority-3, and so on.

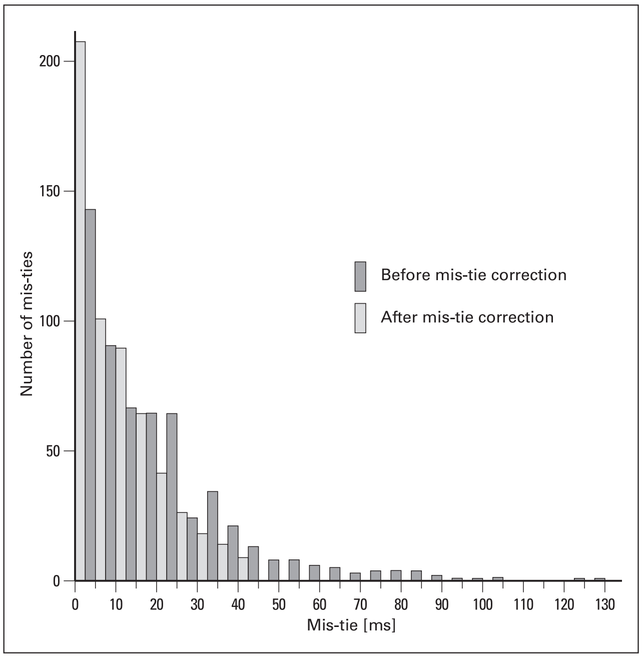

Fig. 3.10: Number of seismic line intersections relative to mis-tie values before and after mis-tie correction procedure. The average mis-tie was 18.1 ms and 12.2 ms respectively before and after correction.

3.3 Velocities within stratigraphic units from well data

We calculated seismic velocities within stratigraphic units from the well TZ-curves and if necessary completed them with typical values from published data or by graphical interpolation. TZ-curves provided the stratigraphic unit thickness and one-way time difference between each boundary from which velocities were calculated (see Figure 3.5). In the first (top) unit (Cenozoic), the velocity was calculated relative to 500 m amsl (see Figure 3.6). Velocity calculations for all used wells are shown in Appendix 2.5.

TZ-curves, however, do not always provide accurate interval velocity information, especially if the stratigraphic unit is very thin (this is for example the case for the Liassic unit in the southern part of the SMB), if data along the TZ-curve were measured at depths far from the formation boundaries or if the formation is not completely drilled. In such cases, velocities were estimated from interval velocity versus depth diagrams that resulted from the compilation of all available P-wave velocity data for a specific unit (see Figure 3.11). Appendix 3.3 shows velocity compilations for each interpreted formation in the Swiss Molasse Basin as derived from well data.

3.4 Calculation of horizon maps

To obtain a continuous data distribution across the entire SMB, we interpolated TWT grids from the interpreted seismic profiles for each interpreted seismic horizon over the entire extent of the SMB. We constructed these grids as an array of data points that define a surface with regular spacing in the X and Y directions. Subsequently, the interpolated TWT grids were converted to depth using interval velocities. Because velocities within units vary laterally, velocity grids were constructed for each interpreted formation over the entire basin. Finally, vertical thickness grids of the different units were computed from the depth grids. TWT, velocity, depth and vertical-thickness grids were graphically displayed on maps with isolines indicating map values.

A procedure sometimes used to derive depth maps consisted in shifting the seismic horizons until their depths exactly coincide with formation boundaries at well locations (see for example SPRECHER & MÜLLER 1986, DIEBOLD et al. 1991). This procedure requires local shifting or sometimes distorting seismic horizons around the well locations in a way that cannot be reconstructed easily and that does not necessarily have geological justification. We refrained from applying this procedure to retain the original recorded geometry of the horizons. Consequently, discrepancies between depth-converted seismic horizons and depths of corresponding formation boundaries at well locations may occur and must be addressed on an individual basis. They may depend on a number of factors such as the presence of faults that offset the seismic reflections near the well but that are not documented by the seismic data, or by lateral velocity variations near the well. Uncertainties resulting from misfits between depth-converted seismic reflections and formation boundaries in wells are discussed in paragraph 3.6.

3.4.1 TWT horizon map calculation

Two-way traveltime (TWT) data from the interpreted seismic profiles were interpolated to 100 x 100 m grids (i.e. an array of data points with 100 m spacing in the X and Y directions that defines a surface). Computations were carried out with the ArcGIS 9.3 software (ESRI Inc.) using a spline interpolation algorithm, a mathematical function that minimizes overall surface curvature.

In order to account for important faults or fault zones affecting the interpreted seismic horizons, the spline interpolator allowed us introducing discontinuities or breaks in the interpolated grids. These discontinuities, referred to as «barriers» in the ArcGIS terminology, are introduced as linear features that prevent data located on one side of the barrier to be used in the interpolation of data on the other side (and vice versa). In this procedure, the calculated minimum curvature surface honours both the input data points and the barrier discontinuities (see e.g. ZORASTER, 2003).

In our interpolations, we used large faults or faults observed on several adjacent profiles and assumed to belong to the same fault zone, as «barrier» features. Dipping or curved faults could not be exactly represented. Instead, such faults were replaced by a several vertical segments (see Figure 3.12). The accuracy with which faults are defined does not justify introducing a barrier for each horizon, and therefore the same «barrier» features were sometimes used for con-

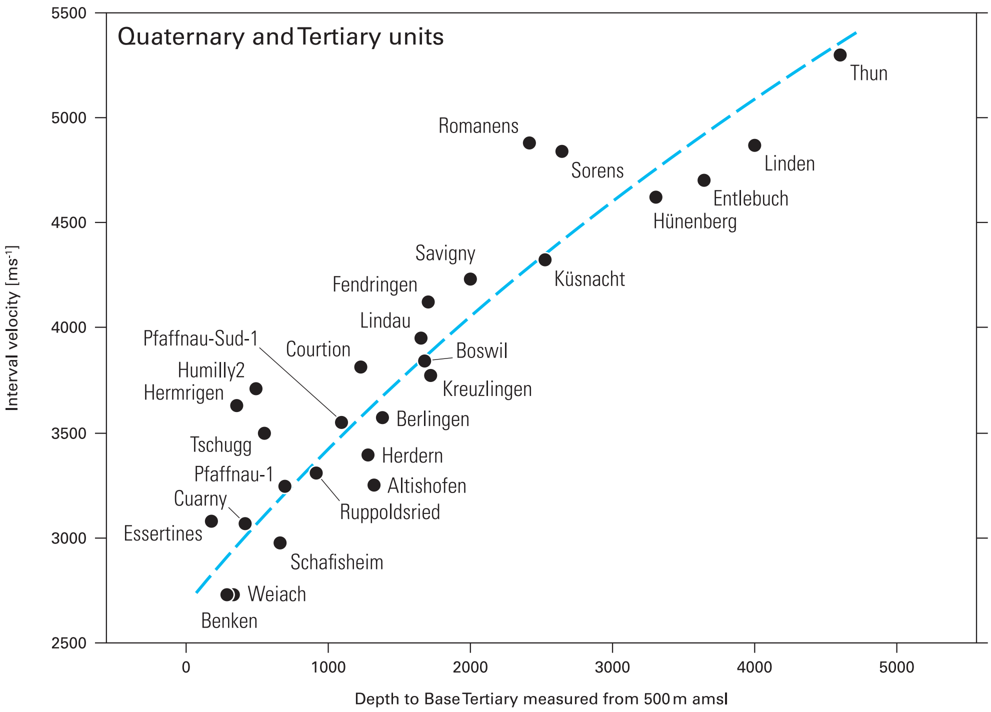

Fig. 3.11: Interval-velocity-versus-depth diagram for the combined Quaternary and Tertiary units. Velocities are derived from TZ-curves in wells in the SMB. The dashed line indicates a general velocity trend with depth. It was traced manually, and it does not represent some calculated average. Such diagrams were used to estimate interval velocities in wells without, or with poor-quality, velocity information. Diagrams for all interpreted units in the SMB are shown in Appendix 3.3.

secutive horizons. The barrier locations are shown on Enclosure 21. Note that faults that are small and isolated, and therefore do not correspond to a major horizon offset, were not used as «barrier» features. As a result, the interpolated surfaces sometimes show small undulations in the vicinity of such faults.

After this first-pass interpolation of the TWT data, we used the seismic horizons of the profiles included in the transects and subjected to a more in-depth interpretation (see paragraph 3.5) in a second-pass interpolation. These horizons were digitized and re-introduced in the larger data set that was then re-interpolated.

Machine interpolation may introduce artefacts in grid values due to under- and overshooting effects, mainly due to insufficient data density (see Figure 3.13). To compensate for this effect, we smoothed the grid values. We used a routine that assigns to each data point the average value of the surrounding points within a 3 km radius. The smoothing radius was selected such that artefacts were almost completely removed. Of course, this process tends to smooth out the surface discontinuities resulting from the introduction of barriers as described above. The TWT surface maps for the eight interpreted horizons are shown in Enclosure 17; their geologic content is discussed in chapter 5.

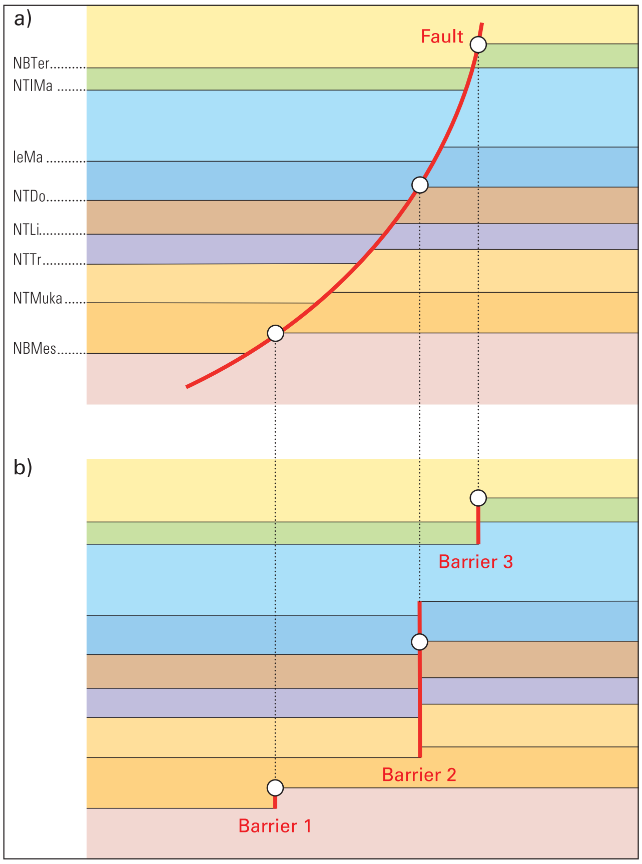

Fig. 3.12: a) Schematic view of a curved fault on an interpreted seismic profile offsetting the interpreted seismic horizons. b) During interpolation of the interpreted horizons and grid-surface calculations, the curved fault is replaced by a series of vertical breaks, called «barriers». Grid points on one side of the barrier are interpolated independently from grid points on the other side of the barrier allowing for a break in the grid. The segment fault offsetting the NBTer horizon and the one offseting the NTlMa horizon are combined into the same barrier. In the same way, fault segments offsetting the IeMa, NTDo, NTLi, NTTr and NTMuka horizons are regrouped. The barrier in the NBMes horizon is the deepest. This grouping of faults is justified by the limited accuracy with which a fault location is defined on the seismic profile. The horizon to which each barrier is associated is indicated with a white circle.

3.4.2 Velocity map calculation

Velocity maps were calculated using interval velocity data at well locations plus some constraint points at additional locations. Constraint points were necessary to enable realistic extrapolation of the gridded surface into areas with no data. They were mostly set at a few locations at the edge of the basin in areas not controlled by any existing well. Velocities at constraint points were either estimated from TZ-curves in wells or from velocity-versus-depth plots (see Figure 3.11 and Appendix 3.3). In the southern part of the basin, velocities at constraint points were taken from values determined by laboratory measurements on Alpine rock samples (Wagner et al. 1999).

The velocity grids were computed using the «thin-plate» spline algorithm available from the ArcGIS Geostatistical analyst extension. The procedure is based on a statistical cross-validation technique to determine optimal calculation parameters. It uses an exact interpolation technique (radial basis functions), meaning that the calculated surface goes through each data point. As for the TWT maps, interpolated velocity grids were produced with a 100 m spacing. Note that since the velocity information provided by the wells is spatially sparse, interpolation between data points (well locations) cannot provide a detailed image of lateral velocity variations. Thus, the interpolated grids provide general velocity trends within the Swiss Molasse Basin. The velocity maps are shown in Enclosure 18.

3.4.3 Calculation of horizon depth and vertical thickness maps

Horizon depth maps were computed by combining TWT and velocities grids in a top-to-bottom approach (see Figure 3.14). First, the depth value of the Near Base Tertiary horizon was computed from 500 m amsl. Each subsequent horizon depth was then computed by adding its thickness to the previous horizon's depth. The depth maps of the interpreted horizons are shown in Enclosure 19; depths are given from 500 m amsl. At any given location, the depth between the horizon and the surface topography can easily be inferred. If the local elevation is higher than 500 m, the horizon depth is calculated by adding to the depth map value the difference between 500 m and the local elevation; if the local elevation is less that 500 m, the difference between 500 m and the local elevation is subtracted from the map value.

Vertical thickness maps within units were computed by taking the difference between the depth values of two consecutive horizons. They were calculated for the following eight units: Cenozoic, Cretaceous, Late Malm, Early Malm, Dogger, Liassic, Late Triassic, and Early Triassic (see Enclosure 20). Strictly speaking, vertical thickness maps are not

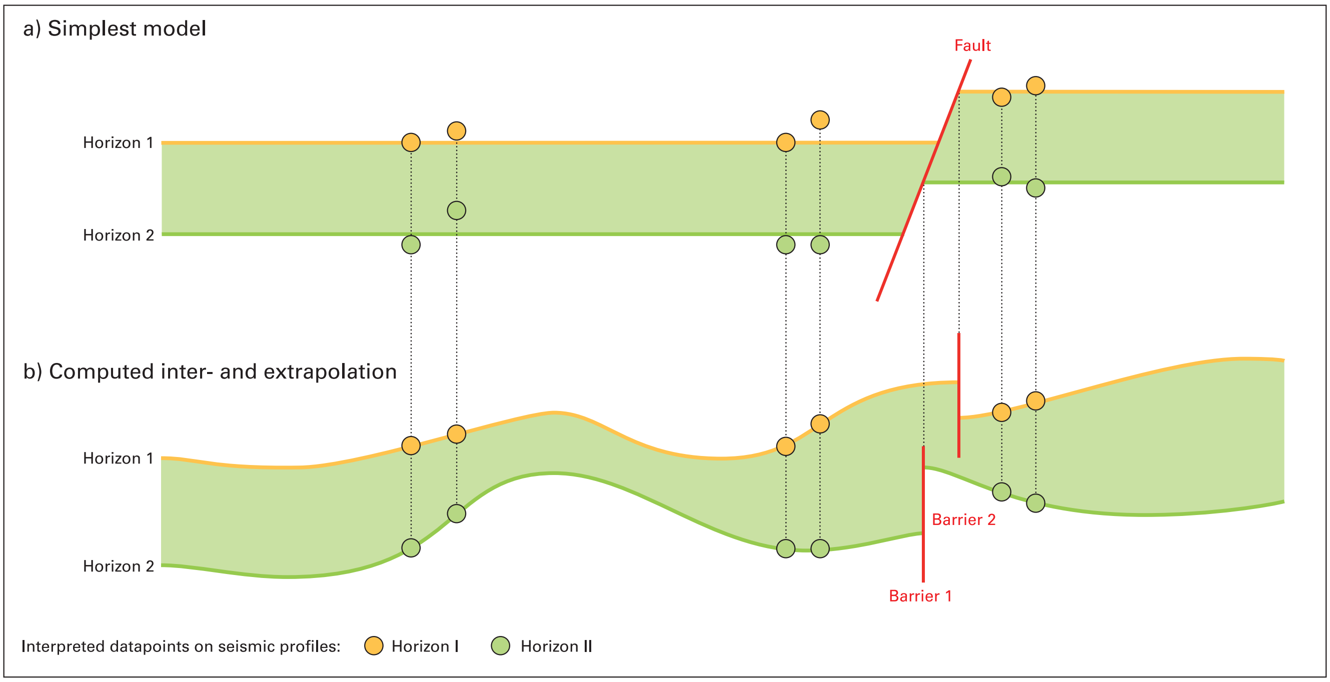

Fig. 3.13: Schematic comparison between (a) a simple horizontal datapoint interpolation and (b) a more elaborate computed data interpolation. In this process, faults are allowed. The green and blue dots indicate digitised datapoints from the seismic horizons, and the green and blue lines are the corresponding interpolated and extrapolated horizons. In case (b), computation results are influenced by small data variations causing under- and overshooting effects. In the vicinity of faults (represented by vertical «barriers» in our computations, see text and Figure 3.12), similar effects may occur. To minimize such effects the computed horizon surfaces were smoothed.

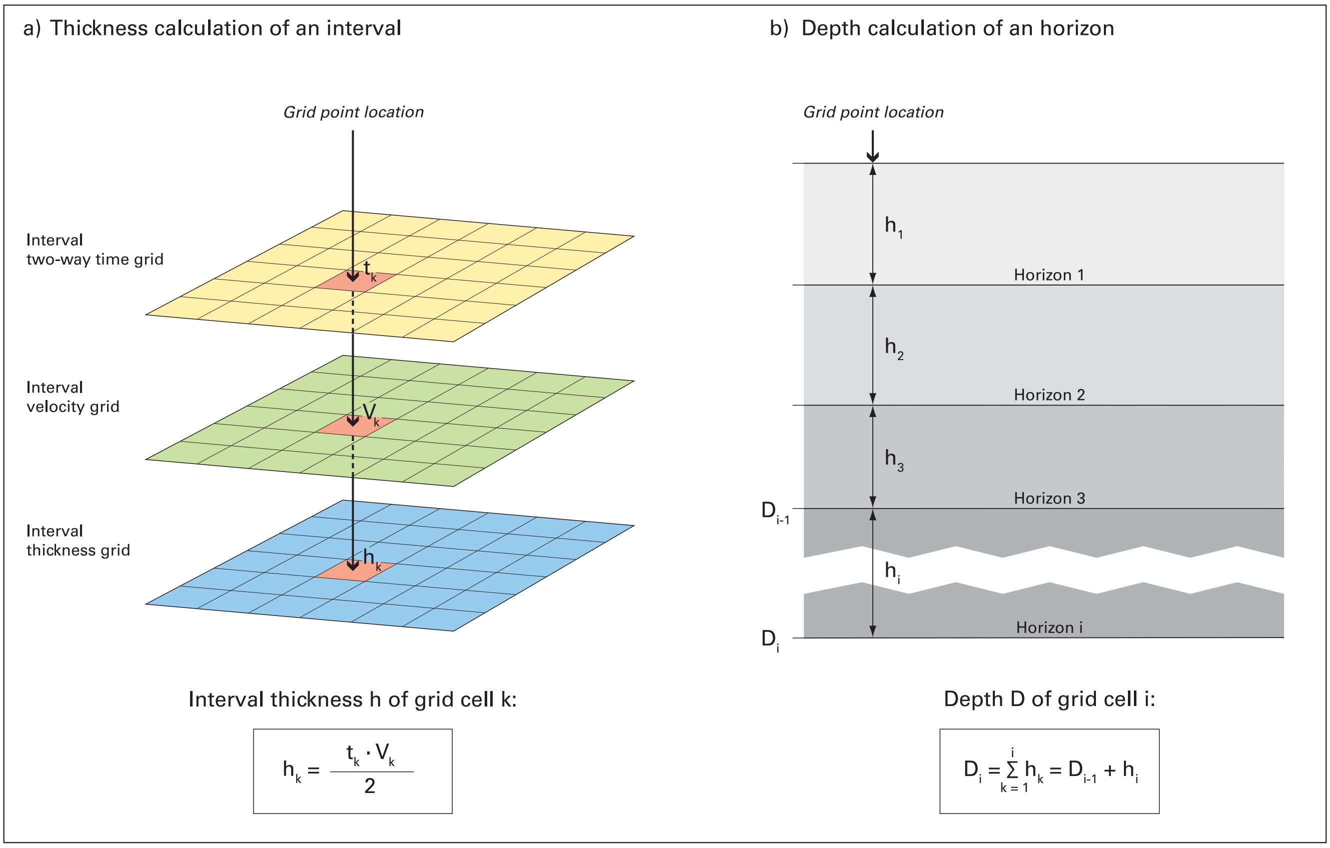

Fig. 3.14: a) Calculation of stratigraphic unit thickness at a grid point. The half-TWT value between two horizons t_k is multiplied by the velocity value V_k at the same location (half-TWT between 500 m amsl and Base Tertiary for the first horizon), and the resulting thickness h_k is stored in new (interval thickness) grid. The same calculations are repeated for all grid points. b) Calculation of depth surfaces of the interpreted horizons. For a given grid point, depth D_i of horizon «i» is computed by adding the thickness of all units situated above that particular horizon.

isopach maps because thicknesses are not measured perpendicularly to the bedding plane but vertically. A vertical thickness corresponds to an isopach value where layers are horizontal. Where layers are dipping, the vertical thickness exceeds the real isopach value. Uncertainties in the maps are discussed in paragraph 3.6.3; the geological map content is discussed in chapter 5.

3.5 Transect interpretation

3.5.1 Transects

To illustrate the 3D structure of the Swiss Molasse Basin we constructed a series of transects using interconnected seismic profiles crossing the Swiss Molasse Basin in the dip and strike directions. To realise this we performed a more in-depth interpretation of the 1248 km of seismic profiles that are part of the transects using more elaborate principles taking data quality into account. In addition, the uncertainty of the horizons in TWT and in depth was quantitatively assessed. The transects are also a means of presenting a significant part of the data sets (seismic and well). The transect enclosures (Enclosures 03 to 15) include non-interpreted seismic profiles (top section), interpreted seismic profiles together with some nearby wells (central section), and finally a depth-converted seismic interpretation that includes additional geological data and some conceptual elements (bottom section). The transects are described in details in chapter 4, whereas the principles followed for their seismic and geologic interpretation are described below.

Seismic reflections were differentiated into three quality classes and faults in two quality classes. Identical criteria apply to the Cenozoic and Mesozoic units, whereas different quality classes are defined for the pre-Mesozoic rocks because of the generally poorer quality of the seismic data in this unit. The definition of the quality classes rely on criteria that enable the interpreter to make some objective judgement on the data quality and therefore on the degree of confidence that one can have in the interpreted reflections. Finally, absolute and relative errors of the TWT interpretation of the seismic profiles and of the depth-converted profiles were estimated. A geological model is the result of a compilation of several types of data of variable certainty and information quality, and it is important to know the quality of the data in order to judge the reliability of the overall model and of specific model features. Thus the transect interpretation relies on clearly identified seismic information, well information, and additional geological information. To each of these features a quality class is associated and error estimates of the reflections are provided.

3.5.2 Quality classes for seismically derived features in the Cenozoic and Mesozoic units

a) Seismic reflections

The quality classes of the seismic reflections in the central and bottom sections in the Cenozoic and the Mesozoic units are defined in Table 3.3. Quality classes rely on two

Tables 3.3: *Definition of quality classes for the interpretation in transects of (a) seismic reflections and (b) horizons not based on seismic data in the Cenozoic and Mesozoic units.*

a) Seismic reflections		
Reflection quality on interpreted seismic profiles	Certainty of geological identification	Reflection quality (quality class) 1: well defined 2: fairly well defined 3: poorly defined
Good	Clear	1
Good	Uncertain but likely	2
Medium	Clear	2
Weak	Clear	2
Weak	Uncertain but likely	3
Weak	Uncertain or no identification	3

b) Horizons in the geological interpretation (not based on seismic data)		
Horizon based on	Certainty of geological identification	Horizon quality class 1: well defined 2: fairly well defined
Geological observations	Surface exposure	1
Geological observations	Borehole	1
Geologically inferred	Regional geological concept	2
Published data	Geological publication	2

factors. Firstly, the visual quality of the reflections are defined as good, medium or weak according to their amplitude strength, signal shape, signal to noise ratio, etc (see first column in Table 3.3a). Secondly, the certainty of the stratigraphic identification of the reflection is assessed (see second column in Table 3.3a). This depends on whether or not the considered reflection makes sense together with the surrounding reflections, i.e. if it can be linked to them in a meaningful way. According to the combinations of these two factors a seismic reflection is defined as quality class one (well defined), two (fairly well defined) or three (poorly defined). Each class is displayed on transects with a different symbol (see chapter 4).

b) Horizons

The bottom section, i.e. the-depth converted seismic interpretation, includes geological information or conceptual reasoning that justify defining a horizon that extends observed seismic reflections (first column in Table 3.3b). Certainty of the geological information depends on whether it is provided by surface geology and borehole data or if it relies on a geological concept or some geological publication (see second column in Table 3.3b). Depending on the combination of these factors, horizons are set in quality class one (well defined) or two (fairly well defined). These are displayed on transects with a colour different from the observed seismic reflections (see chapter 4).

c) Faults

Similarly to observed seismic reflections and geologically derived horizons, faults can be derived from seismic observations or they can be based on other considerations. Seismically identified faults are either observed or inferred (see first column in Table 3.4a). The type of information used to define a fault depends on the nature and the quality of the seismic reflections (see second column in Table 3.4a). This requires careful examination of the reflections considering their previously assessed quality class. Only two quality classes were set for seismically derived faults: well defined or poorly defined.

In the depth-converted seismic interpretation (bottom section), additional faults were introduced based on information other than seismic data. Faults can be observed or they can be geologically inferred or derived from published papers (see first column in Table 3.4b). Décollement zones and major faults also fall in this category since they are not directly observed in seismic data. The second factor to assess the quality of faults not determined seismically is information that originates either from surface or borehole observation or from some geological concept (see second column in Table 3.4b). Features that we have determined in this way are labelled «conceptual». As for seismically derived faults, two classes of such faults are defined, well defined and poorly defined. The two types of faults are displayed with a different colour code on the bottom section of transects.

3.5.3 Quality classes for seismically derived features in the pre-Mesozoic unit

a) Seismic reflections

The reflection quality in the pre-Mesozoic unit is much lower than in the above units, and a different classification was therefore adopted. Individual reflections were not identified, but instead three zones of seismic reflectivity were defined and displayed in the transects: a reflective zone (A), an intermediate zone (B) and a non-reflective zone (C) (see Table 3.5). The different zones tentatively assess the probability of the presence of Permo-Carboniferous rocks in the pre-Mesozoic unit. However, previous works in the Swiss Molasse Basin have shown that seismic reflectivity beneath the Mesozoic unit may occur within crystalline basement (Birkhäuser et al. 2001). Thus in the depth-converted seismic interpretation, zone A is interpreted as possibly containing Permo-Carboniferous sediments, zone B as an uncertain extension of PC-sediments and zone C as presumably containing crystalline basement. The interpretation of this last zone assumes that there is no sedimentary accumulation without seismic reflectivity.

Tables 3.4: *Definition of quality classes for the interpretation of tectonic elements (faults) in the Cenozoic, Mesozoic and pre-Mesozoic units in transects. a) Seismically determined faults, b) faults not based on seismic data.*

a) Seismically determined faults		
Fault structure identified as	Based on type of information	Fault quality class 1: well defined 2: poorly defined
Seismically observed	Offset of stack of seismic reflections of class 1	1
Seismically observed	Clear lateral and / or vertical change of reflectivity pattern in well-defined seismic region	1
Inferred	Offset of stack of seismic reflections and horizons of class 2 or 3 only	2
Inferred	Termination of seismic horizons	2
Inferred	Variation of seismic facies (overburden effects excluded)	2
Inferred	Offset of stack of seismic reflections with highest class 3	2

b) Faults in the geological interpretation not based on seismic data		
Fault structure identified as	Based on type of information	Fault quality class 1: well defined 2: poorly defined
Geologically observed	Surface exposure	1
Geologically observed	Borehole	1
Geologically inferred faults and décollement zones	Regional geological concept	2
Published	Geological publication	2

Criteria that define the zones are sometimes associated with additional conditions to either exclude reflections that are not geologically meaningful such as processing artefacts and multiple reflections or to include weak reflections for which additional information is available. When additional well data indicate the presence of Permo-Carboniferous or crystalline rocks in the pre-Mesozoic unit zones are classified as reflective zone (A) or non-reflective zone (C), respectively, in the depth-converted seismic interpretation.

b) Faults

Fault classification in the pre-Mesozoic unit is identical to the one for the Cenozoic and Mesozoic units. However,

Table 3.5: *Definition of reflectivity zones for the interpretation of the pre-Mesozoic unit in the Transects..*

Observed reflections on seismic profiles	Additional conditions	Reflectivity zone A: reflective B: intermediate C: unreflective
Strong reflections, tested to be PC in a well	–	A
Structural extension of reflections with tested PC in a well		
Continuous reflection from a well on intersecting line		
Similar reflection characteristics as in well controlled basin	Probable multiples excluded (dip angles of reflection make it independent marker), artifacts excluded, (e.g. on ends of profiles, or migration smiles), reflections must have a plausible geometry for a sedimentary basin.	A
Angular unconformity with Base Mesozoic horizon		
Series of reflections with identical dip		
Series of reflections that are terminated by faulting		
Weak reflections that could be extensions of tested PC reflections	In the vicinity of a well	B
Angular unconformity with Base Mesozoic horizon	Short segment only	B
Series of weak reflections with identical dip	Multiples excluded, plausible geometry for sedimentary basin fill, unconformities (dip angles of reflection make it independent marker). Doubtful reflection quality.	B
Series of reflections that are terminated by faulting		
Absence of all above criteria	Above conditions not fulfilled	C

because individual seismic reflections in the pre-Mesozoic unit are not classified, the fault classification relies only on the presence of more or less clear reflections. This is consequent with the fault definition of the Cenozoic and Mesozoic units for class 2 faults only.

3.5.4 Extraction of digitized TWT and depth-converted reflections from the GIS database for the transect interpretation

The interpretation of the seismic profiles along transects was first controlled by extracting the TWT of the interpreted horizons from the GIS database along the transect tracks and by superimposing them on the seismic profiles. Then the criteria described in paragraph 3.5.1 to paragraph 3.5.3 were applied. Occasionally, some digitized reflections were adjusted to better fit the data, most of these changes affected interpreted faults. Attributing quality classes to reflections had consequences on the definition of faults. In the Tertiary unit, no reflection had originally been interpreted because they are generally discontinuous and could not systematically be followed from one seismic profile to another, and a detailed interpretation of this unit was out of the scope of the project. However, for the transects we interpreted some particularly strong and well-defined reflections in the Tertiary unit (Top UMM, base and Top OMM, Intra USM) for clarification of the overall unit structure.

Depth-converted interpreted horizons within the Mesozoic units were extracted from the GIS database along the transect tracks. They were then slightly adapted to correspond to changes introduced in the interpretation of the transect seismic profiles in TWT. Depth conversion of interpreted horizons and faults within the Cenozoic unit was done with a constant velocity of 3.5 kms^{-1}; reflectivity zones within the pre-Mesozoic units were depth-converted with a velocity of 5 kms^{-1}. Although velocity variations within these units are known to occur, especially within the Cenozoic unit (see Figure 3.11), a detailed velocity analysis exceeded the scope of this project.

3.6 Data uncertainties

Seismic data, like any other physical measurement, are prone to errors and they have their own limitations that affect data resolution. Seismic processing also affects data quality and thus contributes to further reduce resolution. Ultimately, interpretation of seismic data may also be affected by errors. Together these successive steps contribute to uncertainties that are intrinsically linked to the data and that should be quantified as much as possible. In the following we discuss data limitations and quantitatively estimate main sources of errors with special attention to the transects.

3.6.1 Main sources of errors

Table 3.6 gives some insights into the possible interpretation errors in the seismic method in general and in this project in particular. It is a non-exhaustive list of items for which quantitative estimates of uncertainties involved in the seismic interpretation are provided. Table 3.6a provides

Table 3.6a: *Uncertainty estimates for well data interpretation.*

Data-related uncertainties	Operation, calculation, method	Estimated maximum uncertainty	Estimated average uncertainty		Remarks
		[m] or [m/s]	[m/s] or [ms]	[m]	
Well-data interpretation	Determination of stratigraphic boundary	100 m	–	1–5	Correlation of various log curves with cuttings or core analysis
Well-data interpretation	Interpretation of stratigraphic unit	–	–	–	Although errors in the stratigraphic interpretation are possible, an accuracy value cannot be estimated
Well-data interpretation	Depth-conversion of stratigraphic boundaries in well to TWT	–	10–30 ms	10–50	
Velocity in stratigraphic unit	Calculation from TZ-curves	500 m/s	0–500 m/s	–	May include interpolation along the TZ-curve when the depth at which the OWT was measured did not correspond to the depth of an interpreted stratigraphic boundary
Velocity in stratigraphic unit	Definition of replacement velocity	–	50 m/s	50	Only applies when 0 level of TZ-curve is below 500 m amsl

Table 3.6b: *Uncertainty estimates for seismic data interpretation.*

Data-related uncertainties	Operation, calculation, method	Estimated maximum uncertainty	Estimated average uncertainty		Remarks
		[m] or [m/s]	[ms]	[m]	
Seismic profile interpretation	Seismic line positioning in GIS	–	–	20–500	Depends on error on the seismic location map (see Chap. 2). Horizontal error will translate into vertical (TWT) error for dipping reflectors
Seismic profile interpretation	Well to seismic tie	–	0–150	0–300	See chapter 3.2.2
Seismic profile interpretation	Seismic data processing	–	5–20	10–40	Due to unknown processing parameters such as replacement velocity for DP adjustment or static corrections
Seismic profile interpretation	Signal polarity	–	10–20	50	On many old profiles signal polarity is not reported
Seismic profile interpretation	Reflection picking	–	10	20	For low signal frequencies (e.g. 25–30 Hz) the exact TWT of reflection onset is not accurately picked.
Seismic profile interpretation	Skipping of a reflection period	–	10–20	50	Interpreter error
Seismic profile interpretation	Horizon following	600 m	100	250	Following a horizon relies on signal-to-noise ratio. It can be very difficult on poor quality profiles as well as in tectonized zones.
Seismic profile interpretation	Distortion of the paper seismic profile	–	20	40	Due to photocopying and paper shrinking / paper expansion
Seismic profile interpretation	Accuracy of hand drawing on seismic profile and transferring to transparency	–	10–20	50	–
Mis-tie reduction	Correcting mis-ties between seismic lines	94.5 ms * 40 ms **	12 * 8.4 **	100	Maximum corrections were distributed along the boundaries of the seismic line grid, away from calibrated data near the basin axis (see chapter 3.2.5). Depth uncertainties are velocity dependant

* for 519 intersections between seismic profiles
** for 28 intersections between transect profiles only

a list of errors and derived uncertainties related to identifying horizons and deriving the velocities of stratigraphic units in wells. Table 3.6b deals with errors in the interpretation of seismic horizons and their associated uncertainties. The indicated uncertainties are not mathematically calculated, rather they represent reasonable estimates. They are based on observations made during the working process as well as on experience from geophysical data gathering in the field and years of data interpretation. The resulting total uncertainty is not simply the sum of the uncertainties of each individual step. The mathematical propagation rises rapidly beyond reasonable limits. Some constraints come from the internal logic of the data: e.g. stratigraphic horizons do not cross each other nor do they pinch out without geological reason, velocities cannot exceed «reasonable» values, i.e. a range of velocity values known from other sources for the same type of rocks, etc. The next section provides some quantitative estimates of relative and absolute uncertainties in two-way traveltime (TWT) and in depth for the interpreted seismic transects.

3.6.2 Quantitative uncertainty estimate for the transects

a) Well data

The link between seismic horizons and stratigraphic boundaries relies on the identification of the individual unit and its location in the drillhole (Table 3.6a). Boundary depths are assumed to be relatively accurate; they are estimated to be associated with an uncertainty of the order of a few metres. It is very difficult, however, to give a quantitative estimate for the identification of the stratigraphic unit itself. While unit identification is generally likely to be correct, a mis-identification may result in uncertainties of up to hundreds of meters. Uncertainties in velocity calculations within stratigraphic units depend on the availability and accuracy of a TZ-curve down the well. Uncertainties involved in establishing connections between seismic horizons and unit boundaries in wells largely depend on uncertainties in the horizons themselves. In the transects, some apparent discrepancies between horizons and stratigraphic boundaries in wells are observed. They are, however, believed to be mostly due to local geological heterogeneities. For all wells located within 100 m of the transects (Table 3.7) the maximum discrepancy of 32 ms is observed at well Eclépens-1. This well is located above a complex structure with strong lateral variations.

b) Seismic interpretation

The main sources of errors that affect the interpreted seismic horizons are listed in Table 3.6b and the resulting quantitative uncertainties are estimated. Summing all uncertainties in this table would not provide a reasonable uncertainty estimate. For the depth-converted horizons, another cause for uncertainties comes from the fact that migration of the seismic data was not taken into account. If only unmigrated seismic profiles would have been used it would have been appropriate to carry out 3D migration of the two-way traveltime horizon surfaces. The data that were used, however, were a mixture of migrated and unmigrated seismic profiles making such procedure pointless.

Table 3.7: *Maximum TWT offsets observed between the eight interpreted seismic horizons and corresponding stratigraphic boundaries in wells located at distance of 100 m or less for Transects 1 to 15.*

Well name	TWT offset [ms]
Altishofen-1	8
Eclépens-1	32
Hünnenberg-1	~0
Lindau-1	<32
Pfaffnau-1	16
Tschugg-1	~0

One way of estimating interpretation uncertainties involved in this work is to assess them statistically. Our interpretation is based on a large number of seismic profiles that intersect each other (519 intersections in total). Thus, one can assume that the large number of intersections in the mis-tie reduction computations (based on mis-ties between the interpreted seismic horizons, see paragraph 3.2.5) provide some statistical estimate of uncertainties in the seismic data interpretation. After mis-tie reduction, the average mis-tie for the 519 intersections was 12 ms and the largest mis-tie 94.5 ms (see last line of Table 3.6b). These numbers were computed by taking average values over the eight horizons within the seismic profiles; however, some mis-ties between individual horizons reach larger values.

When the only 28 intersections between transects are taken into account, the average mis-tie reduces to 8.4 ms and the maximum mis-tie is 40 ms. This last number is in agreement with the maximum deviations observed between well stratigraphy and interpreted seismic horizons on nearby seismic profiles that belong to a transect (Table 3.7). We therefore estimate a relative uncertainty of 40 ms (or ± 20 ms) in TWT gives and depth uncertainty of 200 m (or ± 100 m, for an average velocity of 5000 ms^{-1} within the Mesozoic strata).

The other intersections (519) between all interpreted profiles may be taken as an expression of the overall absolute TWT and depth uncertainty. Rounding up the maximum TWT value of Table 3.6b (94.5 ms) we obtain a maximum TWT absolute uncertainty of 100 ms (± 50 ms) and a maximum absolute depth uncertainty of 400 m (± 200 m for a velocity of 4000 ms^{-1}, an average velocity for seismic signals travelling through the Cenozoic and Mesozoic strata).

We believe that these estimates are rather pessimistic. They are attempts to estimate uncertainties as the result of a succession of errors in the complex processes involved in the interpretation of seismic data. Larger values may occur locally, for example, due to interpretation errors in areas of poor data quality. The uncertainty estimates, both in two-way traverltime (TWT) and in depth, are indicated on the transects where they are also graphically expressed.

3.6.3 Uncertainties in the TWT, velocity, depth, and vertical thickness maps

The causes for uncertainties in the seismic horizons either in TWT or in depth are of course also valid for the corresponding maps. However, uncertainties in the maps are evidently larger than along the transects for several reasons. First, the maps are constrained only along the seismic profiles, and as mentioned earlier, machine interpolation may create some over- and undershooting effects between them. Secondly, although these effects are largely suppressed by subsequent smoothing, smoothing itself introduces some additional uncertainties. This is the case because the original data points along the seismic horizons are not fixed when they are involved in the averaging calculations. As a result, uncertainties in the maps are expected to be larger than in transects. On depth and vertical thickness maps (see Enlosures 19, 20 and 21), map values and well values are indicated at well locations. Although some isolated large discrepancies may be caused by some local structural anomaly, the difference between the two values provides some insight into the map uncertainties.

4. Deep structure of the Swiss Molasse Basin from seismic transects and well data

We elaborated the deep structure of the Swiss Molasse Basin (SMB) from the interpretation of seismic profiles calibrated with well data within the Cenozoic, Mesozoic, and pre-Mesozoic units. Eight seismic horizons were interpreted and correlated through the entire SMB. The horizons and the faults affecting them were digitized and introduced in a GIS database as explained in chapter 3. Based on a selection of profiles from the interpreted ones (see Figure 2.2), fifteen basin transects were constructed (see Figure 4.1), each of them being composed of several seismic profiles. As explained in chapter 3, the seismic profiles included in transects were interpreted following more rigorous rules than the rest of the seismic data set. Together with the horizon-, velocity- and vertical thickness maps and the well data, the transects build a new 3D geological model that is described in this chapter and in chapter 5.

The transect locations were selected according to several criteria: firstly, the transects together should provide insight into the entire of the SMB based on a more or less regular transect distribution; secondly, the transects should make maximum use of public seismic profiles in order to offer access to a large audience and, finally, the transects should run through or close to as many wells as possible to ensure a good control of the interpretation.

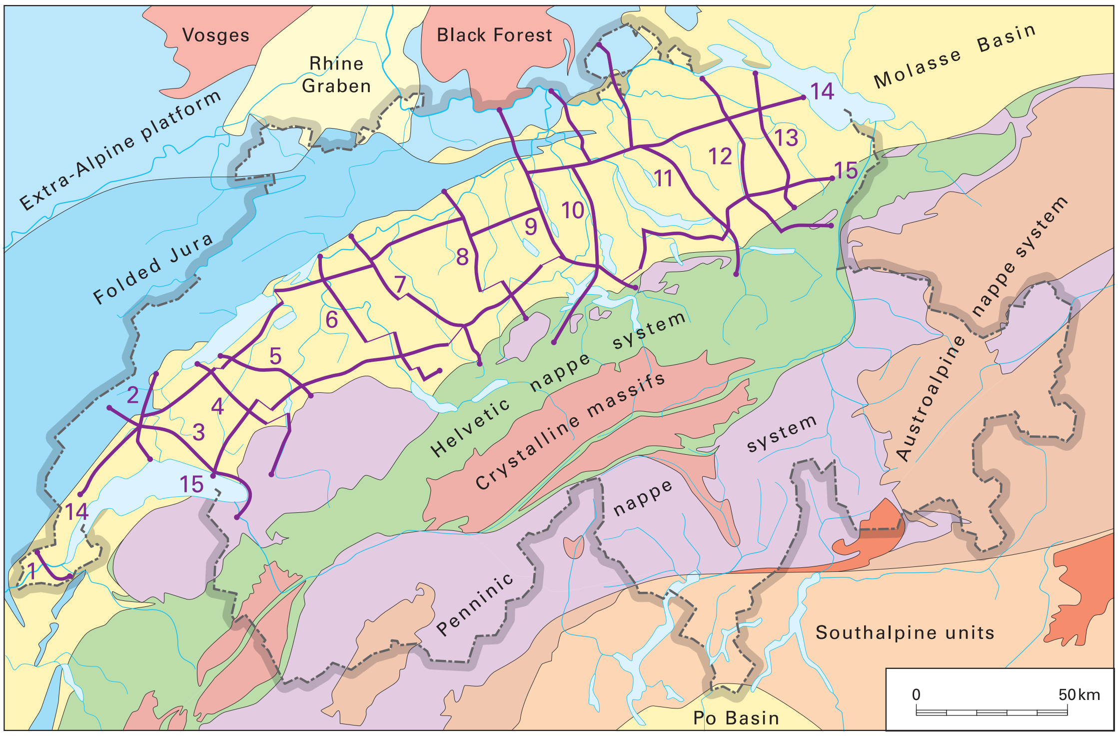

Fig. 4.1: Location map of transects with their respective number and tectonic situation.

4.1 Transect construction and display

Fifteen transects were constructed and are displayed on Enclosures 3 to 15. Thirteen transects are dip sections (1: 80 000 vertical and horizontal scales) that extend from the foot of the Jura Mountains to the Subalpine Molasse (SAM) and the Alpine nappes. The last two transects are strike sections that extend across the SMB from west to east (1: 250 000 horizontal scale and 1: 80 000 vertical scale).

Each transect enclosure includes three sections: un-interpreted seismic profiles on the top section, seismic interpretation superimposed on the seismic data on the central section and, on the bottom section, depth-converted seismic interpretation (see Figure 4.2).

4.1.1 Top section: seismic profile

Seismic profiles or parts of profiles that compose a transect were selected such that together they build an approximately continuous basin cross section. Seismic profiles were oriented such that the transect's left end is located to the north or to the west. For this reason, some profiles that were originally displayed in the opposite direction had to be inverted from left to right. Under each seismic profile, the type of stack (non-migrated or migrated) is indicated.

The profiles were vertically lined up to make the main Mesozoic reflections appear continuous. As a consequence, the different profile DPs (300 m, 400 m, 500 m or 700 m) do not align (Figure 4.3). In transect parts separated by gaps, the seismic profiles were vertically positioned by adjusting their DPs relative to the DPs of the transect profiles flanking them.

SLP annotations on top of the seismic profiles correspond to the ones indicated on Enclosure 2 (for the definition of SLPs, see paragraph 2.2.2). Locations of intersections between the interpreted seismic profiles are indicated on top in blue. If an intersecting profile also belongs to a transect it is indicated in purple.

4.1.2 Central section: seismic interpretation

This section presents the geological seismic interpretation superimposed on the seismic profiles. The seismic interpretation consists of all seismically supported information elements (reflections and faults) in the Cenozoic, Mesozoic, pre-Mesozoic units. This section helps the reader better understand the interpretation and evaluate the quality of the inferred information.

The seismic interpretation of transects was done following the working steps described in chapter 3; this includes defining quality classes for reflections and faults (see paragraph 3.5). Units separated by the seismic horizons interpreted across the entire SMB are coloured. In chapter 5, we will discuss the coloured regions in terms of a 3D geological model. In areas of marginal seismic quality, no colours are shown. These areas are outside of the geological model, and only clearly identifiable reflections are interpreted. The estimated relative and absolute TWT uncertainties of the interpreted reflections are shown as scale bars (for detailed explanations see paragraph 3.6).

The interpreted seismic reflections within Cenozoic and Mesozoic units are set in three quality classes (see paragraph 3.5.2 and Figure 4.4): well defined (quality class 1), fairly well defined (quality class 2) and poorly defined (quality class 3). These are shown respectively as black solid lines, dashed lines and dotted lines. Where seismic reflections are missing, horizons are freely interpolated and indicated as colour boundary only. Within the Tertiary unit, horizons (e.g. near base OMM, intra USM) were interpreted only where there were good reflections.

In the pre-Mesozoic unit, individual reflections are not interpreted because of the much poorer quality of the seismic data, instead types of reflectivity zones were defined (see paragraph 3.5.3): a reflective zone (A), an intermediate zone (B) and a non-reflective zone (C). Inside of the geological model, zone A is shown in light brown, zone B with purple and brow stripes and zone C in purple. Outside of the geological model, zones are defined the same way, but they are shown in grey only: light grey in zone A, with light grey stripes in zone B and dark grey in zone C.

Only two quality classes were defined for faults within the Cenozoic and Mesozoic units (see paragraph 3.5.2): well defined (quality class 1) or poorly defined (quality class 2). These two fault classes are respectively shown in red as solid lines and dashed lines. In areas of marginal seismic quality, only clearly visible faults are interpreted.

The wells used in the interpretation are indicated on the transects. Wells that lie within 4 km from the transect and are distinguished from those that lie further away (Figure 4.4f). The well information was either projected along a direction perpendicular to the seismic profile or parallel to important structural trends. The calibration of the seismic data with wells is described in paragraph 3.2.2 and paragraph 3.3.

4.1.3 Bottom section: depth-converted seismic interpretation (with additional conceptual geological information)

This section displays all seismically defined elements of the central section after depth-conversion using the same quality classification. Additional geological information from other sources is also shown.

Interpreted seismic horizons from Near Base Tertiary to Near Base Mesozoic were converted to depth in the GIS database using appropriate seismic velocities (see paragraph 3.5.4). Graphically, this corresponds to applying a specific stretch factor at each location between the two-way traveltime seismic profile and the depth converted profile. Faults were graphically converted to depth using the same stretch factor at each particular location.

Reflections and faults within the Cenozoic unit were depth-converted using a constant average velocity of 3.5 kms^{-1} (see paragraph 3.5.4). For this reason, we expected shallow features to be deeper than they should (because for this depth range the average velocity is too high) while deep features were expected to be shallower (because for this depth range the average velocity is too low). Thus, depth conversion within the Cenozoic unit is not as accurate as the one used for horizons of the Mesozoic units, and it has an informal character.

Top section:

Seismic profile names

Well information: name, location

Intersecting transects and profiles

Seismic location point numbers

Datum planes

Seismic profiles without intepretation

Used datum planes; courtesy

Central section:

Well stratigraphy in seconds (TWT)

Interpreted seismic horizons

Reflectivity zones

Extent of the geological model

Bottom section:

Tectonic information (swisstopo 2005b)

Geographic information

Well stratigraphy in meters

Interpreted seismic horizons

Reflectivity zones

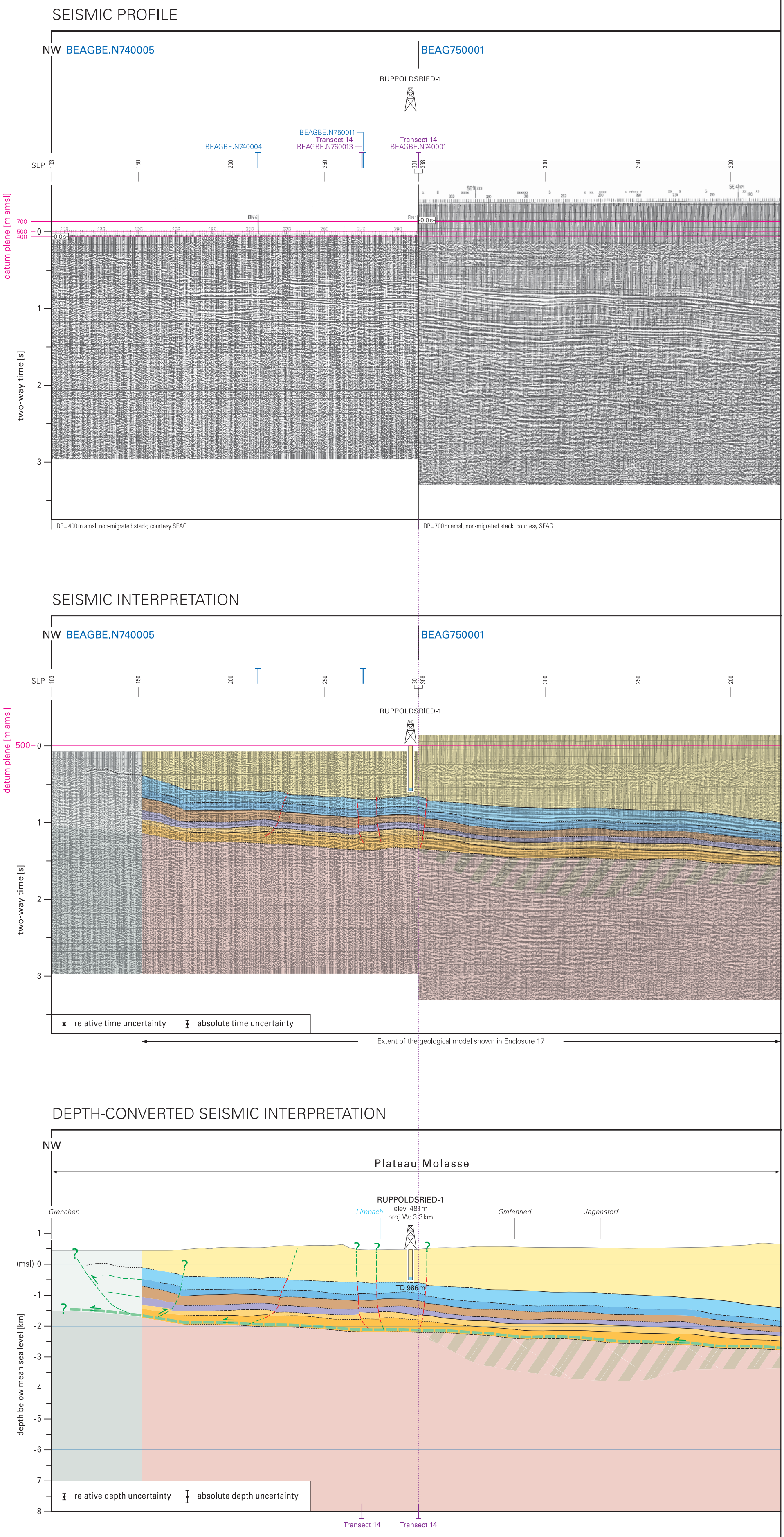

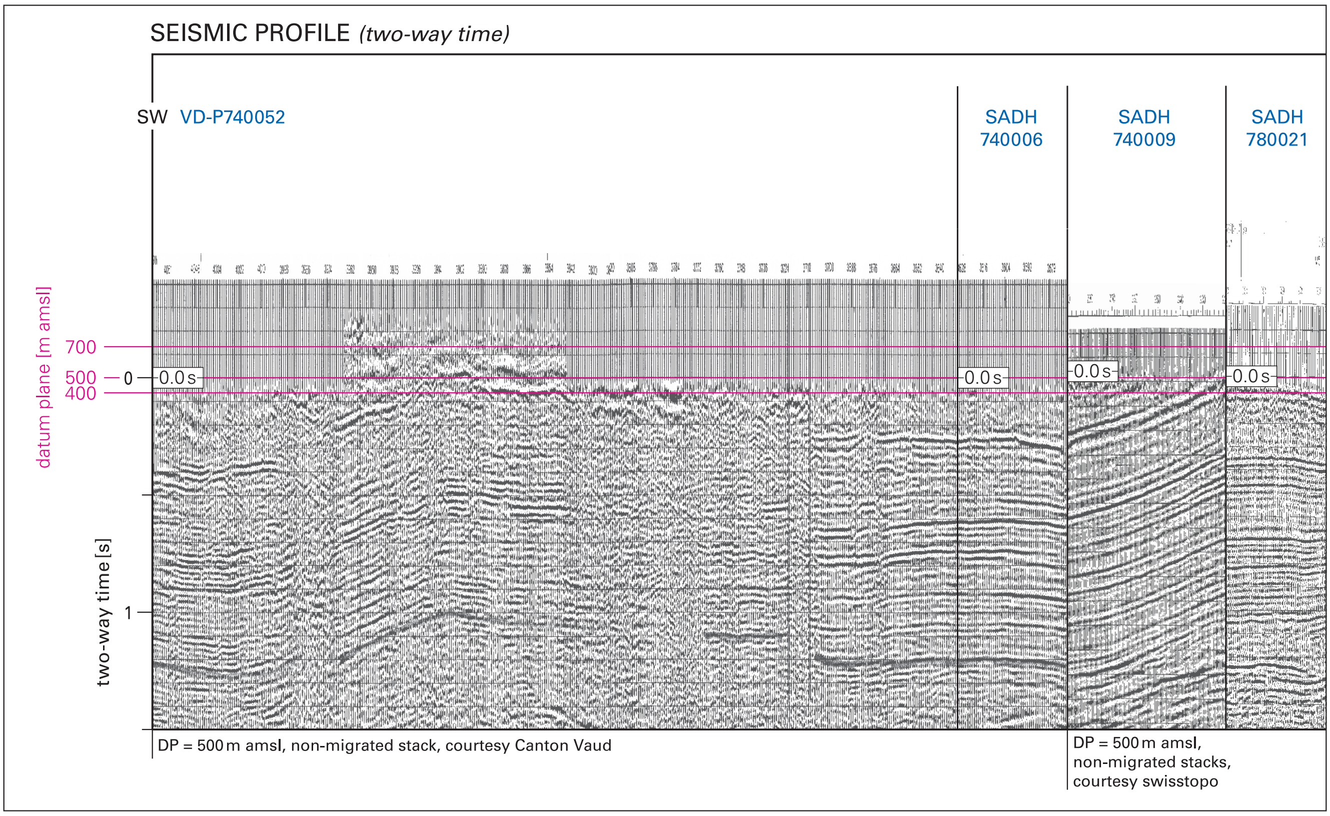

Fig. 4.3: Details of a transect top section (Transect 14). Red lines indicate the DPs of the different seismic profiles in the transect. They are drawn relative to the DP of the first transect profile to the left (in this case 500 m). Two-way time (TWT) differences between the red lines are based on average time offsets between DPs of the different seismic surveys (see Table 3.2). The zero-time of each individual seismic profile is also indicated (0.0 s). On some profiles the zero-time may not exactly align with a DP red line. This is due to mis-ties between seismic profiles. For more information see paragraph 3.2.4 and paragraph 3.2.5.

Reflective zones and faults in the pre-Mesozoic units were depth-converted using a constant velocity of 5 kms^{-1}. Translated to geological terms, these seismic reflectivity zones denote likely or possible presence of Permo-Carboniferous sediments (zone A), uncertain extension of Permo-Carboniferous sediments (zone B) or presumably crystalline basement (zone C).

Conceptual geological information was added to the seismically-defined depth-converted features (see Figure 4.4 e). The information based on outcrops and well data was drawn as solid lines, whereas conceptual elements are displayed as dashed lines. We indicated the increasing importance of conceptual faults by thicker lines.

At the top of the depth-converted section, orientation elements are added such as location names, changes in profile orientation and encountered tectonic units defined at the surface. Geological surface information is taken from the 1:500 000 tectonic map (Swisstopo 2005b) and complemented by information from the 1:25 000 geological maps.

The estimated relative and absolute uncertainties of the depth-converted reflections are shown as scale bars (for detailed explanations see paragraph 3.6).

4.2 Geological description of the seismic transects

The geological interpretation of the 15 transects, representing 1284 km of seismic profiles are described below. From west (Trans. 01) to east (Trans. 13), between the cities of Geneva and Romanshorn, they cross several cantons (see Table 4.1 for abbreviations, Figure 1.2 for location). The two strike sections (Trans. 14 is located to the north of SMB and Trans. 15 to the south) show changes along the basin axis. The transects present the Tertiary sediment accumulation thickening from northwest to southeast in the Swiss foreland basin. The Mesozoic and pre-Mesozoic units are found at maximal depths of 5 – 6 km under the Alpine thrust front.

Fig. 4.2: Example of a transect display (using elements of Transect 7) showing seismic profiles (top section), seismic interpretation (central section) and depth-converted seismic interpretation (bottom section). Explanations of transect content are shown on the left side.

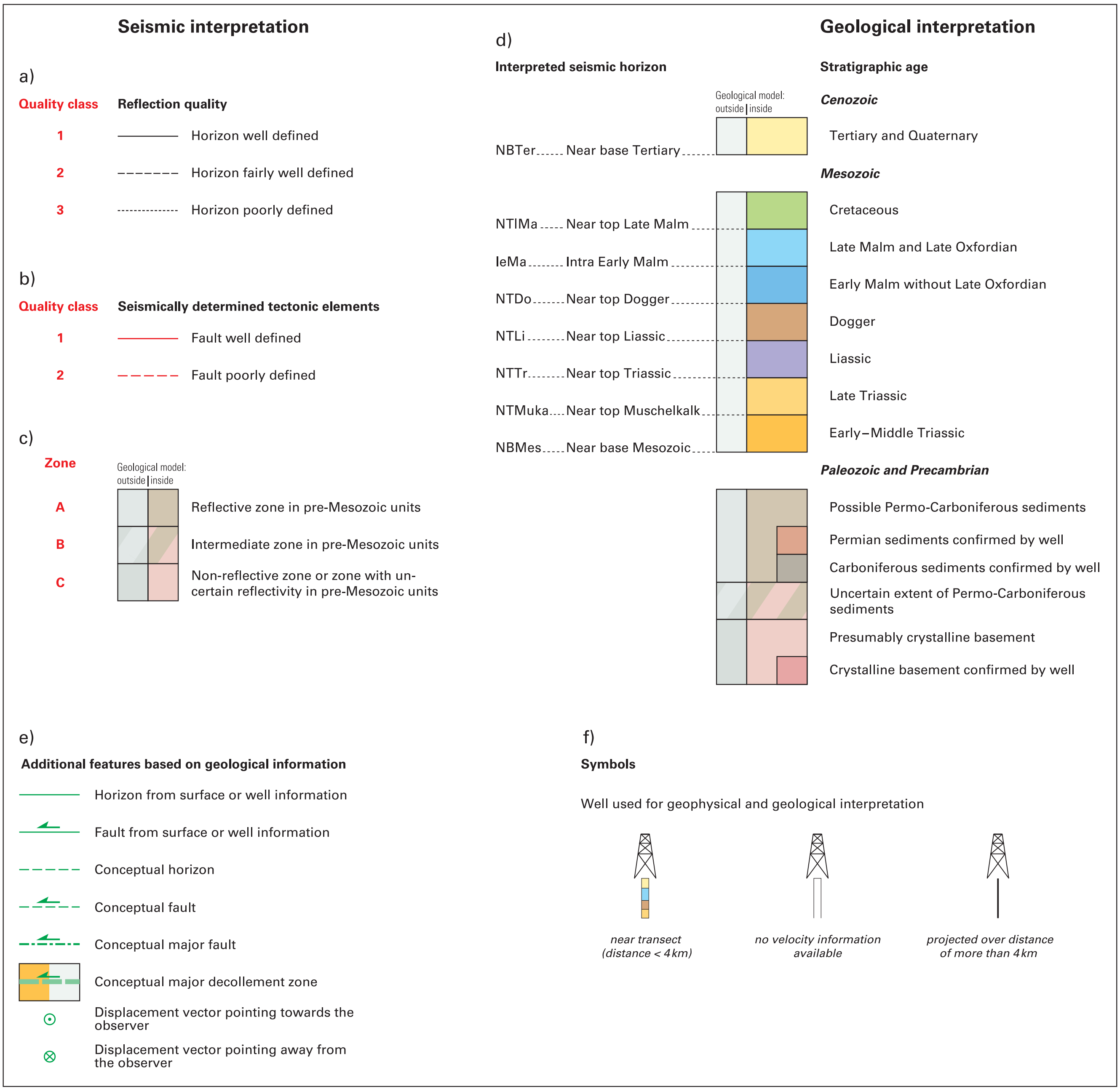

Fig. 4.4: Transect legend. a) Seismic-reflection quality classes and their graphic symbols in the Tertiary and Mesozoic units. b) Quality classes for seismically defined faults and their graphic symbol. c) Seismic-reflectivity zones and their graphic symbols in pre-Mesozoic units. d) Eight interpreted seismic horizons and the Cenozoic and Mesozoic unit boundaries indicated by coloured column e) Conceptual features based on additional geological information. f) Well information, well stratigraphy is shown only for wells that lie within 4 km from transect, wells within the 4 km radius, but for which no velocity information could be obtained are are indicated by open rectangles, wells lying outside of the 4 km radius are indicated by a black solid line. For detailed information about abbreviations of interpreted seismic horizons see Table 3.1 and text.

4.2.1 Transect 01: Genève (Enclosure 03)

This westernmost transect is located in the Plateau Molasse (PM) within the Geneva Basin, between the relief of the Jura Mountains to the north and the Mount Salève fold to the south. It comprises three seismic profiles GG87-2, GG87-4 and GG87-5, acquired as part of the same survey. The first two seismic profiles are perpendicular to the SMB axis and the third one is oriented W–E almost parallel to the basin axis. The length of this transect is 16 km. This transect coincides with part of Figure 5 and Plate 1 of Gorin et al. (1993) and Figure 9 of Signer & Gorin (1995). No direct well control was used in the interpretation of this transect; Humilly-2 and Thônex-1 wells (see Enclosure 16) are located too far from the transect, but they were considered for calibration of the seismic horizons and units. Transect 1 presents horizons with a good lateral continuity and a high reflection quality, mostly in quality classes 1 and 2.

Table 4.1: *Swiss Cantons in French and German with corresponding abbreviation and capital*

Name of Canton in French	Name of Canton in German	Abbr.	Capital
Appenzell Rhodes-Extérieures	Appenzell Inner-Rhoden	AR	Herisau
Appenzell Rhodes-Intérieures	Appenzel Ausser-Rhoden	AI	Appenzell
Argovie	Aargau	AG	Aarau
Bâle-Campagne	BaselLand	BL	Liestal
Bâle-Ville	BaselStadt	BS	Basel
Berne	Bern	BE	Bern
Fribourg	Freiburg	FR	Fribourg
Genève	Genf	GE	Genève
Glaris	Glarus	GL	Glarus
Grisons	Graubünden	GR	Chur
Jura	Jura	JU	Delémont
Lucerne	Luzern	LU	Luzern
Neuchâtel	Neuenburg	NE	Neuchâtel
Nidwald	Nidwalden	NW	Stans
Obwald	Obwalden	OW	Sarnen
Saint-Gall	Sankt Gallen	SG	Sankt Gallen
Schaffhouse	Schaffhausen	SH	Schaffhausen
Schwytz	Schwyz	SZ	Schwyz
Soleure	Solothurn	SO	Solothurn
Tessin	Tessin	TI	Bellinzona
Thurgovie	Thurgau	TG	Frauenfeld
Uri	Uri	UR	Altdorf
Valais	Wallis	VS	Sion
Vaud	Waadt	VD	Lausanne
Zoug	Zug	ZG	Zug
Zurich	Zürich	ZH	Zürich

The Tertiary seismic unit has a wedge shape and presents onlaps toward the north (at the Base Tertiary unconformity) on the underlying thick Lower Cretaceous layers (see Charollais et al. 2007 for a precise description of stratigraphy and thickness). Within the Mesozoic sequence, the Jurassic and Cretaceous strata have an approximately constant thickness and they dip to the south, whereas the thickness of the Middle – Early Triassic seismic unit is variable. South of the village of Choully, the latter thickens showing oblique reflectors that are interpreted as duplex structures.

The section shows steeply dipping, poorly defined faults with minimal apparent reverse or normal movement. These faults are well defined in the Mesozoic outcrops of the Jura Mountains and of Mount Salève with a significant lateral offset, but, as shown on the interpretation, these faults are not clearly visible on the seismic section. For example, the poorly defined Coin tear fault on the eastern part of the GG87-5 profile is oriented NW–SE on the geological map (see Figure 4.5), and it has an important sinistral offset in the Mount Salève. The interpreted faults on the seismic profiles terminate within the Middle Triassic layers within the conceptual major décollement zone. No clear connection with pre-Mesozoic units is observed.

Two separate pre-Mesozoic reflective zones are interpreted at both extremities of the section, and angular unconformities (toplaps) are observed within these zones toward the Base Mesozoic horizon (e.g. north and south of SLP 100 on GG87-2 profile). As already described in Gorin et al. (1993), these reflective zones show in the upper part a less reflective package of presumably Permian clastics and, at deeper level, they give way to high-amplitude facies (presumably coal-bearing Carboniferous sediments). These zones could be interpreted as Permo-Carboniferous half-grabens (see also Gorin et al. 1993, Signer & Gorin 1995). Permo-Carboniferous sediments are present in the Humilly-2 (Enclosure 16) and Faucigny-1 wells (Appendix 2.5).

4.2.2 Transect 02: Orbe – Morges (VD) (Enclosure 03)

Transect 02 is located in Canton Vaud across the Plateau Molasse and includes the first relief of the Folded Jura. It comprises four seismic profiles from three different surveys: VD-P740038, SADH740009, VD-P760057 and VD-P760068. The first three profiles run NNE–SSW and the fourth one is oriented NW–SE, perpendicular to the fold structures of the western SMB. The length of this transect is 31 km. No direct well control was used for the interpretation of this transect. The Treycovagnes-1 and Eclépens-1 wells (see Enclosure 16) are located further than 4 km away from transect, however they were considered for calibration of the horizons and seismic units of the intersecting seismic profiles (see Enclosure 1). Transect 2 mainly presents horizons with good lateral continuity (except to the northern part of the section) and good-quality reflections, mostly of quality classes 1 and 2, except for the Near Base Tertiary horizon that is generally poorly defined. For the interpretation of seismic profile VD-P740038 see also Jordi (1993).

The Tertiary unit, in the southern part of the section, is characterized by a sequence with poor quality reflections. The underlying Cretaceous unit is thinner than in the western area (Geneva basin). The Mesozoic units have a constant thickness except for the Early–Middle Triassic units. The northern part of the section between the Orbe and Venoge rivers shows a thickening of the latter unit. The section obliquely intersects the southern flank of the first fold of the Jura Mountains. To the north of Morges (SLP 200), an evaporite-cored detachment fold is observed (see also Sommaruga 1997); these folds are developed above a conceptual major décollement zone.

The La Sarraz tear fault zone is a main feature in this section. Its main fault is seismically well defined (quality class 1) whereas minor associated faults are poorly defined. The main branch of the fault dips toward the south and ends within Triassic beds. Horizon offsets are visible along the tear fault, but no major lateral change in thickness is observed across the fault. The La Sarraz tear fault zone, also known in the literature as the Mormont–Vallorbe fault (Jordi 1990, Baujard et al. 2007; see also Figure 4.5), represents the conjugate dextral system of the sinistral Pontarlier tear fault (see the description of Transects 03 and 14 paragraph 4.2.3 and 4.2.14). Another important feature of this transect is the Pipechat–Chamblon–Chevressy (PCC) tear fault zone. All Mesozoic horizons are seismically poorly defined especially on the northern side of the fault (SLP 1800), but the presence of this fault associated with vertical and lateral offsets across it have been shown by previous seismic studies (Jordi 1990, 1993; Muralt et al. 1997). The extension into pre-Mesozoic units of both the La Sarraz and the Pipechat–Chamblon–Chevressy tear fault zones is not observed.

An extended reflective zone is observed along the whole transect within the pre-Mesozoic units that presents high-amplitude seismic facies, presumably coal-bearing Carboniferous sediments. About 400 m of Permian rocks were drilled in the Treycovagnes-1 well.

4.2.3 Transect 03: Lac de Joux – Villeneuve (Enclosure 04)

Transect 03 is located in Canton Vaud and runs from the first anticline of the Folded Jura to the Prealpine Klippen across the Plateau Molasse and the Subalpine Molasse. It comprises three seismic profiles from three different surveys SADHU8401, PSBRU8308 and PSBRU8424. The first two profiles are oriented NW–SE, perpendicular to the structures of the Swiss Molasse Basin and the third one runs around the eastern end of Lake Geneva, its orientation changing from N–S to NE–SW. The length of this transect is 66 km. Well control is provided by Savigny-1 giving information on the Near Base Tertiary (NBTer) horizon and by Chessel-1, located in the Quaternary sediments (160 m thick) of the Rhône River plain, and providing information on the underlying Prealpine tectonic unit. Other wells are located more than 4 km from the transect (e.g. Eclépens-1) but they have been considered for the calibration of horizons of intersection profiles. Horizons beneath the Plateau Molasse (in the Tertiary USM and Mesozoic units) display good lateral continuity and high-quality reflections, mostly of quality classes 1 and 2. To the south, in the Mesozoic units beneath the Subalpine Molasse, the reflection quality decreases to classes 2 and 3.

The NBTer horizon is a single fairly strong reflection contrasting with the highly reflective underlying Cretaceous unit characterized by one to two reflections. The quality of the NBTer reflector largely depends on the lithology of the lowest Tertiary unit. To the north, the impedance contrast is weak between the USM layers (mainly poudingue) and the Cretaceous unit. To the south the impedance contrast is stronger due to the presence of UMM layers (mainly sandstone). The Tertiary seismic unit, in the Plateau Molasse, is wedge shaped, and it includes onlaps to the north over the underlying thin Lower Cretaceous layers (the Near Top UMM onlaps the Base Tertiary unconformity at SLP 3580 on profile SADHU8401). In the Subalpine Molasse, Tertiary sediments consist of slices; thrusts are observed at the surface and their extension to depth is well to poorly defined on seismic profiles. The transition from Subalpine Molasse to Folded Molasse is enhanced by few reflections (quality class 3), and it represents a wedge or crocodile structure next to the Savigny-1 well. The faults and the different Molasse units encountered in this well provide important information for the interpretation of the above-mentioned crocodile structure. The Tertiary unit within the Subalpine Molasse is detached from the Mesozoic layers below (conceptual major fault).

The thickness of each Mesozoic seismic unit decreases to the southeast except for the Late Malm unit which thickness increases slightly. To the north of the geological model, the transect crosses the Folded Jura and displays an interesting feature within the Mesozoic unit. The Jurassic layers are folded above a very important thickening of Early–Middle Triassic layers. This anticline is the lateral continuity of the Mt. Tendre fold, and its structure is known to be more complex than interpreted here (Aubert 1941, 1977, Rigassi 1977): a north-vergent thrust ramp fault that we do not identify on this seismic profile (between SLP 2004 and 2200), should be present. The oblique reflectors within the Triassic layers are interpreted as small thrust faults imbricating parts of the units, which results in an overall layer thickening in a duplex geometry (Boyer & Elliot 1982). These duplexes are bounded by a roof thrust below Top Late Triassic or Top Middle Triassic units and a basal thrust, presumably within the Base Middle Triassic above the Buntsandstein beds. This anticline, cut by the Pontarlier tear fault zone (see description below) developed above a major décollement zone.

Beneath the Subalpine Molasse unit, faults of quality class 2 are observed. They are mainly normal faults within Cretaceous and Late Malm beds. Beneath the Plateau Molasse unit, south of Cossonay village, a tear fault of quality class 2 is present across the Mesozoic layers. At its northern extremity, outside the geological model, the transect crosses the major Pontarlier tear fault zone, a geologically well-defined left lateral fault with two fault branches (Aubert 1959). On the depth-converted section, the tear faults are displayed as «conceptual» because no direct evidence is observed in the seismically transparent zone. The Pontarlier tear fault zone is well defined on several intersecting seismic profiles and on Transect 14 (see Enclosure 14). In map view, it extends southwards to Lake Geneva (see Figure 4.5).

Two separate pre-Mesozoic reflective zones are observed: a first one at the foot of the Folded Jura and a second major one under the eastern end of Lake Geneva at the transition between the Subalpine Molasse and the Ultra-Helvetic and Prealpine tectonic units (beneath the Penninic cover nappes). The first one shows high-amplitude seismic facies, presumably coal-bearing Carboniferous sediments. About 400 m of Permian-rocks were drilled in the Treycovagnes-1 well. However, the presence of Carboniferous rocks in this well is questionable (M. Weidmann, personal communication 2011). To the south, in the second zone, a pronounced large-scale anticline, highlighted by Mesozoic reflections is observed. Still deeper, the reflective zone gives way to high-amplitude facies (presumably coal-bearing Carboniferous sediments). The main geological question is whether this structure developed by partial inversion of a Permo-Carboniferous trough or whether it developed as a ramp anticline above the sole thrust of the Jura fold-and-thrust belt as it cuts down into Permo-Carboniferous series or even the basement.

The latter interpretation is presented in the depth-converted seismic interpretation: a gentle ramp in the pre-Mesozoic unit could have played a significant role in the development of this large anticline, as it appears to extend further into the Triassic conceptual major décollement zone. This zone presumably extends to the south. This major anticline has already been described in the literature with thicker Triassic beds (Fig. 11 and Plate 3 in Gorin et al. 1993; Plate 6 in Sommaruga 1997) and has been drilled in 2009–2010 by Petrosvibri SA (Noville-1 well). The drilled length is 4298 m and the depth reached is 3535 m. First evaluations of the unit thicknesses were presented orally by W. Leu (seminar at University of Lausanne in 2011): Triassic units about 400 m, Permian sediments 150–200 m and Carboniferous rocks 300 m.

To the south, outside of the geological model, few reflections highlight folds within the upper Mesozoic layers located under the Prealpine units above the Penninic base thrust. The lateral position of this thrust, observed in the Chessel-1 well, is questionable.

4.2.4 Transect 04: Yvonand – Gruyères (Enclosure 05)

Transect 04 is located in Cantons Vaud and Fribourg, and it runs from the southwestern shore of Lake Neuchâtel across the Plateau Molasse, the Folded Molasse to Subalpine Molasse units and the Penninic cover nappes. It comprises three seismic profiles SADHU8603, FR.S750002 and FR. S750009 of three different surveys. The first two profiles are oriented NW–SE perpendicular to the western SMB axis, and the third one is oriented NNE–SSW along Lake Gruyère and the Sarine River valley within the Prealpine Klippen (Penninic cover nappes) with a highly oblique trend relative to the regional dip of the Mesozoic series. There is a jump of about 8 km between the second and the third profile. The length of this transect is 52 km. Well control is provided by the Romanens-1 well yielding information from the Tertiary unit down to the Late Triassic beds. Transect 4 presents Mesozoic horizons under the Plateau Molasse with quality classes 1 to 3 reflections depending on the certainty of the geological identification. To the south, under the Subalpine Molasse and especially under the Prealpine Klippen (Penninic cover nappes) the reflection quality decreases strongly and the geological identification of reflections becomes very difficult (quality class 3).

The wedge-shaped Tertiary unit displays no major features within the Plateau Molasse; the Near Base OMM horizon is correlated along the Plateau Molasse series. For detailed studies within the Tertiary unit on seismic profiles SADHU8603 and FR.S750002 the reader is referred to the work of Strunck (2001) and Strunck & Matter (2002). The Romanens-1 well is located at the Subalpine Molasse front. At this location, a north-dipping thrust is observed within the Tertiary Molasse unit. Within the Subalpine Molasse, several slices of Molasse units and south-dipping thrusts have been mapped at the surface (see Gruyères geological map from Pasquier 2004), but no correlation at depth can be inferred from the seismic data. Therefore, these thrusts are shown as conceptual faults. The Subalpine Molasse series are detached at the Base Tertiary level (conceptual majorfault). The Mesozoic series are calibrated with the Romanens-1 well. The thickness of the Dogger and Liassic units decreases strongly from north to south by more than 50 % in front of the Folded Molasse. The thickness of the Early–Middle Triassic unit varies. To the north and to the south of La Baume-Yvonand evaporite-cored detachment folds can be identified. The southernmost one (SLP 1050) is the lateral northeast extension of the Essertines anticline. The Romanens-1 well is located over a small thickening of Middle-Early Triassic strata. The southern section along the Sarine Valley shows thicker Late Malm versus thinner Early Malm strata. Liassic beds thin out under the Prealpine Klippen. Along the southernmost end of the profile, correlating horizons becomes difficult.

The fault zone near the village of Lucens is composed of two main faults and an antithetic one with apparent normal movement; it represents a main structure in the Plateau Molasse. The Broye River channel is located here over this wide normal fault zone that affects the entire Mesozoic unit. A major normal offset is visible across this fault zone (fault quality classes 1 and 2). The faults appear to be linked with deformation of Triassic layers. A fault outcrops on the southern side of the channel. The associated graben structure seems to be oriented NE–SW parallel to the channel (Ibele 2011). North of La Baume village, the seismically identified fault seems to be related to the Cuarny Fault (Jordi 1990). Two normal faults (SLP 140 and 210 on profile FR.S750002) offset the Near Base Tertiary and Near Top Late Malm horizons with a change of thickness across them. These faults appear to be synsedimentary faults. At the base of the Mesozoic layers, there is a conceptual major décollement zone where the structures and faults root.

An extended intermediate zone in the pre-Mesozoic units is observed beneath the Plateau Molasse. Within this region, a small reflective zone has been interpreted. To the south, outside of the geological model, and under the Penninic cover nappes, the Mesozoic levels appear to be uplifted on profile FR.S750009 (SLP 350–111). Here, the interpretation becomes difficult due to poor seismic resolution (low signal to noise ratio): we can either interpret a velocity pull-up caused by carbonates of the Prealpine Klippen, or an inverted Permo-Carboniferous trough or ramp anticline related to a gentle thrust cutting into the basement.

4.2.5 Transect 05: Estavayer-le-Lac – Le Cousimbert (Enclosure 05)

Transect 05 is located in Cantons Fribourg and Vaud, and it runs from the Canton Fribourg enclave of Estavayer-le-Lac at the southern shore of Lake Neuchâtel to the foot of the northern flank of Le Cousimbert Mountain across the Plateau Molasse, Folded Molasse and Subalpine Molasse units. It comprises three seismic profiles from three surveys FR.N8504, FR6001 and FR.S750015. There is a jump of circa 1 km between the second and the third profile. The first one is oriented WNW–ESE and the other two are oriented NW–SE; they are all more or less oriented perpendicular to the main structures. The length of this transect is 34 km. No direct well control was used in the interpretation of this transect. The Courtion-1 and Romanens-1 wells (see Enclosure 16) are more than 4 km distant, but they were considered for calibrating the horizons and seismic units of intersecting profiles. Profile FR.N8504 shows horizons with good lateral continuity and reflection quality classes 1 to 3. The seismic quality of the FR6001 profile (acquired in 1960) is very poor, and it cannot be reliably interpreted. This profile is not considered in the three quality types of seismic profile display defined in paragraph 3.5.2 (see Figure 2.8). In the bottom section, we nevertheless attempted to correlate units across this profile from the two adjacent ones. To the south, at the front edge of the Subalpine Molasse, the reflection quality decreases to classes 2 and 3 because of the uncertain geological identification.

In general, the thickness of the Tertiary unit increases to the south. An intra USM horizon was interpreted. Other Tertiary horizons are not recognized on the seismic profile, although they have been mapped at the surface (base OMM, SLP 620 and 940). For a detailed study of the Tertiary unit on seismic profile FR.N8504, the reader is referred to Strunck (2001) and Strunck & Matter (2002). The thickness of the Mesozoic series is constant in the northern and central part of the profile. To the south of the transect, the thickness of the Dogger and Liassic units strongly decreases while thickness of the Late Malm unit increases; these variations are similar to those observed on Transect 04. The seismic units are constrained by six intersecting profiles, among them Transects 14 and 15.

Transect 15 shows two main anticlinal structures that occur on profile FR.N8504, one at SLP 700–1050 and one at SLP 200–450. Both anticlines show a thickening of the Early–Middle Triassic unit, which induces an evaporite-cored detachment fold that developed over a décollement (conceptual major zone). USM Tertiary beds are also folded. The northern anticline has a large wavelength, and it represents the extension of the Essertines anticline that here becomes the Payerne anticline. The southern anticline located between the Broye Channel and Onnens village is the extension of the Misery–Courtion anticline (Jordi 1990). Several reverse faults with dip angles of up to 70° are related to this anticline structure. South of the Fribourg agglomeration, thickening is also visible within the Early–Middle Triassic unit, however no anticline is observed in the overlying beds. Instead, a half-graben structure is observed bounded by a normal fault that roots in the Triassic layers. South of Estavayer-le-Lac, we interpret two steep antithetic faults on the seismic data (quality classes 1 and 2) associated with the La Lance–Fétigny fault zone, a dextral tear fault zone oriented NW–SE (see Figure 4.5). This fault zone extends over several kilometers up to the Jura Mountains (Mt.-Aubert). It is observed both in outcrop (geological map of Meia 1969) and on seismic profiles (Sommaruga 1997). A seismic study of Lake Neuchâtel (Gorin et al. 2003) showed that at the bedrock surface, the La Lance fault can be mapped as a NW–SE trending fault zone 1 km wide; recently disturbed overlying Quaternary sequences suggest episodes of fault reactivation. Ibele (2011) attempted to correlate this seismically defined fault zone with surface outcrop data.

No reflective zone was interpreted in pre-Mesozoic units, whereas two intermediate zones are observed, one to the north and the other one to the southeast at the transition between the Plateau Molasse, Folded Molasse and Subalpine Molasse.

4.2.6 Transect 06: Biel / Bienne – Thun (Enclosure 06)

Transect 06 is located within Canton Bern, and it runs from Lake Biel to the Thun-1 well, mainly across Plateau Molasse and partly across Folded Molasse and Subalpine Molasse units. It comprises five seismic profiles of different surveys BEAGBE.N740007, BEAG750004, BEAGBE.S70B017, BEAGBE.S8504 and BEAGBE.S8503TV. The first four seismic profiles are oriented NW–SE, perpendicular to the main structures of the SMB, and the southern seismic section is oriented WSW–ENE, parallel to the structures. They are two gaps in this profile: one of about 10 km between the second and the third profile and one of about 2 km between the third and the fourth profile. The total length of this transect is 59 km. Well controls are provided by Hermrigen-1, Linden-1 (projected over distance more than 4 km) and Thun-1: they all give information down to the Middle Triassic unit. The transect includes horizons in the Plateau Molasse with a fairly good lateral continuity and reflections of quality classes 2 and 3. At the southern edge of the Plateau Molasse, on profile BEAGBE.S70B017 north of the Linden-1 well, the reflection quality is poor and interpretation is tentatively carried out by correlation with adjacent profiles.

The wedge thickness of the Tertiary unit increases to the south except at the northwest end of the transect. Very few horizons were interpreted within this unit. For a detailed interpretation of the Tertiary unit in this area the reader is referred to Vollmayr (1992) and Schlunegger et al. (1993). Well Linden-1 is located in front of the Folded Molasse and well Thun-1 within the Subalpine Molasse. The latter gives information on faults which have no visible link with the seismic data. Nevertheless, north-vergent thrusts observed on seismic section between the Linden-1 and Thun-1 wells are linkable to outcropping thrust faults. North of well Linden-1, within the Plateau Molasse, a south-vergent thrust fault has been added on the bottom section as a conceptual fault. This thrust fault merges with a very low-angle (1° to 2°) south-dipping conceptual major thrust fault (SLP 2015 on profile BEAGBE.S70B017). It is also linked to faults of quality class 2 at depths of approximately 2 km. The Mesozoic series are calibrated with well Hermrigen-1 to the north and well Thun-1 to the south. The thickness of the Dogger and Liassic units decreases progressively to the south, especially under the Folded Molasse and Subalpine Molasse. The thickness of Triassic layers varies significantly along the transect.

The remarkable structure of the Hermrigen anticline shows a thickening of the two drilled Triassic units. This structure is interpreted as an evaporite-cored detachment fold. Steep north-vergent reverse faults are also related to this structure; their associated offset, however, is limited. At the base of the Mesozoic layers, there is a conceptual major décollement zone where faults root. The northern part of this transect coincides with the western seismic profile of Pfiffner et al. (1997). These authors interpret the Hermrigen anticline as an inversion of a Permo-Carboniferous trough.

The Mesozoic strata beneath the Plateau Molasse unit (BEAGBE.S70B017 seismic profile) are cut by several steep faults with a normal or reverse apparent offset. The extension of these faults to shallower Tertiary units or to the surface is uncertain. To the south, the Thun-1 well is located on a structure showing Triassic beds that thicken towards the southeast and to the southwest. Because the seismic profiles change direction in this area, they do not image the entire anticlinal structure.

Reflective zones in pre-Mesozoic unit are not very extended, whereas intermediate zones are more frequent. No clear link between these reflective or intermediate zones and the Mesozoic structures is observed.

4.2.7 Transect 07: Grenchen – Kemmeribodenbad (Enclosure 07)

Transect 07 is located in the Cantons of Solothurn, Bern and Lucerne, and it runs from the southern edge of the Jura Mountains to the Subalpine Flysch across the Plateau Molasse, the Folded Molasse and the Subalpine Molasse. It comprises six seismic profiles of five different surveys BEAGBE.N740005, BEAG750001, BEAGBE.S700013, LEAGLUZN760014, LEAGLUZN740001 and LEAGU8408. The first four seismic profiles are oriented NW–SE and the last two are NNW–SSE, mostly perpendicular to the direction of the structures within the western SMB. At its south end, within the Subalpine Flysch, the transect is oriented in the N–S direction. There are three profile gaps in this transect: a major one of about 6 km between the second and the third profile. The length of this transect is 62 km. Nearby well control is provided only by the Ruppoldsried-1 well that reaches the Late Malm unit. The general reflection quality is poor (quality classes 2 and 3), especially in the central and south part of the transect.

As observed on the other dip transects, the thickness of the Tertiary unit increases toward the south, and it reaches more than 4 km beneath the Subalpine Molasse. Only a few Tertiary horizons were interpreted. Top or base OMM horizons are interpreted on the bottom section based mainly on surface geological information. A south-vergent thrust fault is observed on a seismic profile at the front of the Folded Molasse (SLP 211–100 on profile LEAGLUZN740001). North-vergent thrust faults are observed at the boundaries between the Folded Molasse, the Subalpine Molasse and the Subalpine Flysch. A major, very low dip-angle (1° to 2°) conceptual thrust fault is located within Tertiary layers at the base of these north-vergent faults. We based our depth intepretation on the neighbouring transects. Here the Mesozoic cover dips gently towards the south. Thickness of the Mesozoic layers decreases progressively to the south, except for the Late Malm layers where the thickness remains constant.

The northernmost part of the transect shows an anticlinal structure that corresponds to the Seeketten thrust fold of Laubscher (2008). Well Ruppoldsried-1 is located on a gentle anticlinal structure bordered by three steep reverse faults and shows a thickening of the Early – Middle Triassic layers. The Mesozoic units under the Plateau Molasse are cut by several steep faults with a normal or reverse apparent offset. The extension of these faults to the surface is uncertain. At the base of the Mesozoic layers, there is a conceptual major décollement zone where the folds and faults root.

No reflective zone within the pre-Mesozoic unit was interpreted. Limited zones of intermediate reflection quality are observed. The poor quality of profile BEAGBE.S700013 may obscure some pre-Mesozoic structures.

4.2.8 Transect 08: Egerkingen – Entlebuch (Enclosure 08)

This transect runs from Egerkingen at the foot of the Jura Mountains in SSE direction, passing by the Pfaffnau wells (profile SOTN740016) and from there towards the Napf Mountain at the boundary between Canton Bern and Canton Lucerne (profile LEAGU8403). The trace jumps 8 km to the east of the Napf where profile LEAGLUZNR880998 continues southward into the Entlebuch valley. The total length of the transect is 51 km.

Both the Pfaffnau-1 and Entlebuch-1 wells drilled through the entire Mesozoic sequence, but only the latter found some Paleozoic sediments. At Pfaffnau several other wells were drilled (Pfaffnau south area), but only Pfaffnau-1 drilled through 19 m of the crystalline basement. Well Entlebuch-1 is the only place in the deep SMB where a Carboniferous section has been drilled (from 4948 m down to TD at 5152 m). There are no Permian rocks reported from well Entlebuch-1. Both wells Entlebuch-1 and Pfaffnau-1 are important calibration points for our interval velocity calculations and depth conversion.

The seismic profiles that contribute to this transect are not the best quality. Most reflections have quality classes 2 and 3. Reflections from the NBTer are often interrupted or absent, and reflections at the top of the Oxfordian shales (Intra Early Malm; IeMa) do not show up at several places. The NTDo and NTLi horizons rarely correspond to good-quality reflections except in the area south of well Pfaffnau-1. The lowest reflection quality is found north of well Entlebuch-1 where we explain the absence of clear seismic imaging by structural complications in the overburden as well as in the Mesozoic and Paleozoic itself.

Seismic and well data confirm the general thinning from north to south of the middle Triassic, the Dogger and the lower part of the Malm sections.

On profile SOTN740016, the Jura deformation is visible north of the Aare River. The compressional feature within the Malm unit south of Neuendorf may extend to the east of the profile into the Born Mountain. This structure stands out as the southernmost surface anticline of the Jura fold belt in the area. Small normal faults at basement level (SLP 270) are not strongly supported by the seismic data; they could be interpreted as additional conjugate thrusts that sole in Triassic sediments. Pfiffner (2009) interprets the high position of the basement north of SLP 270 as an expression of a thick skin compressional feature. However, in our data there are no reflections in the basement that could support this hypothesis.

South of well Pfaffnau-1, on profile LEAGU8403, reflections within Tertiary and Mesozoic units display irregular seismic quality. The NBTer reflection is sometimes absent, which could mean that the Malm surface is locally eroded. As in other profiles, internal differentiation of the Malm is not very convincing, but the sedimentary reduction of the Oxfordian layer between wells Pfaffnau-1 and Entlebuch-1 is represented by a gradual transition from almost three reflections to a single one. The Dogger series forms a wedge whose thickness gradually decreases to the south. It is apparently offset at several places by small normal faults, most clearly at SLP 3270. Note that the thin Liassic unit entirely falls within one black coloured amplitude trough, and that there is no proper top Liassic reflection to be followed along this profile. Because the Liassic unit remains thin throughout the eastern part of the Swiss Molasse Basin, it rarely shows up on seismic profiles, and its interpretation is based on geological information.

A south-dipping reflection in the pre-Mesozoic section is observed south of well Pfaffnau-1. It is interpreted to be the expression of Permo-Carboniferous sediments thickening to the south. The well is located just north of the truncation of this reflection at the base of the Mesozoic unit. Along profile LEAGU8403, the presence of reflections at Paleozoic level between SLP 3300 and SLP 3800 is confirmed by adjacent seismic profiles. Further to the south along this profile, the seismic quality decreases, and the potential presence of Paleozoic sediments remains doubtful.

On profile LEAGLUZNR880998, the thick Tertiary sequence is affected by dip changes observed at surface from north to south, and the resolution of the seismic data is generally poor. The conceptual interpretation of the Tertiary structures within the Folded and Subalpine Molasses proposes a triangle zone with a roof thrust that is cut by (later?) north-verging thrusts, bringing the Lower Marine Molasse (UMM) to the surface. This triangle zone is better defined in adjacent transects to the east.

We interpret compressive structures under the village of Entlebuch on top of the structurally thickened Triassic and inverted Paleozoic sedimentary trough. Although there is little evidence for such structuration, we believe that the Tertiary heterogeneity is insufficient to produce such an image within the Mesozoic unit. Alternatively, the discontinuity of reflections within the Mesozoic section can be explained by scattered ray paths in the deformed Tertiary overburden. Well Entlebuch-1 lies above a structural high that could be the result of an inversion of a pre-Mesozoic graben under Alpine compression. The strong reflections between two-way traveltimes 2.2 s to 3.0 s are interpreted, by analogy with the Carboniferous trough of northern Switzerland, to be caused by continental or paralic Paleozoic sediments rather than by a deeper slice of Mesozoic sediments. Their origin could not be checked in the Entlebuch-1 well. A more detailed interpretation of this profile has been published by Vollmayr and Went (1987).

4.2.9 Transect 09: Laufenburg – Schwyz (Enclosure 09)

This transect extends from the southern margin of the Black Forest at Laufenburg across the Aargau Jura fold and thrust belt and the allochthonous part of the Molasse Basin to the front of the Alpine nappes near the town of Schwyz. The Tabular and Folded Jura are visible on the seismic profile U82-NF-10. Further south, profile SEAGLEAGRU8307 runs along the western shoulder of the Seetal above Beinwil am See and Hochdorf in Canton Lucerne. Profiles LEAGLUZN770024 and SEAGR770031 take an ESE-direction, they cross Transect 10 and run at a low angle to the structures of the Subalpine Molasse from Ebikon via Immensee to Arth, at the north slope of Mount Rigi. Profile SEAGR750023 ends near the town of Schwyz. The total length of Transect 09 is 81 km. Along the southern part of the transect, 21 km are shared with Transect 15.

Two wells provide calibration data. To the north of the Jura fold belt, well Kaisten-1 defines the depth position of the Middle Triassic and older markers, including some 172 m of Permian sediments and a significant portion of crystalline basement (1009 m). Well Schafisheim-1 provides control for the Quaternary, Cenozoic, and Mesozoic sections. The Quaternary fill under the Aare valley is drawn schematically. Schafisheim-1 also evidences formation thicknesses that are comparable to other wells in northern Switzerland, except for the Late Malm layer that is thinned by erosion. There are no Paleozoic sediments on top of the crystalline basement in Schafisheim-1.

Along this transect, older profiles generally have lower frequency content than more recent profiles, and along each profile the quality of the reflections varies considerably. On profile U82-NF-10, seismic quality appears to be deteriorated by structures close to the surface. Down the slope of the Molasse Basin, three profiles (SEAGR750023, SEAGR770031 and LEAGLUZN770024) were available to us as unmigrated stack versions. Structural complications in this area add to the generally poor reflection quality. On profile SEAGLEAGRU8307, reflections from the middle Triassic to middle Jurassic series are better resolved north of SLP 1800, and the Tertiary section is seismically well imaged. Due to absence of well calibration, however, none of the seismic reflections can be ranked over long distances to quality class 1.

Frontal structures of the Jura thrust belt are recognized on the Nagra profile U82-NF-10 (SP 2050–2100, Mandach thrust) 10 km to the north of the main fold belt. Seismic interpretation of the Homberg and Geissberg thrust anticlines cannot match the complexity of surface geology. These structures correspond to the Chillholz and Gisliflue anticlines (Nagra 2008). Our interpretation is a compromise between visible reflections and published interpretations including surface geological data (Diebold et al. 2006).

Within the Tertiary unit, a triangle zone is interpreted based on strata that rise to the south all the way to profile SEAGR770031, and that plunge to the south on profile SEAGR750023. Near Hochdorf, between SLP 1800 and 2100, a paleovalley up to 250 m deep and up to 5 km wide is interpreted within the late Malm unit. This valley was cut into the Mesozoic platform during Paleogene exposure, prior to the deposition of late Eocene and younger deposits. Along the common part of Transect 09 and 15, reflections in the Mesozoic unit are often interrupted, and they occur as packages with variable dips. In the poor-quality data area along profiles SEAGR770031 and SEAGR750023, we adopted a conceptual interpretation based on a compressional model, but an alternative solution including normal faults is possible too. The Triassic sediments are thickest at the southernmost part of the transect under small thrust anticlines that point to the north as well as to the south.

The deep Permo-Carboniferous trough of northern Switzerland just to the south of well Kaisten-1 is seismically well defined by reflections along its southern slope. The northern margin has probably been complicated by strike-slip movements (Laubscher 1986, Ustaszewski 2004, Ustaszewski & Schmid 2007). It is too steep to be correctly imaged by seismic profiling. The southern margin of the trough, however, is the clearly visible edge of the adjacent basement slope. It may well have mechanically contributed to the emplacement of the thrusts that cut the Homberg and Geissberg anticlinal structures (Diebold et al. 1991). Further south under the Molasse Basin, seismic-facies changes at Paleozoic level cannot be interpreted unequivocally. Graben structures are more likely to be present to the south of SLP 1900 on profile SEAGLEAGRU8307 or at the north ends of profiles SEAGLUZN770024 and SEAGR750023, where south-dipping reflections are observed.

The concept of a triangle structure within the Tertiary unit cannot be based on the reflections of profile LEAGLUZN-770024 only. Outcrop information and projection of seismic observations from both sides of the transect contribute to the conceptual geological model. At the south end of the transect, the Subalpine Flysch and the Helvetic base thrust (Hbt) are projected from the southwest into the profile. Nagra (2008) published an interpretation of the north part of Transect 09, and more information on the seismic profiles at the south end of the transect can be found in Bodmer & Gunzenhauser (1992).

4.2.10 Transect 10: Koblenz – Sarnen (Enclosure 10)

Transect 10 runs across Cantons Aarau, Zurich, Lucerne and Nidwalden. Profiles U83-NF-55 and SEAGU8306 run from the Rhine River at Koblenz to the Limmat Valley. After a jump of almost 5 km to the west, the transect continues along profile SEAGU8511, it follows the River Reuss across the Plateau Molasse (well Hünenberg-1), and it reaches the Subalpine Molasse of Mount Rigi along profile SEAGR-750025 (thermal water well Weggis-1). From there, the transect crosses Lake Lucerne, and it ends in the external Helvetic Nappes (LEAGLUZNRU7609) at the boundary between Cantons Nidwalden and Obwalden. Because of the generally poor seismic quality of profile SEAGR750025 and because of the absence of well calibration along profile SEAGU8511, reflections are set into the quality classes 2 or 3. The total length of Transect 10 is 92 km.

Near the towns of Koblenz and Zurzach, at the north end of the transect, several wells have been drilled for the exploration and production of thermal water resources. They all confirm the presence of a shallow crystalline basement (also found in outcrops), and the erosive reduction of Mesozoic sediments. Between wells Zurzach Z3 and Zurzach-Jungrebe, Permian sediments are present as a thin layer of clastics that extends southwards into the Permo-Carboniferous graben of northern Switzerland. In well Weiach-1, 456 m of Permian sediments, 572 m of Carboniferous sediments and 457 m of crystalline basement were drilled. This well is shown on the transect because it provides the most complete stratigraphic calibration point in the area (projected from the east over 10 km). Well Hünenberg-1 went through several Tertiary closures, and it reached the top of the Malm unit at a depth of 3259 m (TD at 3288 m). To the south, in the Subalpine Molasse, well Weggis-1 provides geological information down to 2302 m. Unfortunately, there is no geophysical data available for velocity calculations in this well.

Seismic quality varies along the five profiles that constitute Transect 10. Profile LEAGLUZNRU7609 crosses Lake Lucerne, leaving a large data gap that is only filled at large TWTs. South of well Weggis-1, the seismic interpretation becomes difficult because only few reflections dominate the seismic noise level.

To the north end of the transect, the Jura fold belt is crossed close to its east end. North of the Lägeren fold, several north-verging thrusts are apparent within the Mesozoic unit, mainly affecting Triassic and Jurassic strata. The details of the Lägeren thrust-fold are hardly visible on the seismic profiles, and the complex reflections within the Triassic unit can be interpreted in various ways. South of the Lägeren, an anticlinal structure could well be cut by several south-verging thrusts, at least one is shown by Müller et al. (2002). The Permo-Carboniferous trough of northern Switzerland produces a set of strong reflections from SLP 100–250 on profile SEAGU8306. They are calibrated by a perpendicular profile running through well Weiach-1 (Müller et al. 2002). There are no indications of shortening in the tabular Jura north of well Weiach-1, and we stop the major décollement horizon within the Triassic unit under the Lägeren anticline. Small compressional features within the Mesozoic unit extend up to 8 km north of the Lägeren.

Further south, the seismic data show a rather smooth Paleozoic basement top. Gently undulating reflections within the Mesozoic unit are interrupted at several places (quality class 2). The curved shape of the reflections within the Malm layer indicates the nature of south verging small thrusts on profile SEAGR750025 at SLP 720 and 400, and possibly at SLP 240 and 270.

South of well Hünenberg-1, the Upper Marine Molasse (OMM) strata starts to rise over a triangle structure with a roof thrust that culminates north of Immensee. South of that culmination, surface geology indicates that all Molasse strata dip southward, and they are tectonically overlain by North Helvetic Flysch units, Helvetic nappes and even Pennine elements (Stanser Klippen, not shown on the transect). A sliver of Lower Marine Molasse (UMM) sediments surfaces north of well Weggis-1 where this unit was drilled.

The complex structure and the low signal-to-noise ratio of the seismic data along the entire profile make it difficult to comment on reflections within the Mesozoic and Permo-

Carboniferous units. Our structural interpretation in this area is sometimes conjectural, and it cannot be confirmed because of the absence of cross-profiles. An alternative, somewhat more detailed interpretation of the north part of Transect 10 is shown in Nagra (2008), and additional information on the Weggis-1 well can be found in Greber et al. (1994).

4.2.11 Transect 11: Siblingen – Glarus (Enclosure 11)

Transect 11 starts in Canton Schaffhausen near the northernmost point of Switzerland, and it runs to the south-southeast (profiles U84-NF-65 and SEAGU8305). After a 4 km jump to the east, three old profiles (SEAGR74001, SEAGR75001 and SEAGR750015) were combined into a more recently reprocessed one (SEAGR880999). This profile crosses the south half of the Swiss Molasse Basin and it ends in the Helvetic nappes near the city of Glarus. Clear, continuous seismic reflections are scarce, and the good quality attributed to the seismic horizons is related to their correlation with well discontinuities. This is for example the case for the good-quality horizons within the Triassic unit south of Lindau. The total length of Transect 11 is 95 km.

Well Siblingen-1 calibrates the northernmost part of the transect by sampling Liassic, Middle and Early Triassic units conformably overlying crystalline basement. Well Weiach-1 is projected onto the profile because it is the best control point of Paleozoic sediments in north Switzerland. Well Lindau-1 marks the beginning of the SE trend of the transect. With the exception of well Küsnacht-1, well Lindau-1 is the only well east of Zürich that provides information on the entire Mesozoic section in a basin slope position. Well Tuggen-1 that was drilled to a depth of 1600 m, gives some interesting dip information on the Subalpine Lower Freshwater Molasse (USM), however, there is no geophysical data from this old well to calibrate two-way tavertime seismic profiles.

The generally smooth monoclinal dip of the Mesozoic section is interrupted to the north by the Baden–Irchel–Herdern lineament visible under the Irchel Mountain. This lineament coincides with the southern limit of the Permo-Carboniferous trough of northern Switzerland (Weiach Trough). The seismic facies of the Paleozoic section within the trough includes sub-horizontal and south-dipping reflections down to two seconds TWT. For details see Diebold et al. (1991) and Naef et al. (1995). The Baden–Irchel–Herdern lineament is clearly expressed on profile U84-NF-65 around SLP 400 by a north-heading normal fault that displaces also the Mesozoic and Tertiary series. This feature is believed to be a Pliocene strike-slip reactivation of the Paleozoic trough shoulder. West of Basel, the reactivation of Permo-Carboniferous extension faults shows transpressional strain (Ziegler & Dèzes 2007 and Ziegler & Traefel 2009). The seismic data suggest that the basement shoulder behind the lineament forms an outstanding regional ridge.

The deeper part of profile SEAGR880999, in eastern Canton Zurich, shows a much poorer quality seismic image, and the interpretation of Paleozoic sediments in that part of the transect remains speculative.

Gentle undulations of seismic reflections visible on profile SEAGU8305 in the Triassic, Liassic and Dogger units are underlined by small thrust faults that explain reflection interruptions. They may be related to salt-solution features (P. Ziegler, personal communication).

Within Tertiary units an onlap reflection configuration is observed on profile SEAGU8305, and reflections at the base of the Tertiary unit show some irregularities on profile SEAGR880999 that may be related to erosion of the top Malm carbonates. Our interpretation is rather smooth, and it leaves room for alternatives. For instance, gentle Paleogene paleovalleys may be present between SLP 400 and 600 or between SLP 900 and 1000. To the south, we interpret a triangle structure under Uznach where both south and north dipping strata are observed at the surface. The Mesozoic unit is offset by a dominant normal fault (at SLP 760 on SEAGR880999) stepping down into the basin. Tertiary reflections are not displaced. Note that the vertical displacement is of the order of the thickness of the Middle Triassic bed.

Where the transect reaches the Central Alps, seismic reflections are less continuous, and they finally disappear under a complex overburden with variable dips and rock properties. Therefore, compressive structures interpreted south of the intersection with Transect 15 must be taken with caution; they have conceptual value. The deepest parts of the Tertiary basin may be reached near the southern end of this transect. The Helvetic nappes that plunge to the east in the Glarus–Walensee region are not visible on these seismic data. At the extreme south end of profile SEAGR880999, there is some seismic noise between 1 and 3 seconds two-way traveltime. At this level, we could conceptually place the imbricated slices of the decaying frontal Aar Massif (see Pfiffner 2009).

4.2.12 Transect 12: Stein am Rhein – Buchs (Enclosure 12)

Transect 12 runs from Stein am Rhein, at the west end of Untersee, to Wil (profile SEAGR8301), and from there it follows the upper reaches of River Thur that cuts obliquely through the Subalpine Molasse (profile SEAGR750004). The southern portion of this transect (profile SEAGR750009), runs sub-parallel to the strike of the external Helvetic nappes from Alt St. Johann to Buchs. The reflection quality class is often 2 or below. The NTMuka horizon is the one that can best be followed over long distances. Under the triangle zone, quality class 1 was attributed to the NBMes and NTMuka horizons even though there is no well control. The total length of Transect 12 is 77 km.

Well Herdern-1 at the north end of the transect drilled through the entire Tertiary and Mesozoic sedimentary sequences down to the crystalline basement which was encountered at 2129 m. This well is the only calibration point for this transect; it is located 3 km to the west of profile SEAGR8301. The Liassic section is so thin (only 20 m thick in the well) that its top and base could not be correctly represented in the interpretation of profile SEAG8301; instead two neighbouring reflections were selected for the base and top of this unit.

As observed along other transects, the reflection associated with the unconformity between the Tertiary and Malm series strongly varies laterally. This can be attributed to the irregular erosional surface of the karstified Jurassic carbonates and to the variable lithology of the transgressive basal Molasse deposits.

To the south of the transect, the Mesozoic units and particularly the Malm unit are very thin. The thin Liassic layer corresponds to half a reflection period on profiles SEAG R750004 and SEAGR750009. The best correlation between reflections along the profiles is achieved by aligning the black amplitude of the Near Top Triassic horizon and by drawing the Near Top Liassic horizon parallel to it. The NTDo horizon falls close to a white amplitude signal in between.

On profile SEAGR8301, there is some evidence for reflections within the pre-Mesozoic unit between SLP 103 and 400 as well as between SLP 800 and 1000. Further south, there is some indication for the presence of shallow Permo-Carboniferous sediments in our stack version of profile SEAGR750004 e.g. near SLP 270 or SLP 400. However, this observation is not confirmed by the interpretation of the migrated data by Stäuble & Pfiffner (1991).

According to Müller et al. (2002), well Herdern-1 was drilled on the margin of the Permo-Carboniferous trough of northern Switzerland.

The small faults shown on profile SEAGR750004 that cut through the Mesozoic units often coincide with poor data zones, in particular under the triangle structure. The reverse fault at SLP 580 could equally be interpreted as the edge of a small graben zone. We interpret the abrupt changes in reflection dips within the Mesozoic units (between SLP 430 and 350 on profile SEAGR75004) as synthetic and antithetic normal faults. However, the effect of strong seismic-velocity variations in the triangle zone of poor data quality cast some doubt on the interpretation of these faults.

The triangle zone (culminating under the Toggenburg valley at Ebnat-Kappel) is cut at an oblique angle, and it appears therefore wider than it really is. Its south-pointing top thrust seems to be steepened by later squeezing of the series. Stäuble & Pfiffner (1991) present a migrated version of this profile with much better resolution, that resolves the internal configuration of the triangle zone, and that confirms the generally thin Mesozoic series. These reprocessed seismic data also allow for alternative fault positions across the NBMes horizon.

We can only «conceptually» interpret the west–east running profile SEAGR750009. It parallels the strike direction of the Helvetic Säntis nappe, and it runs on the dip-slope of the Churfirsten system in the area of Alt St. Johann. Reflections probably all come from outside the seismic profile plane, and therefore it cannot be properly migrated. We show this profile to present some conceptual tectonic relationships. Under the Helvetic Säntis nappe, there is room for the frontal part of the Glarus nappes that should cut across the southernmost part of Transect 12. For an alternative interpretation and the southward extension of this transect see Pfiffner et al. (1997). Note that in this area, far from the Jura thrust and fold belt, there is no indication for transport of the Mesozoic and Tertiary units above a décollement zone within the Triassic unit.

4.2.13 Transect 13: Kreuzlingen – Säntis (Enclosure 13)

Transect 13 starts at the west end of Lake Constance near Kreuzlingen, and it runs through Gossau and Urnäsch to end in front of the Helvetic Säntis nappe. It is based on the seismic profiles SEAGR790008 and SEAGR750008 that were available to us as unmigrated stacks only. The absence of well control along most parts of this transect results in reflections of quality classes 2 and 3 only. Despite the poor data quality and despite the possibility of reflections originating from pre-Mesozoic units, the interpretation of the NBMes horizon at rather shallow level along the transect is corroborated by intersecting profiles. The total length of Transect 13 is 49 km.

Well Kreuzlingen-1 provides calibration data from close to the surface OSM to crystalline basement at a depth of 2530 m. Without this information it would be very difficult to attribute stratigraphic levels to the variable, discontinuous seismic reflections. On both seismic profiles, the Dogger and Triassic carbonates create locally strong reflections. The seismic resolution within the Mesozoic and Tertiary units is limited, and it hardly enables us to map the NBTer horizon under the triangle zone or in the area north of SLP 300 along profile SEAGR790008. The small-scale faults near well Kreuzlingen-1 are therefore uncertain.

Profile SEAGR790008 provides information on the possible occurrence and configuration of Permo-Carboniferous troughs between SLP 660 and 600 as well as between SLP 360 to 540. Near SLP 185, a south-dipping normal fault apparently affects the Mesozoic series and the basement, as indicated by diffractions. Our interpretation puts the fault at the northernmost position possible.

Along profile SEAGR750008, the presence of low-frequency dipping reflections below the Mesozoic series is interpreted as an indication for a Permo-Carboniferous trough that may extend to the north all the way to the normal fault observed at SLP 185 on profile SEAGR790008.

The triangle zone within the Tertiary unit at the southern end of this profile is shown with realistic angles where the profile runs in a direction perpendicular to the structures. Unfortunately, the internal geometry of the triangle zone and of the Subalpine Molasse is poorly imaged along profile SEAGR790008. The internal thrust stack is here interpreted in a schematic conceptual way; individual thrusts may well be located elsewhere, but the interpretation respects the slight dip-changes and indications from reflection terminations.

The anticlinal feature observed in the Mesozoic unit between SP 200 and 250 may be a velocity pull-up artefact. This would involve velocity changes of almost 10 % over a distance of 5 km. The thrust stack (of possible high-velocity strata) interpreted on the bottom section is purely conceptual. An alternative interpretation was presented by Nagra (2008).

4.2.14 Transect 14: Nyon – Pfaffnau – Romanshorn (Enclosure 14)

Transect 14 crosses Cantons Vaud, Fribourg, Bern, Solothurn, Lucerne, Aargau, Zürich, and Thurgau, and it runs from the western end of the SMB (Lake Geneva) to its eastern end (Lake Constance). It comprises eleven seismic profiles of different surveys. They are many minor gaps (ca. 2 km) between the seismic profiles and a major one 5 km long, west of well Schafisheim-1. The west profiles are oriented SW–NE and the eastern profiles WSW–ENE; they follow the general axis trend of the main structures within the SMB along the southern border of the Jura fold-and-thrust belt. The length of this transect is 286 km. It is constructed with a vertical scale of 1:80 000 and a horizontal scale of 1:250 000; therefore, the structure geometry is vertically exaggerated by a factor of approximately 3. Thus this scale influences the apparent quality of the displayed seismic horizons. The horizontal compression makes some flexures appear as faults, and it generally makes reflections of quality classes 2 and 3 appear as higher quality-class reflections.

The transect intersects twelve dip transects from transect 02 to transect 13. Interpretations of seismic profile SADH780021 were published by Jordi (1993) and of the western part of profile SEAGU8507 by Nagra (2008). Transect 14 is controlled by nine wells distributed along the profile: Eclépens-1, Essertines-1, Tschugg-1, Hermrigen-1, Ruppoldsried-1, Pfaffnau-1, Altishofen-1, Schafisheim-1 and Lindau-1. Seven of these wells give significant information on deep horizons because they reach Triassic sediments or basement rocks. The transect shows seismic horizons of variable reflection quality from quality-classes 1 to 3. Using the well data we could upgrade the seismic quality-classes.

The thickness of the Tertiary unit varies depending on the location of the profiles (more external or internal relative to the SMB) and increases progressively from west to east. The top and base OMM horizons were interpreted in the eastern part at a few locations only, whereas in the easternmost area, these horizons correspond at some places to high-quality reflections and their interpretation is more continuous. The Tertiary unit lies discordantly on the Cretaceous unit to the west, but on Late Malm layers to the east. Cretaceous beds disappear east of Hermrigen-1, where 8 m of this unit only are present in this well. The transect shows progressive thinning of all Mesozoic units from west to east, from more than 3000 m to the west to less than 800 m to the east. Within the Early–Middle Triassic series, local thickness variations are observed on the seismic profiles; these are related to a detachment fold with local thickening of the series (Eclépens-1, Essertines-1, Tschugg-1, Hermrigen-1 and Ruppoldsried-1). To the west, these low-amplitude folds reach the surface as anticlinal structures oriented NW–SE such as the Mormont–Essertines anticline (near wells Eclépens-1 and Essertines-1). Steep reverse faults are associated with these structures, but other steep faults, with normal or reverse movement, unrelated to anticlinal structures are also observed.

In the western part of the transect, the seismic profiles display a series of tear fault zones: St-Cergue, Pontarlier–Aubonne, La Sarraz and La Lance–Font–Fétigny. These faults affect the entire Cenozoic and Mesozoic cover. Some of the faults belong to conjugate system Pontarlier–Aubonne (sinistral) and La Sarraz (dextral, Fig. 4.5). The seismic data show that the St-Cergue and La Sarraz fault zones include several splays, with fault plane quality-class 1 to 2. The Pontarlier–Aubonne fault zone, however, is represented on the seismic data by only one singificant quality class 1, fault plane. Yet, in most places, this tear-fault zone is characterized by a wide unreflective, deep-reaching zone. Across the fault zone, thickness changes are observed, small ones within the Malm, Dogger and Liassic beds and a large one within the Early–Middle-Triassic units. The latter are thicker on the western side of the fault, which may explain the higher elevation of the same beds on this side of the fault. At the base of the Mesozoic layers, there is a conceptual major décollement zone, where folds and faults root. This décollement zone extends to the east almost as far as Bassersdorf i.e. to the extension of the Lägeren fold, the last Jura anticline in the east.

In the eastern part of the Swiss Molasse Basin, no major structures are visible. Beds, especially Triassic evaporites, are thinner. Rare faults cut Mesozoic and Cenozoic sections, and a few of them offset the Mesozoic - pre-Mesozoic boundary. Near Romanshorn, a steep normal fault has a north-south trend (Müller et al. 2002, Nagra 2008), and it affects the whole cover with a marked offset.

Thick reflective zones are observed in the pre-Mesozoic unit on the west seismic profiles that show high-amplitude seismic facies at great depth, presumably coal-bearing Carboniferous sediments. In the central area, only one reflective zone in pre-Mesozoic rocks is observed, this is beneath Altishofen-1, whereas in the eastern part of this transect only intermediate zones occur.

4.2.15 Transect 15: Vevey – Entlebuch – Appenzell (Enclosure 15)

Transect 15 is a combination of fourteen seismic profiles that run more or less parallel to the axis of the Swiss Molasse Basin. These profiles were selected because they are the southernmost part of our interpreted profiles. The Transect extends from the Mt. Pélerin, north of Vevey, where it crosses the Basin axis to that itse northern flank, and it follows the edge of the Folded Molasse up to Lucerne where it zigzags in and out of the basin while keeping the general WSW–ENE trend. Several jump correlations were necessary to provide continuation, for example, near well Sorens-1, or to bridge gaps between seismic surveys, for example, to the east of Eggiwil (BE), west of Ebikon (LU) or between Schwyz and Morgartenberg (SZ). The transect is constructed with the same vertical and horizontal scales of Transect 14 resulting in a vertical exaggeration of approximately 3. The total length of the transect is 240 km.

Stratigraphic calibration of the seismic profiles along this transect is only available at a few locations. Wells Savigny-1, Servion-1 and Sorens-1 provide insight into the structure and thickness of the Tertiary units, whereas Romanens-1 gives additional information on Mesozoic units down to Middle Triassic strata. Well Linden-1 (TD within lower Keuper beds) and well Entlebuch-1 (TD within Carboniferous sediments) are the only wells to the south of the SMB that provide data on stratigraphic boundary depths and OWT times (and thus velocities) for the seismic interpretation. To the east of well Entlebuch-1, there is no calibration of Mesozoic or deeper strata in Switzerland. The next deep well lies in Austria southeast of Lake Constance.

The seismic quality of the profiles in the southern SMB is poor, not only because of the acquisitions parameters of

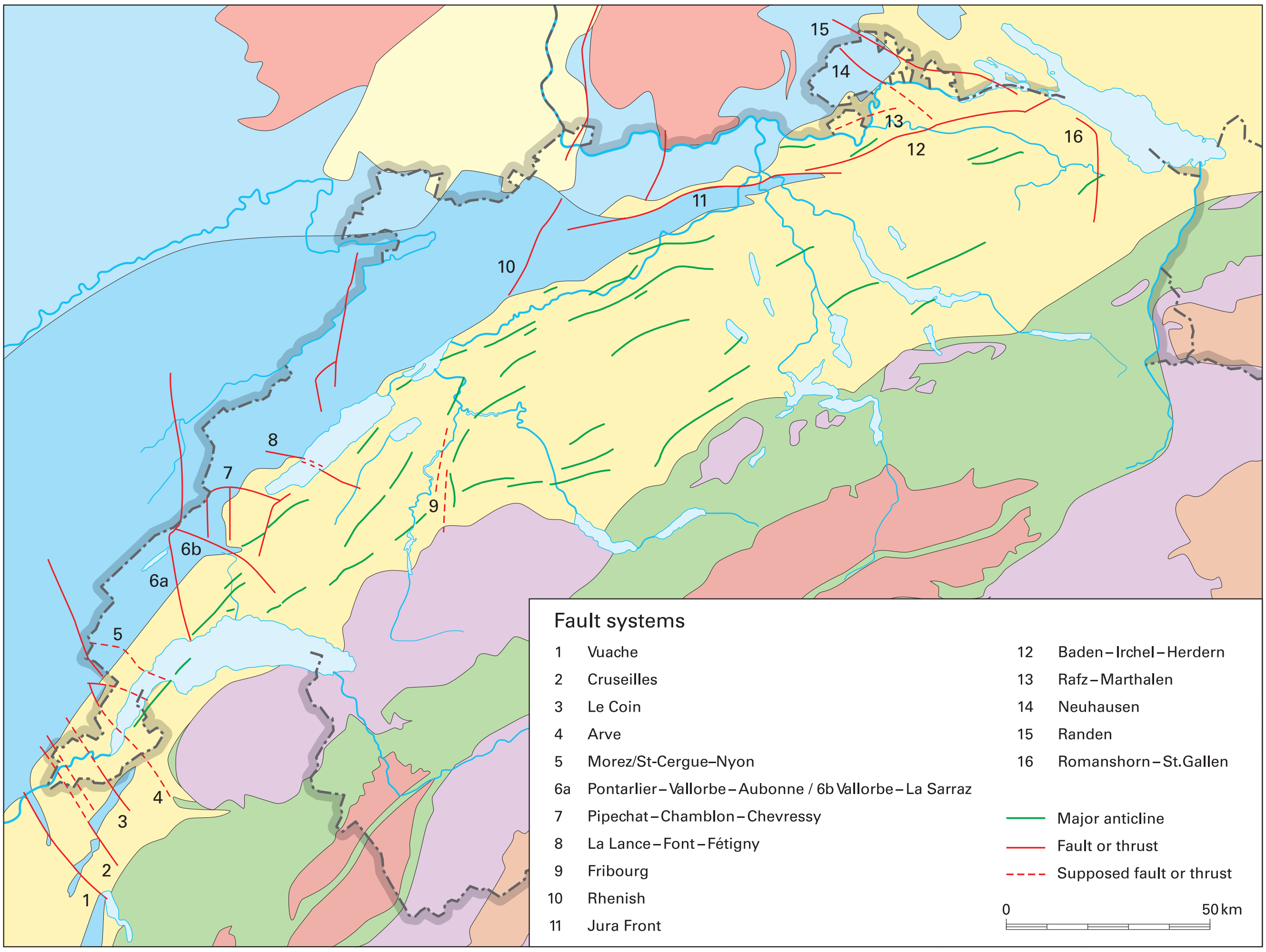

Fig. 4.5: Location map of main tear faults in the SMB (modified from Chevalier et al. 2010; for tectonic units see Figure 4.1).

the (old) surveys, but mainly due to structural complications within Tertiary units and orientation of the profiles that strike at low angle to the dip direction of the structures. Profiles BEAGBE.S70A / B010 and SEAGR750023 are examples of profiles with strong absorption and dispersion of seismic wave energy and therefore almost devoid of reflections from Mesozoic strata.

Nevertheless, some major changes along the basin axis are clearly visible. From west to east, the thickness of Mesozoic sediments decreases. The Cretaceous layer is totally eroded east of the Aare River. Originally, however, Cretaceous deposits extended at least as far east as well Entlebuch-1 as evidenced by remnants of Cretaceous sediments found in Malm karst pockets in the well. All Mesozoic units thin between the southern Canton Berne (Guggisberg) and Canton Lucerne (Ebikon). The NBTer horizon is often difficult to identify and follow, particularly in central Switzerland where it appears to be eroded. The separation between Early and Late Malm units must be considered with caution. This is especially the case near the city of Lucerne where poor-quality reflections dominate. Thickness changes of the Dogger and Liassic units along profiles SADH780023, FR.S750006 and FR.S74A001 are related to the massive sedimentary accumulation to the NW and thinning towards SE whereas thickness variations of the Triassic units may be influenced by tectonic strains. The top of Middle Triassic carbonates (Muschelkalk and Rötidolomit) creates what appears to be the strongest seismic signal in central and eastern Switzerland. Within Permo-Carboniferous units, reflectivity zones were identified near wells Savigny-1 and Romanens-1 and between SLP 126 and 300 on profile FR.S74A001. Such highly reflective zones are also observed in the Entlebuch area where Permo-Carboniferous rocks were found in well Entlebuch-1. Potentially, more Permo-Carboniferous sediments may be present. They are only identified locally as reflectivity zones of uncertain extension because of their poor seismic quality.

Many small structures that offset Mesozoic horizons are interpreted along the poor-quality profiles. Some horst and graben structures are apparent, but also many small thrusts are observed on intersecting profiles that appear to point to the north and more rarely to the south. There is no structural model to support these observations; they are drawn as we interpret them. They seem to end in Triassic evaporites because they cannot be traced further down. The transect nicely images the Linden anticline structure, but unfortunately it does not go through the structure where well Entlebuch-1 is located. The transect crosscuts the triangle zone of the Subalpine Molasse at various angles (e.g. profiles LEAGLUZN770024, SEAGR770031 and SEAGR750023). Under Arth and Morgartenberg for example, this directional change results in opposite dips. The «M»-shaped structures within the Molasse near Egg also comes from changes in the profile direction. Along some profiles (LEAGLUZN770024, SEAGR760028 and SEAGR750016), the top of the Tertiary triangle structure is strongly squeezed and steepened, and therefore it is not observed on the seismic profiles. When extrapolating the few dipping features in the southern part of the triangle roof, however, these structures could be interpreted as dominant north-pointing thrust that reactivated the south-dipping thrusts at a later stage of compression. This hypothesis has not been expressed so far in the literature. The unconventional presentation of this transect in the strike direction prompts questions about the geometrical logic of structures within all stratigraphic levels. This underlines our still limited understanding of the structure in this region. For more information in the area of Transect 15, see also Micholet (1992), Greber et al. (1994), Naef (1999), Habicht (1945) and Pfiffner (2009).

4.3 Wells

Information on all available and known deep wells in the SMB was gathered and checked for its utility to calibrate the interpreted seismic horizons. To control the basin stratigraphy we used forty-three deep wells. Thirty-four wells contributed directly to the seismic interpretation (see Enclosure 16) and thirty-three of them to the definition of velocities. Ten wells were used for the evaluation of the pre-Mesozoic units. Wells are not ideally distributed in the SMB; in the Subalpine Molasse area and in the eastern SMB there is scarce or no information at all (see Figure 2.1).

We gathered information on the wells from the literature and from unpublished reports (see appendix 2.5). Although well data have been published in scientific papers more often than seismic sections, they are not always useful for calibration since velocity data is often missing. We did not reinvestigate the stratigraphy of wells in our work. The lithological descriptions and even the nomenclature adopted by different authors are not always consistent; therefore some correlations between wells may be uncertain. Many wells were drilled for hydrocarbon exploration and are located on geologically high structures such as anticlines, pop ups, horst blocks; and as a result almost no data exist on syncline structures. Therefore, the stratigraphical thicknesses reported from wells can either be reduced by erosion and non-deposition or be thickened by thrusting and salt flow.

On the well penetration chart (Enclosure 16), we present the stratigraphic column of thirty-three wells. The wells are graphically aligned at the Base Tertiary boundary in order to highlight thickness differences between the Cenozoic units on one hand and Mesozoic and pre-Mesozoic units on the other hand. Correlation between wells runs from west to east between five groups and from north to south within each group. These may contain 2 to 9 wells. Wells are displayed vertically from ground elevation, using the total vertical depth (tvD, see paragraph 3.2.2) when available, and assuming small deviations for wells with only along hole depth (ahD). For specific details on the wells, TWT intervals, and calculated velocities, refer to paragraph 3.3.

Wells are displayed on transects (see Enclosures 03 to 15) for the geophysical and geological interpretation. The detailed correlation between stratigraphic boundaries in wells, the nearest seismic profile and the interpreted seismic horizons is shown in Appendix 2.5. This appendix also includes general information on the wells and the data used to calculated velocities in the interpreted units.

4.4 Main units and their boundaries in the Swiss Molasse Basin: a geological description from well and seismic data

Eight seismic horizons have been interpreted that correspond to the top or the base of units that are main stratigraphic systems and epochs (lithological groups and super groups, see Remane et al. 2005). In the following sections, each unit is described separately together with its boundaries in geological terms based on well data and on seismic characteristics observed across the entire SMB. Where data resolution permits, we address certain details, but we do not interpret sequence stratigraphy or describe seismic sequences based on unconformities (Mitchum & Vail 1977, Mitchum et al. 1977) or on maximum flooding surfaces (Galloway 1989).

We present units from top (youngest) to bottom (oldest); they are first described based on the well data and then on their seismic characteristics. For a geological description of the units based on previous knowledge the reader is referred to chapter 1. Details of the Quaternary unit were not a focus of this work, and they are therefore not addressed here. We treat the Quaternary and Tertiary units together in the seismic interpretation, and both units are not distinguished either in cross sections or in the different calculated maps (see chapter 5).

4.4.1 Tertiary unit and Near Base Tertiary horizon (NBTer)

Tertiary units have been penetrated by about thirty wells (Enclosure 16), i.e. more than any other deeper unit in the SMB. Their base is therefore the best constrained boundary. Thickness of the drilled Tertiary wedge strata in the Basin ranges from 0 m (erosion contact with the Jura Mountains) at the northern border of the SMB to 5100 m (Thun-1 well) in the outcrop area of the Subalpine Molasse in front of the Alps. The southernmost parts of the SMB are covered by Alpine thrust sheets, e.g. frontal Ultra-Helvetic, Helvetic and even Penninic units. Therefore, the transition from Molasse-type strata into North Helvetic Flysch south of the Subalpine Molasse unit is not very well known. The northern limit of Tertiary sediments coincides with the limit of the erosional wedge in the foothills of the Jura Mountains. The age of the onlapping sediments becomes younger from south to north. However, in the proximal part, i.e. along the southern border of the SMB, there is strong internal deformation observed in outcrops and wells. The Tertiary unit lies on Cretaceous beds in the western SMB, whereas in the central and eastern SMB it rests on Late Malm unit.

The NBTer seismic horizon corresponds to the foreland unconformity (see Figure 1.4). It is clearly visible on most seismic profiles. It is the limit between a heterogeneous, sometimes chaotic, seismic unit with local onlap configuration at the top (i.e. Molasse sediments) and a set of clear, high-amplitude horizons of the Mesozoic layer-cake stratigraphy at its base. The quality of the NBTer reflection depends on the lowest lithology of the lowest Tertiary strata and on the level of erosion of Jurassic and Cretaceous sediments below them. To the north, the impedance contrast is weak between the USM layers and the Cretaceous unit. To the south the impedance contrast is stronger due to the presence of UMM layers. In the western SMB, the NBTer horizon is a fairly high-amplitude reflection due to the underlying hard Cretaceous limestone unit, whereas in the eastern part the eroded Malm gives a less-pronounced seismic impedance contrast and therefore weaker reflections.

Although stratigraphic subdivisions of the Tertiary formation (OSM, OMM, USM, UMM) are documented in most wells, these groups were not interpreted consistently throughout the basin in this work. The low resolution for these intervals on most of the seismic profiles did not allow a regional correlation of different horizons. Quality class 1 reflections are rarely observed. The Upper Marine Molasse (OMM) stands out in some seismic profiles as a band of clear, continuous high-amplitude reflections whereas the seismic signature of the OSM varies strongly and is often influenced by surface weathering zones or irregular and locally deep Quaternary accumulations. Seismic reflections within the lower fresh water Molasse (USM) are interpreted as low continuous clastic channel units, coarse-grained fan systems and shoreline deposits (Strunck 2001). Top UMM and base and top OMM are indicated on some transects for clarification of the overall structure of the Tertiary units. On some transects, especially where those markers are absent, an intra Molasse reflection (e.g. intra USM, near Top Chattian–Base Aquitanian, in Transect 04) was locally interpreted to clarify regional structures. In the Subalpine Molasse, no stratigraphic horizon was interpreted. A few papers present local interpretations (SMB western part: Signer 1992, Gorin et al. 1993; SMB central part: Strunck 2001; SMB eastern area: Diebold et al. 1991, Kempf & Pfiffner 2004, Stäuble & Pfiffner 1991), but they are too spread apart to enable lateral correlations at the SMB scale.

4.4.2 Cretaceous unit

In general, Mesozoic sediments show strong reflections where shaly series alternate with thick limestone or dolomite beds (e.g. Early Triassic and Middle Jurassic unit). Less reflective sediments are shaly evaporites (e.g. Triassic beds) or Malm reefs. The Jurassic series (Malm, Dogger, and Liassic) is rather well organized with several regressive sedimentary cycles, the top of which produce some of the strongest reflections within the SMB.

The Cretaceous unit was identified only in 14 wells in the western part of the SMB. The well penetration chart (see Enclosure 16) shows the west-east wedging out of the Cretaceous strata, with its thickness (from well data) decreasing from 380 m (Humilly-2 well in France) to 8 m (Hermrigen-1). The eastern limit of the Cretaceous sediments in the SMB is an erosional limit. Wells Ruppoldsried-1, Thun-1 and Linden-1 do not include Cretaceous strata because of the pre-Miocene erosion of the rather thin accumulation of coastal sediments of presumably Early Cretaceous age. Lower Cretaceous (Hauterivian) erosional remains are known from karst pockets as far east as Entlebuch-1, whereas Late Cretaceous sediments are mainly encountered in the westernmost drillholes of the basin, e.g. Humilly-2. In the Geneva basin and the Jura Mountains, the top of the Mesozoic substratum includes karst pockets filled with siderolitic sediments (Charollais et al. 2007). The absence of Cretaceous layers to the north of a line between Biel and Besançon is explained by a close shoreline and non-depositional area; their absence to the east of the Aare River seems to be caused by post Cenomanian (Late Cretaceous) uplift and erosion (Stampfli et al. 1998).

On the seismic data, the Cretaceous unit can be followed only over the western part of the SMB (see Enclosure 17). It disappears in Canton Bern along a north-south oriented zone west of the Aare River. Cretaceous strata are limited at the top by the NBTer horizon and at the base by the NTLMa horizon. The Cretaceous layers show few strong reflections. The seismic profiles indicate that their presence is restricted to an area SW of a line running approximately through the cities of Besançon, Biel and Thun. In most parts of Cantons Vaud and Fribourg, two seismic reflections can be distinguished. The internal structure shows discontinuous packages. It is not clear if those are separated by faults and thrusting or by sedimentary architecture and facies distribution changes. The thickest Cretaceous section is preserved in the Geneva Canton where limestones and marls give rise to three or four high-amplitude reflections.

4.4.3 Late Malm unit and Near Top Late Malm horizon (NTLMa)

Late Malm strata (Tithonian–Portlandian facies, and Kimmeridgian) are present in many drillholes, but the most complete series are preserved in the wells that encountered Cretaceous beds on top, i.e. in the western SMB. This means that in most wells, the Late Malm strata were eroded. The remaining Malm thickness is about 400 – 500 m to the west and decreases to about 200 m to the east and south. The maximum stratigraphic thickness is found in Humilly-2 (830 m). In well Cuarny-1, 1015 m of Late Malm strata were drilled because of layer doubling to due to a thrust fault.

The Near Top Late Malm (NTLMa) seismic horizon (more specifically, the top of the Tithonian limestones) is sometimes marked by a clear double reflection (Transects 04, 06), whereas the homogeneous limestones of the Kimmeridgian layers do not show strong internal reflectivity. More often the seismically heterogeneous Kimmeridgian series grades upward into discontinuous shingled reflections of somewhat higher amplitude. In the western part of the SMB, the Top Late Malm reflection is picked between the two «Cretaceous reflections» and the two «Top Late Malm reflections»; it is a strong and well-defined reflection (e.g. Transect 03). The homogeneous underlying Kimmeridgian is an unreflective facies that appears to thicken towards the deeper parts of the SMB. Some reef geometries can be distinguished in the main basin. In general, there are more parallel low-amplitude reflections to be found in the deeper part of the basin. In the eastern SMB, the thickness of Late Malm unit decreases, and it is represented on the pre-1984 seismic profiles by two reflections only. The pre-Miocene erosion reduced the Top Malm strata in the Aargau and Zürich area down to the Sequanian level (Upper Oxfordian).

4.4.4 Early Malm unit and Intra Early Malm horizon (IeMa)

The Early Malm strata show a more or less constant thickness of 200 – 300 m in the western and central parts (in the Rauracian realm), and they thin to the east and the south. At its base, they are marly or calcareous rocks in the west and more shaly rocks in the east (36 m in Kreuzlingen-1). In the Late Malm stratigraphy, it is difficult to separate the Sequanian (upper Oxfordian limestone) from the proper Kimmeridgian limestone. In most outcrops, a lithological cyclicity is observed which is best visible in the area between Yverdon and Solothurn where marly intervals alternate with limestone beds.

The Intra Early Malm seismic horizon (IeMa) is a reflection of highly variable strength. On Transect 03 this horizon is characterized by a strong almost continuous reflection whereas on Transect 11 it is a weak reflection or entirely absent. It lies at the top of the unreflective Early Malm series. This intermediate horizon coincides with the top of the first two seismic cycles of the Oxfordian marly sediments. It lies below the stratigraphic base of the Late Malm unit within the Oxfordian (Sequanian) limestone series. The Early Malm unit is characterized by small seismic amplitudes. The Early Oxfordian series progrades down in the western Swiss Molasse Basin, and the IeMa horizon disappears into a downlap configuration. The Oxfordian shales («Argovian beds», Effingen or Villigen formations) consist of marly cycles that become richer in limestone and grade upwards into the heterogeneous carbonate of Late Oxfordian series. This package seems to accumulate in the western and central areas, and it thins to the south and to the east, where only a single reflection is observed.

4.4.5 Dogger unit and Near Top Dogger horizon (NTDo)

The thickness of the Dogger beds in wells is variable, and the Late Dogger beds mainly thin from west to east. In some drillholes, thickening is due to tectonic complications (Eclépens-1, Courtion-1). The thinning of the Dogger to the south is particularly pronounced: from more than 500 m thick strata in the Courtion-1 and Hermrigen-1 wells, only 50 m remain in the Thun-1 and Entlebuch-1 wells. At the top of the Dogger units, the «Dalle nacrée» formation that consists of biodetrital limestones, contrasts with the overlying marly Oxfordian (Early Malm) strata. At the base of the Dogger unit, argillaceous beds of the Aalenian «Opalinus Ton» thicken to the east and to the north.

The contrast between the marly Early Malm and the Dogger limestones yield some of the most continuous and strong seismic reflections in the entire Swiss Molasse Basin. The Near Top Dogger (NTDo) horizon is very well defined. Below, within the Dogger unit, we observe two to three high-amplitude reflections parallel to the NTDo horizon. The Late Dogger sedimentary package progrades into the Basin, causing a stack of downlapping horizons. The uppermost reflection that was mapped at the northern edge of the basin becomes the second from the top in the centre of the basin. The underlying seismically transparent zone represents the Aalenian Opalinus Clay. The southern part of the SMB shows the thinnest Dogger series. This is interpreted as a reduced accumulation on the extension of the Early Jurassic high zone of the «Alemannic Land» (see Figure 1.4). At the southernmost part of the SMB, the NTDo horizon is less well defined (e.g. on Transect 03), due to the drastic change of lithology and thickness of the Dogger unit.

4.4.6 Liassic unit and Near Top Liassic horizon (NTLi)

The limit between the Aalenian series (lowest stage of the Dogger unit) and the Liassic series is not always obvious to detect from drill-hole cuttings. Twenty-one wells (Encl. 16) reach the base of the Liassic unit. Liassic sediments are thickest in the southwest (440 m in Humily-2), and they thin to the east and the north (20 m in Herdern-1). They are generally thinning to the SE too and are probably absent south of Lake Lucerne and further east. To the SE of the SMB, palaeogeographic evidence from outcrops suggests a high area of low relief «Alemannic Land» (Trümpy 1980, Figure 1.4).

The seismic facies of the Liassic limestone series shows up to five low to medium-amplitude reflections of regular frequency with varying strength in the western SMB. The uppermost seismic horizon that we mapped becomes clearer as the amplitudes of the Middle Liassic diminish on the Basin flank. The package thins from north to south and from west to east. The Liassic unit is reduced to one single reflection in the southern part of the SMB. Thinning starts to the east of the Sarine River (see Transect 11), and it continues all the way up to the eastern border of Canton Bern. Thickness changes also reflect early salt movements.

The NTLi horizon is well defined on Transect 03 where its shows up as a high-amplitude reflection that is continuous along all seismic profiles, except to the south of the SMB. It coincides with a high seismic impedance contrast with the underlying fairly reflective but well bedded Late Liassic sediments. In the eastern part of the basin, however, the NTLi reflection is weak (see Transect 11). Along this transect, a negative seismic amplitude (as opposed to a positive one in the normal case) was followed for practical interpretation reasons along great distances on profile SEAGR80999.

4.4.7 Late Triassic unit and Near Top Triassic horizon (NTTr)

The stratigraphy of all Triassic layers and their correlations from well to well are difficult to establish for two reasons. First, only 15 of the 25 wells that reached the Triassic unit drilled through the entire Triassic series (12 of them are shown on Enclosure 16). Second, tectonic complications resulted in thinning or thickening, and even doubling of the layers (e.g. resulting in a thickness of 1071 m in well Treycovagnes-1), and such complications appear to be omnipresent in the evaporite layers. This has been interpreted as evidence for a main detachment level (Buxtorf 1907, Heim 1921, Laubscher 1961, Sommaruga 1997). The Triassic sediments of the SMB can best be compared with the German facies that is subdivided into three lithostratigraphic units of different age, from to top to base: Keuper with Rhaetian rocks on top (Late Triassic), Muschelkalk (Middle Triassic) and Buntsandstein (Early Triassic). In the two first formations, anhydrite, gypsum, salt, shales and dolomite alternate (for details see Jordan 1994).

The top of the heterogeneous Triassic series (NTTr) coincides with a strong seismic reflection caused by the lithified Keuper dolomites and by the Rhaetian sandstones that are underlying the marly facies of the Early Liassic beds. To the east of the SMB, the NTTr horizon becomes a relatively weak reflection of variable amplitude (e.g. in the northern part of Transect 11,), while the underlying Late Triassic unit, composed of internal dolomite banks and Schilfsandstein, is reflective and well bedded.

The total vertical thickness of the complete Triassic series reaches a maximum of 750–1000 m at the northwestern limit of the SMB within the first Jura folds. It decreases progressively to the south (see Transect 03) and to the east (Transect 14 and see Figure 5.3). Thickness variations are observed in Late Triassic clastic-carbonate mixed layers although at a lesser degree. These variations appear to reflect early salt movements due to differential loading or subsidence movements. The top series of the Keuper and Rhaetian sediments are often less tectonically disturbed than the Middle–Early Triassic, and they form a package of layer-cake strata. Locally Keuper salt is found, but the Muschelkalk salt in the western and central part of the SMB (see next section) is the most important ductile horizon.

4.4.8 Early–Middle Triassic unit and Near Top Muschelkalk horizon (NTMuka)

Few wells were drilled through the complete Early–Middle Triassic unit and reach the Base Mesozoic surface. In the western and central areas of the SMB, only 4 wells shown on Enclosure 16, drilled this unit. The series between Trigonodus dolomite at the top and the Buntsandstein sediments at the base include variable lithologies. In the western and central parts of the SMB, the Muschelkalk evaporite and salt layer is the most important ductile horizon.

The interpreted intra Triassic seismic horizon lies close to the top of the Muschelkalk facies (NTMuka), and it is an extrapolation of the earlier defined «Top Triassic Unit 2» horizon in the western part of the basin (Sommaruga 1997). In northern Switzerland, where seismic profiles and wells were thoroughly investigated by Nagra and compared to regional and local stratigraphy, there is better understanding of the seismic stratigraphy. The top Muschelkalk horizon, Trigonodus dolomite, causes the most prominent signal over wide areas. This horizon lies at the top of the unbedded Early–Middle Triassic seismic unit, presenting discontinuous and oblique reflections. Important thickness variations also due to tectonic activity are observed in the Middle–Early Triassic unit.

The Middle Triassic series contains evaporites and salt that form gentle accumulations (pillows) in the core of anticlinal structures (evaporite-cored detachment folds). Dolomite and shale packages floating in the evaporites cause a rather high-amplitude chaotic seismic expression. We therefore define the Near Top Muschelkalk horizon (NTMuka) as the upper envelope of a package of variable thickness. At the base of the Middle Triassic series, clastic sediments include calcareous sandstones that contrast with the less sorted Late Permian sediments or the altered crystalline basement surface. Locally, an angular unconformity is visible at the base of the Triassic unit.

4.4.9 Pre-Mesozoic units and Near Base Mesozoic horizon (NBMes)

Pre-Mesozoic units consist of Paleozoic series (Permian and Carboniferous sediments) or of Paleozoic and Precambrian crystalline basement.

Permian sediments were drilled in only 4 wells in the Swiss Molasse Basin (see Enclosure 16) and in 6 wells in the northern and western close surroundings of the SMB. Permian sediments outcrop at the northern rim of the Molasse Basin as well as in the Alps (Swisstopo 2005a). In several wells of northern Switzerland, Permian redbeds, shales and acid volcanoclastics were drilled e.g. in the Weiach-1, Riniken-1 and Kaisten-1 wells. Thin accumulations of crystalline basement (presumably weathering products) were found in wells such as Pfaffnau-1 (Enclosure 16), Buix-1 and Humily-1. The 410 m thick conglomerates drilled in well Treycovagnes-1 were also attributed a Permian age (Petroconsultant database, Otto 1974). They may, however, also contain Carboniferous sediments (Shell, 1978).

Carboniferous sediments are known from the southern rim of the Swiss Molasse Basin in the Alps (Swisstopo 2005a) and were drilled in the wells of Weiach-1 and Entlebuch-1. Close to Switzerland, Carboniferous graben sediments were reached by wells in Germany and France e.g. in Essavilly-1 in the Plateau Jura (Sommaruga 1997) and Humilly-2 (see Enclosure 16).

The crystalline basement of the SMB is rather well understood in northern Switzerland where several wells testify to the heterogeneous crystalline lithologies of Upper Palaeozoic age (Thury and Diebold 1987). Some wells penetrated up to 1400 m of crystalline rocks (Leuggern-1, Böttstein-1, Siblingen-1, Kaisten-1, Weiach-1, see Appendix 2.5 and Enclosure 16). The most frequent situation shows gneiss and granitic basement with fractures and varying degrees of alteration. Radiometric age dating of the crystalline basement ranges from Precambrian to Early Palaeozoic. There are no Mesozoic or Tertiary intrusions known within the Molasse Basin, with the exception of the volcanic intrusions in the nearby Hegau area (Southern Germany; see Figure 1.3 a).

The Near Base Mesozoic seismic horizon (NBMes) is fairly well to poorly defined. Its amplitude is generally weak. It is characterized by the contrast between the overlying reflective Early – Middle Triassic unit and the poorly reflective pre-Mesozoic seismic unit. On some seismic profiles, the NBMes horizon lies at the bottom of the Triassic seismic unit showing well-defined oblique reflections. It is best defined where it presumably overlies crystalline basement. It is more difficult to define where it overlies a reflective or an intermediate reflective zone of possible Permo-Carboniferous sediments.

The accumulation of terrestrial clastics in limited and separated extensional basins can be confirmed after further interpretational work beyond this study. Basin infill is, however, recognized on few seismic-profile segments. Three areas do show strong reflections with high impedance contrasts, which most likely are due to Carboniferous sediments containing coal beds and fluvial clastics. We discuss these in more detail below.

1) The large Permo-Carboniferous trough of northern Switzerland, between Schaffhausen and Basel, was first drilled by Nagra and is best described in their own reports (Sprecher & Müller 1986; Diebold & Naef 1990; Diebold et al. 1991). We can only confirm those observations and use the well data for calibration. The seismic data also show the presence of troughs that are complicated by strike-slip faulting.
2) The Subalpine trough, drilled in Entlebuch-1, seems even more complicated by Alpine thrust movements. Its southern limit is difficult to image seismically because of complex thrust tectonics (Transect 08, Enclosure 8, Profile LEAGLUZNR880998).
3) The visible parts of the western SMB trough are rather flat ramps. In Cantons Geneva and Vaud, strong and deep-reaching reflections are presumably caused by Carboniferous fluvial clastics, shales and coal seams accumulated in rather narrow grabens with steep borders.

The rest of the basement ramp in central and eastern Switzerland only shows a few areas that may contain Carboniferous sediments. Some weak pre-Mesozoic reflections observed on old seismic profiles are often not supported by intersecting profiles.

5. 3D Geological Model of Swiss Molasse Basin

We define our geological model from the surface down to the Near Base Mesozoic (NBMes) horizon based on eight interpreted seismic horizons. At the surface, the model corresponds to the area of the Swiss Molasse Basin (SMB) where seismic data can be interpreted with a reasonable degree of confidence (see chapter 4). In this chapter, we present the geological model through a series of surface maps for each interpreted horizon, 3D views, and a series of superimposed depth-converted profiles. This offers a synoptic view of the SMB's interior. At the surface, the limits of the geological model are defined as shown in Figure 5.1.

5.1 3D surface maps of the interpreted horizons

The surface maps of the eight interpreted seismic horizons (two-way traveltime, velocity, depth and vertical thickness) are displayed at scale 1:1250 000 (see Enclosures 17 to 21). These maps emphasize basin features at a regional scale. At local scale, of course, the structures are more complex. The maps are based on smoothed calculated grids (see paragraph 3.4) using the interpreted seismic profiles, and they are locally constrained by surface geology such as the edge of the erosional limit of Tertiary or Cretaceous sediments to the north.

An area located to the north of Transect 14, near Transects 10 and 11, and south of wells Weiach-1 and Eglisau-1 could contain unreliable map values. The prominent Lägeren structure with stacked Mesozoic layers observed on Transect 10 strongly influences the surface map calculations to the west and to the east of the transect, in areas that are not constrained by seismic interpretation. These areas are cross-hatched on two-way traveltime (TWT), depth, and thickness maps to indicate that the data there should be considered with caution.

5.1.1 Two-way traveltime maps (Enclosure 17)

The TWT maps were calculated by interpolation between seismic profiles or erosion limits using a gridding algorithm described in chapter 3 (see paragraph 3.4.1). The maps show surfaces that dip with an angle of a few degrees towards the southeast. To the west of the SMB, from Canton Geneva up to well Hermrigen-1 and the Aare River, the general direction of the horizon surfaces is NE – SW with minor local variations. In the central and eastern SMB, however, the isoline direction is ENE – WSW.

To the north, the erosion limit of outcrops (from Tertiary and Late Malm beds) represents the limit of the grid for the Near Base Tertiary and Base Cretaceous / Near Top Late Malm maps. The Near Top Late Malm (NTlMa) horizon is

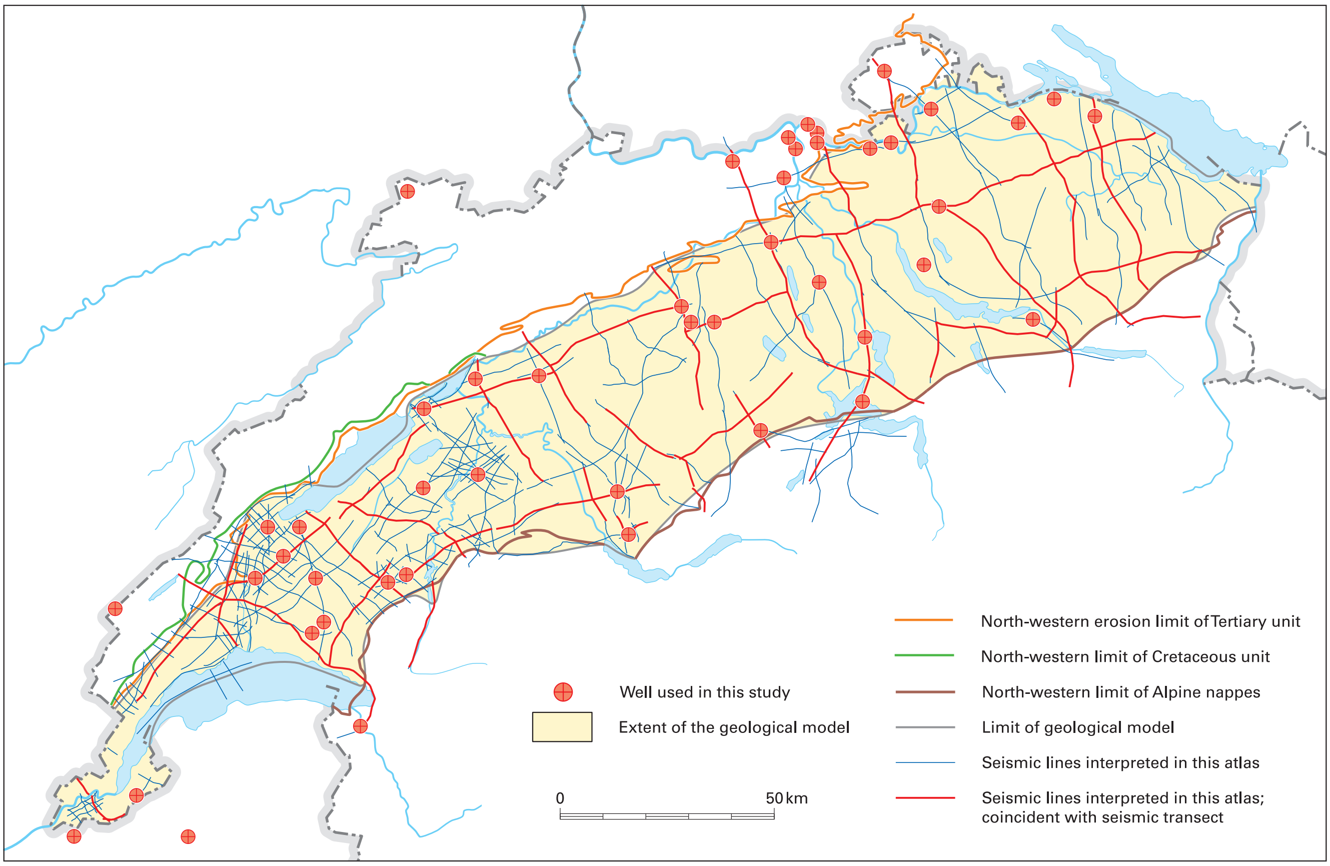

Fig. 5.1: Surface extent of the geological model (in light yellow) as defined in the Atlas. Its limits were defined depending on the grid of interpreted seismic profiles, on the profile quality, and on the boundaries of geological units (Tertiary and Cretaceous units, Alpine nappes). For the identification of wells, see Enclosure 01 and Figure 2.2.

present only where we could identify Cretaceous layers, i.e. from Canton Geneva up to the Aare River in Canton Bern (see also Cretaceous unit in wells in Enclosure 16); further to the northeast, Cretaceous layers are absent.

5.1.2 Velocity maps (Enclosure 18)

For each interval between the interpreted horizons a seismic velocity map was computed by interpolating the velocities calculated from the well data between well locations and by extrapolating to additional constraint points (for more details see chapter 3, paragraph 3.4.2). Velocities vary from 2500 ms^{-1} to more than 6000 ms^{-1}, and increase gradually toward the southeast along a general ENE–WSW direction. The Cretaceous unit map has velocity isolines that follow a N–S direction. The Late Malm and Middle–Early Triassic units map have higher velocities than the other units. We explain this by noting the rock types they comprise: limestones in the Late Malm unit and evaporites (anhydrite and dolomite) in the Triassic unit.

5.1.3 Depth maps (Enclosure 19)

Depth maps of eight seismic horizons are shown in Enclosure 19. They result from the depth conversion of the TWT maps (Encl. 17) using the velocities of Encl. 18. The same colour scheme was used for all units to enable comparisons between maps. Reference elevation of the maps is mean sea level (amsl). Consequently, areas with elevations above this level have positive values; areas below it have negative values.

At the scale of the SMB, Mesozoic layers dip almost regularly towards the southeast at an angle of 5° in the area of Lake Zurich and from 4° to 3° in the area south of Lake Neuchâtel. These dips show the distribution of the Tertiary unit thickness (see paragraph 5.2.4). The Near Base Tertiary surface dips from a depth of +700 m to approximately -4000 m. Similar to the TWT maps, the isoline direction is ENE–WSW in the eastern and central part of the SMB up to a line running from well Hermrigen-1 to the Aare River. West of this line, in Cantons Fribourg, Vaud and Geneva, the direction of the isolines is NE–SW. The depth map of the NBMes horizon shows a smooth surface with wider isoline intervals, especially in the western SMB, corresponding to a low dip angle of 3°. No major differences in the structural trends are observed between the TWT maps (see Enclosure 17) and depth maps (see Enclosure 19).

In the northern part of Canton Vaud around wells Treycovagnes-1, Essertines-1 and Eclépens-1, the depth maps (e.g. Near Top Dogger horizon) show an almost flat area. In the southern part of Canton Vaud, near the east end of Lake Geneva, the horizons rise southwards, and they define a syncline with axis parallel to the Alpine front. At local scale, changes of direction are observed, for example, south of Lake Neuchâtel. These changes are related to a major fault system oriented NS (e.g. the Pontarlier tear fault zone) or NE–SW (e.g. the La Sarraz fault) as shown in Figure 4.5. Seismically defined faults are discussed in paragraph 5.2.

To provide an independent assessment of the depth maps presented in this Atlas, depth values at all well locations were extracted from the horizon grid (blue on the map) and compared to the elevation value (red on the map) measured in wells. Because the two sets of values are quasi-independent from each other, depths do not perfectly coincide; indeed, the approach used in this Atlas does not force the horizons to intersect the well discontinuities. The mapped seismic horizons are defined by their regional expression (see paragraph 3.2.2) and do not necessarily coincide with their corresponding stratigraphic markers in wells. In some cases, large discrepancies can be explained by either a deviation of the well from the vertical direction or by the presence of faults or folds that result in strong horizon topography in the vicinity of the well. This is for example the case for wells Eclépens-1 and Thônex-1. Three-dimensional views of three depth-converted horizons (Near Base Tertiary, Near Top Dogger and Near Base Mesozoic) are shown in Figure 5.2.

5.1.4 Vertical thickness maps (Enclosure 20)

Vertical thickness maps of the eight interpreted units are presented in Enclosure 20, whereas vertical thickness maps of the entire Mesozoic strata and of Triassic beds are shown in Figures 5.3 and 5.4. The term «vertical thickness» is preferred over «isopach» because the unit thickness is measured vertically. In case of dipping layers, the real stratigraphical thickness is less than the vertical thickness.

Quaternary and Tertiary unit thickness map

This map shows thicknesses calculated between the surface topography and the Near Base Tertiary horizon. The map highlights the Tertiary wedge that thickens in the NW–SE direction from 0 m to over 5500 m.

Cretaceous unit thickness map

Cretaceous layers thin progressively from the Geneva basin (> 300 m) to the northeast, where they disappear along the Aar Valley between Lake Thun and well Hermrigen-1 well. No Cretaceous strata are observed eastward of this valley. Isolines are oriented NNW–SSE.

Late Malm unit thickness map

The Late Malm unit progressively thins from Lake Geneva (>1000 m) to Lake Constance, in a direction parallel to the axis of the SMB. Isolines are oriented NW–SE. Minimum thickness values (< 50 m) are located between Lake Lucerne and Lake Zurich.

Early Malm unit thickness map

At basin scale, The Early Malm strata progressively thin from Lake Geneva to Lake Constance. Isolines are oriented NNW–SSE. At local scale, patches of thinning are observed, indicating irregular thinning of the sedimentary basin facies.

Dogger unit thickness map

This map shows progressive thinning of the Dogger layer to the east and the south from > 600 m to 50 m. Isolines trend mainly NE–SW, a direction different from the direction in the maps described above. The Dogger beds are the thickest between Lake Neuchâtel and Lake Geneva. Zones of local thickening such as near well Cuarny-1 are due to the presence of thrust-related structures leading to a doubling of the beds. Strata are also thicker along the Jura Mountains (e.g. Canton Vaud) and decrease towards the central and east part of the SMB.

Liassic unit thickness map

This map highlights a major difference between the eastern and western regions of the SMB. The east and the central parts of the Basin have very thin Liassic sediments. To the WNW, the thickness of Liassic strata increases regularly from a line from the east end of Lake Geneva to Lake Biel. The maximum thickness is encountered along the first Jura folds of Canton Vaud (north of Lake Geneva). In that area, presence of thrust faults and thus tectonic thickening cannot be excluded.

Late Triassic unit thickness map

Late Triassic beds thin from west (> 400 m) to east (< 100 m) across the SMB. Locally, e.g. in Cantons Vaud and Fribourg, zones of thickening or thinning are observed with a patchy distribution; no obvious trend is visible.

Middle–Early Triassic unit thickness map

This map shows important variations of vertical thicknesses from east to west. In the western SMB, between Lake Geneva and Lake Neuchâtel, values range from 300 m to more than 900 m. In addition to a thickening to the northwest, there is a series of elongated lows and highs that alternate at a 5–10 km scale trending NE–SW. These highs correspond to stacks of evaporites, salt, and clays in the core of gentle anticlines. In the central and eastern parts of the SMB, thickness variations are very small, ranging from less than 50 m to 250 m. No particular trend is observable. This particular vertical thickness map is one of the most relevant for the understanding of anticline and syncline structures within the SMB. The conceptual décollement zone is located in this unit and it disappears in the eastern part of the SMB (see Transects 14 and 15, Encls 14 and 15). The unusual thickness of the unit in the above-mentioned unreliable zone to the east of the Lägeren should be disregarded.

Mesozoic unit thickness map

The vertical thickness map of the entire Mesozoic cover (from Cretaceous to Triassic layers) illustrates the thickness contrast between the western, central, and eastern parts of the SMB (see Figure 5.3). Thicknesses in the Geneva, Vaud and Fribourg areas range from more than 3500 m to 2500 m, whereas to the east thicknesses are limited between 500 m and 1500 m. Isolines are thus oriented mainly N–S corresponding to thickness variations oriented E–W. This thickness difference affects the style of deformation.

The Mesozoic unit consists of 0 m to 400 m of Cretaceous, 800 m to 2000 m of Jurassic and 150 m to 800 m of

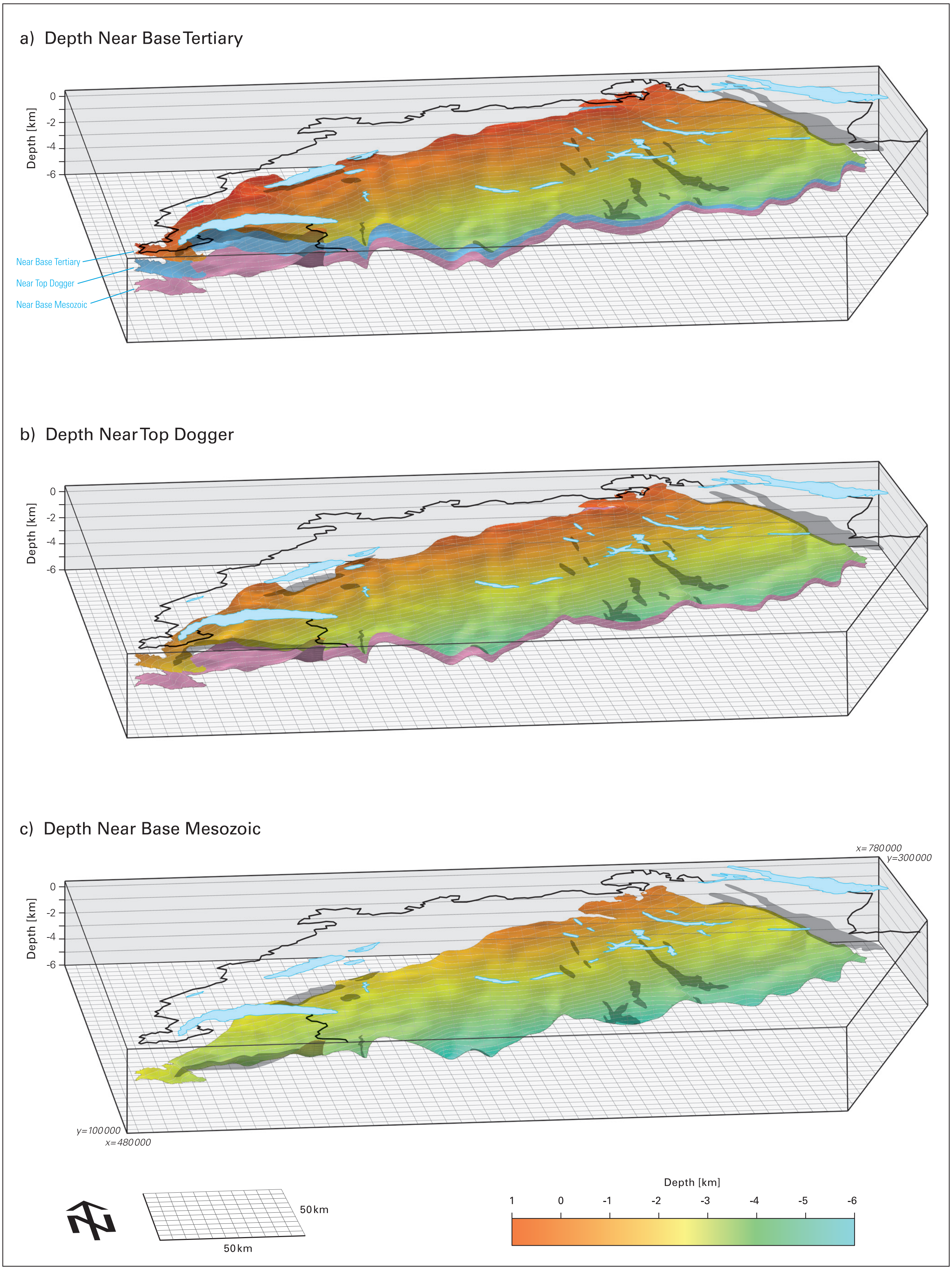

Fig. 5.2: Perspective views of three depth-converted seismic horizon maps. a) Near Base Tertiary horizon, b) Near Top Dogger horizon and c) Near Base Mesozoic horizon (same maps as shown in Enclosure 19). Vertical scale is from +0.5 km to −6 km amsl. A grid with cell size of 5x5 km is projected on the maps. Vertical exaggeration: 5x. Modified from an ArcScene (ArcGIS) image. Swiss border and lakes (blue) are placed at sea level. Vertical projections of lakes (grey) are draped on the displayed surface.

Triassic sediments. An important erosional surface separates various subcropping Mesozoic formations (Cretaceous, Late Jurassic and even Middle Jurassic) from the onlapping Tertiary Molasse units. This erosion represents a foredeep unconformity (see Figure 1.4). The deepest pre-Miocene erosion of the Mesozoic units appears to take place somewhere between Canton Aargau and Lake Lucerne, and it diminishes to the east and to the west.

Triassic unit thickness map

This map includes the Late and Middle–Early Triassic units (see Figure 5.4). Thicknesses vary from 100 m to 1200 m, and decrease from west to east. In Canton Vaud, between Lake Neuchâtel and Lake Geneva, we observe zones of local thickening oriented NW–SE, parallel to the anticline axis (see also SOMMARUGA 1997). To the east of the basin, there is no evidence for relevant thickness variations, but rather thicknesses regularly decrease towards Lake Constance with local patch-shaped isolines.

5.2 Seismically defined faults (Enclosure 21)

5.2.1 Geological characteristics of fault type

Different types of faults were observed on the seismic profiles: normal faults, reverse faults, thrust faults, tear faults or strike slip faults. They are described below.

Normal faults

Normal faults are represented with dip angles of about 70° to 80° in the main extensional direction. They are either isolated or grouped in two, three or more faults, and are either parallel (synthetic) or at high angle (antithetic). A typical family of faults is represented by normal faults offsetting the Mesozoic strata and extending from the Tertiary sediments to the Middle–Early Triassic evaporite strata. Offsets across these faults are generally small (<100 m). To the east of the SMB, a couple of faults cut the Near Base Mesozoic horizon and die in the crystalline or Paleozoic basement (Transect 15). Another fault family is identified in the Paleozoic sediments where normal faults define the graben sidewalls. These Paleozoic faults apparently dip with a lower angle (50° to 70°) than the Mesozoic normal faults.

Reverse faults

The observed reverse faults have dip angles of about 70° to 80° with a reverse offset. In some cases, the fault plane is subvertical and the movement along the plane is not easily identified (normal or reverse sense). These faults cross cut the Cenozoic and Mesozoic cover, and they die out into Triassic evaporites.

Thrust faults

Thrust fault planes are flat or inclined at a maximum of 50°. Often, thrust-faults are detected as stacking of the same strata. Many thrust faults are located either within the Tertiary sediments in the Subalpine Molasse along the southern border of the SMB, or within the Mesozoic cover along the northern border of the SMB (where the first folds of the Jura Mountains occur). Thrusts apparently root in weak to very weak layers, e.g. Triassic evaporites, Liassic, Early Dogger and intra-Malm shales.

Strike-slip faults and tear faults

Strike-slip and tear faults are generally very steep and often occur as diffuse zones of discontinuous reflections or as unreflective zones. Their width ranges from less than 1 km to more than 3 km. In the SMB, tear faults offset the complete Mesozoic cover and appear to end within the Middle Triassic evaporites. There is no evidence that such faults offset the Near Base Mesozoic horizon on the seismic profiles. However, we cannot exclude deep basement-rooted, strike-slip movements beneath the main tear fault zones. These zones are located in the western part of the SMB. They are identified on Transect 14, on the near base Mesozoic map (Encl. 21) and on Figure 4.5: St-Cergue-Nyon, Pontarlier–Vallorbe–Aubonne, Vallorbe–La Sarraz and La Lance–Font–Fétigny.

Synsedimentary faults

Some of the observed normal, thrust, and tear faults seem to line up with zones that were already active during sedimentation in an extensional setting. Dehydration of the sediments and salt dissolution caused differential subsidence and particular geometries in the overlaying sedimentary packages. Their reactivation in the Alpine compressive regime caused inversion of normal faults and offset sedimentary packages of different thickness along tear faults (e.g. the Pontarlier tear fault zone, Transect 14).

Detachment fault zones

The most prominent detachment zones or horizons are located within the two main incompetent formations: the Triassic evaporites and the Early Tertiary claystones and marls. Minor incompetent formations that accommodate tectonic movements are the Early Cretaceous shales (Hauterive Blue Marls), the «Purbeckian» formation at the transition of the Jurassic to Cretaceous strata, the Early Malm marls (Effinger-Schichten or «Argovian» beds) and the Aalenian shales (Opalinuston). They represent minor potential décollement levels or zones.

The detachment zones separate different tectonic styles and seem to accommodate most of the Alpine displacement and shortening throughout the Swiss Molasse Basin (SMB). The Middle–Early Triassic evaporite detachment zone is bound by a roof and a basal décollement. The style of deformation within this zone is very different from the one in the underlying rigid basement or in the overlying Mesozoic layers. Seismic reflections in this zone are locally discontinuous and oblique, suggesting the presence of duplex structures. Over large areas, we cannot observe the basal detachment fault zone on seismic profiles, and infer its presence based on geological information.

5.2.2 Fault display on depth maps (Enclosure 21)

Enclosure 21 presents three horizon depth maps at scale 1:500 000 (Near Base Tertiary, Near Top Dogger and Near Base

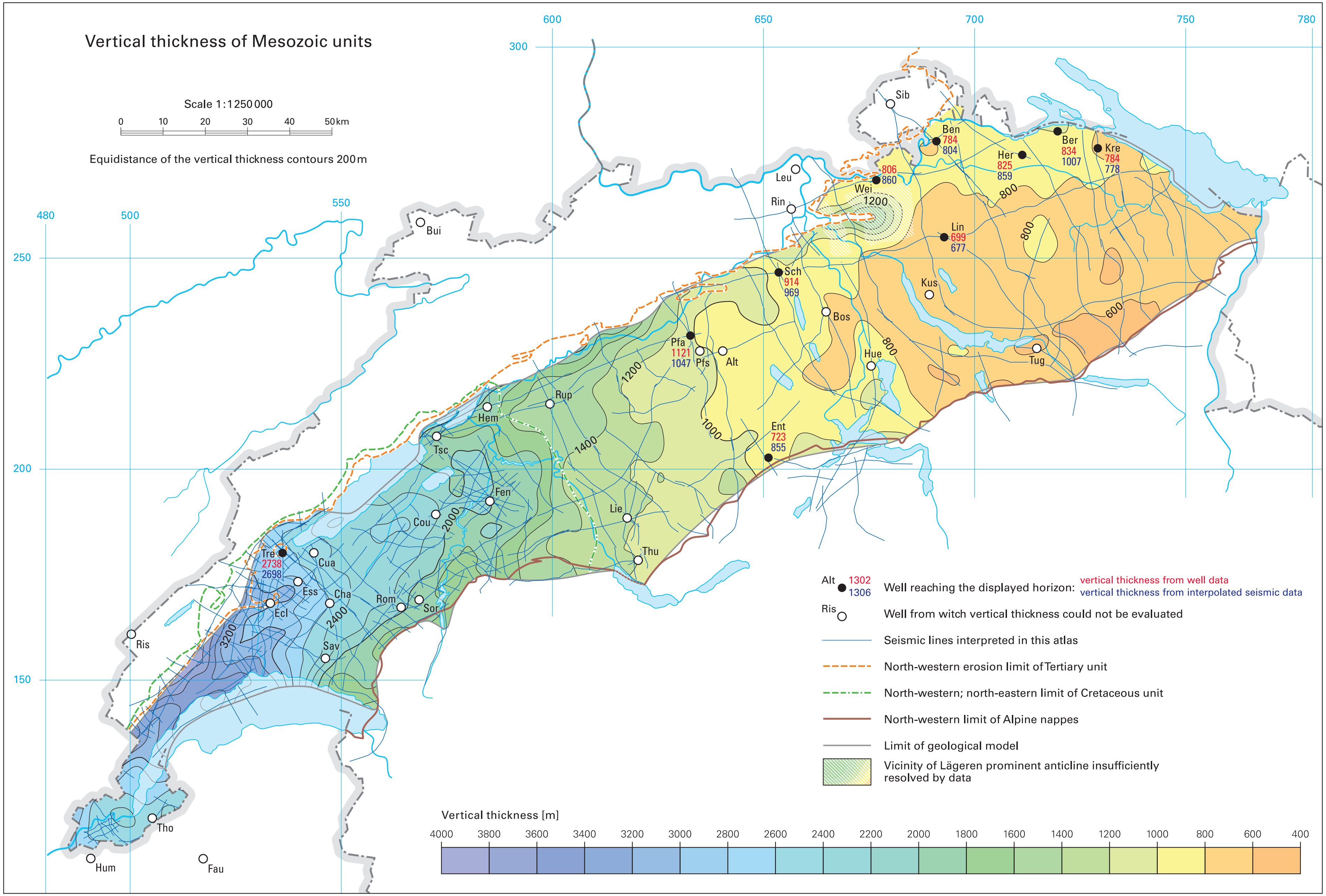

Fig. 5.3: Vertical thickness map of the Mesozoic units in the Swiss Molasse Basin.

Mesozoic). The maps include seismically defined faults and breaks introduced in the surface computations. For technical handling in the GIS system, major faults were considered as single large faults across which vertical offsets were allowed during the grid computation (see paragraph 3.4.1).

Tectonic elements interpreted on the seismic profiles are either normal faults, reverse faults, thrust faults or tear fault zones as described above. To simplify the depth maps, we represent only two different categories of faults: normal and reverse. Fault quality classes are not indicated because such classes were not assigned to faults that were not included in transects. The fault segments are shown along seismic profiles at their correct locations for each specific horizon (hanging wall shoulders for normal faults, footwall edge for reverse faults). The fault symbols are drawn perpendicular to the seismic profiles because the true direction of the fault plane is unknown.

Because of the low profile density of our seismic data set, fault correlations are rarely self-evident. The detailed fault observation on each profile suggests the presence of a series of small faults rather than one single large fault that extends over several kilometres. In some areas, the apparent fault distribution may be biased by the distribution of seismic profiles.

Near Base Tertiary depth map

This map includes a high density of faults in the western area, more particularly to the north (around well Fendringen-1 well) and to the southwest of Canton Fribourg (along Transect 15). Detailed seismic studies in this area have been published (Resun 2008), and little evidence has been found for long, laterally extending faults. The Fribourg zone (see Fig. 4.5 for location) is dominated by a structural style of «en echelon» fault pattern (relay fault) (Mosar 2011, Ibele 2011).

Normal faults dominate the regions south of the geological model, whereas reverse faults are more present along the north, close to the foot of the Jura Mountains. South of Yverdon and in the well Hermrigen-1 area, reverse and thrust faults are also observed at the surface. In Canton Geneva, a series of tear faults were mapped at the surface on geological maps (see Figure 4.5), but surprisingly they were not observed on seismic profiles. The central and eastern areas of the geological model include fewer faults and normal offsets largely dominate. South of Lake Constance, the Romanshorn – St. Gallen fault (Figure 4.5) is interpreted as a normal fault system on the seismic profiles. Despite the uneven distribution of seismic interpreted profiles, we believe that the observed difference in fault density between the eastern and the western areas of the SMB is real. This is supported by the contrasting density of faults observed along seismic profiles in the two areas.

Near Top Dogger depth map

The map is similar to the Near Base Tertiary one, indicating that most faults affect several Mesozoic layers. It also highlights the fact that there are more faults per profile in the west part of the SMB than in its east part.

Near Base Mesozoic depth map

This map shows a higher density of faults in the central and east parts of the geological model than in the west. Faults are generally small, and they do not extend deep into the basement. Most are normal faults, few are reverse.

Figure 5.5 shows two 3D views of faults superimposed on three TWT horizons: Near Base Tertiary, Near Top Dogger and Near Base Mesozoic. Faults are displayed as red line segments. Such a line segment represents the 3D trace of the intersection between a fault plane and the plane of a seismic profile. No fault planes are shown. The faults are the same ones that are displayed on Enclosure 21. The main feature of these figures is the striking contrast between the fault pattern to the east (triangle zone with front thrusts and back thrusts) and the fault pattern to the west (north-vergent thrusts) within the Tertiary sediments (yellow horizon and above). The latter faults root at the base of the Tertiary unit in a decoupling level. The other faults terminate above the Near Base Mesozoic horizon (in purple) in the Early – Middle Triassic unit (conceptual décollement zone).

5.3 Synoptic view of the Swiss Molasse Basin from transects (Enclosure 22)

Enclosure 22 shows a compilation of simplified depth-converted seismic profiles along the SMB. It presents a synoptic view of the basin that enables the reader to observe the spatial evolution of the structural elements of the basin both in the strike and in the dip directions.

5.3.1 Structures within the Tertiary unit

Structures within the Tertiary wedge change from SW to NE as well as from NW to SE depending on the structural domain (Plateau Molasse, Folded Molasse, and Subalpine Molasse). Within the Plateau Molasse, the layers are slightly folded (very low amplitude) following either the geometry of the Mesozoic layers (Transects 03, 08) or with a different one, requiring a décollement horizon at the Base Tertiary unit within shaly beds. The Folded Molasse tectonic unit is a transition zone where layers dip steeply to the SE or NW. The Subalpine Molasse tectonic unit shows a pronounced evolution from SW to NE. To the SW, in Canton Vaud and Fribourg, structures are dominated mainly by a NW-vergent stack of several thrust sheets with presumed internal deformation. Transect 03 includes a wedge-type, crocodile-style structure. Structures within the Tertiary unit are separated from the Mesozoic strata by a décollement zone. The shales of the USM sediments can be considered as an important décollement horizon. In the central and eastern part of the Subalpine Molasse tectonic unit, structures are related to thrust faults pointing either to the NW or to the SE rooting at the base of the Tertiary strata. These structures represent an extended triangle zone. To the east of Lake Thun, the backthrusts of the triangle zone become visible. This SE-vergent thrust plane is rarely doubled, and it can be followed all the way to the southern end of Lake Constance. Transects 06 and 07 are located in the transition area between the thrust Subalpine Molasse of the western SMB and the triangle zone of the Subalpine Molasse of the cen-

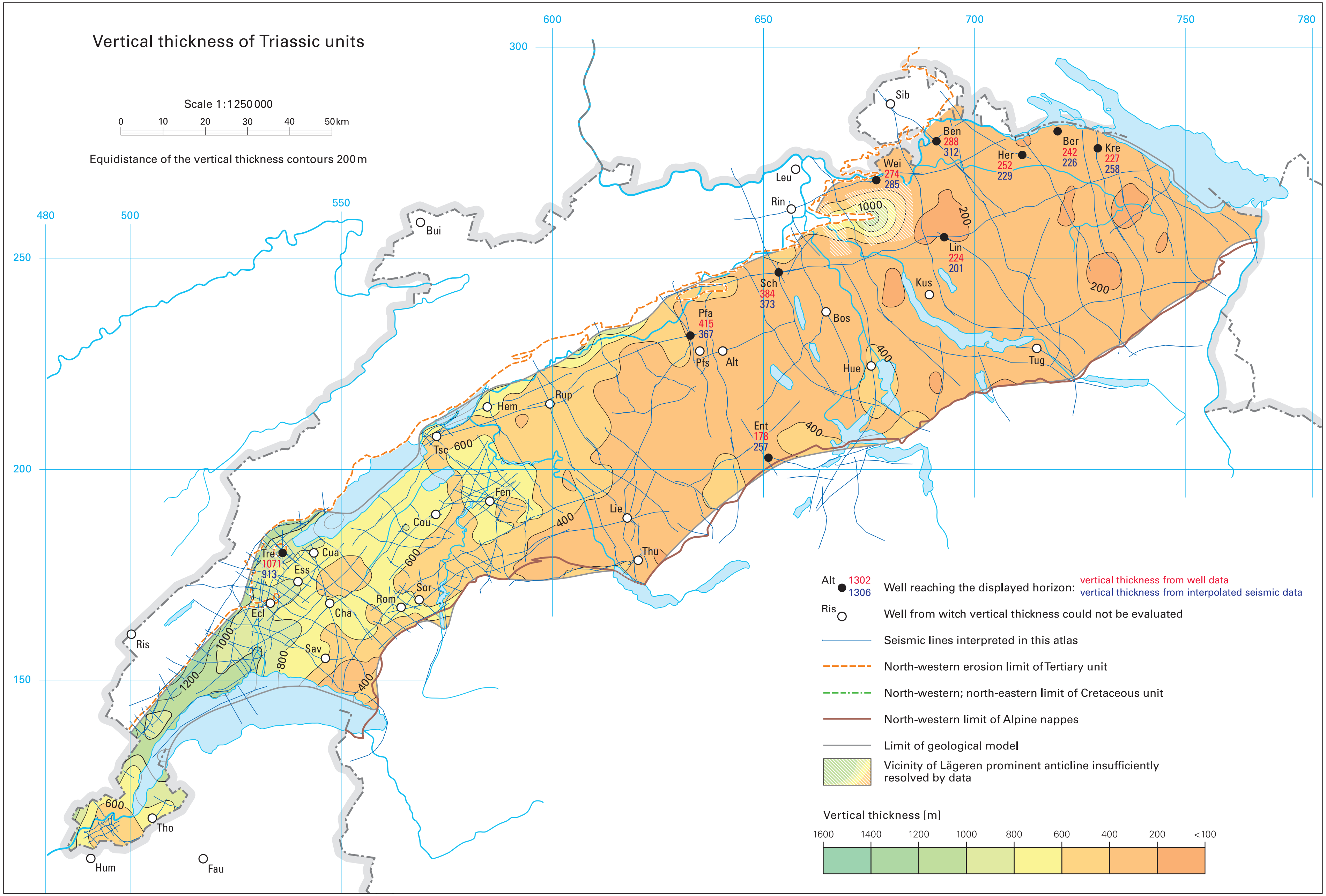

Fig. 5.4: Vertical thickness map of the Triassic units in the Swiss Molasse Basin.

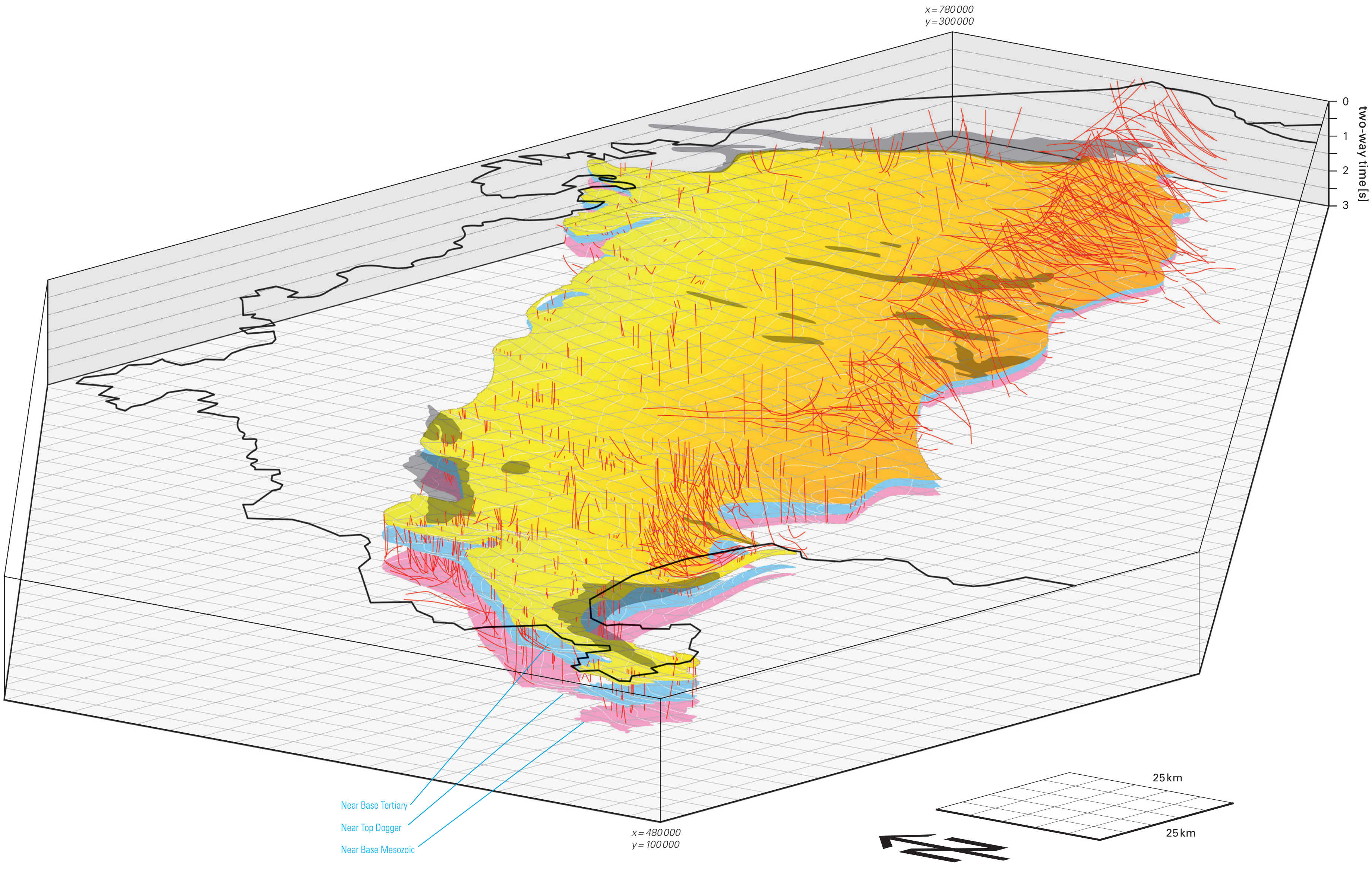
x = 780 000
y = 300 000
0
1
2
3
two-way time [s]
Near Base Tertiary
Near Top Dogger
Near Base Mesozoic
x = 480 000
y = 100 000
25 km
25 km
N

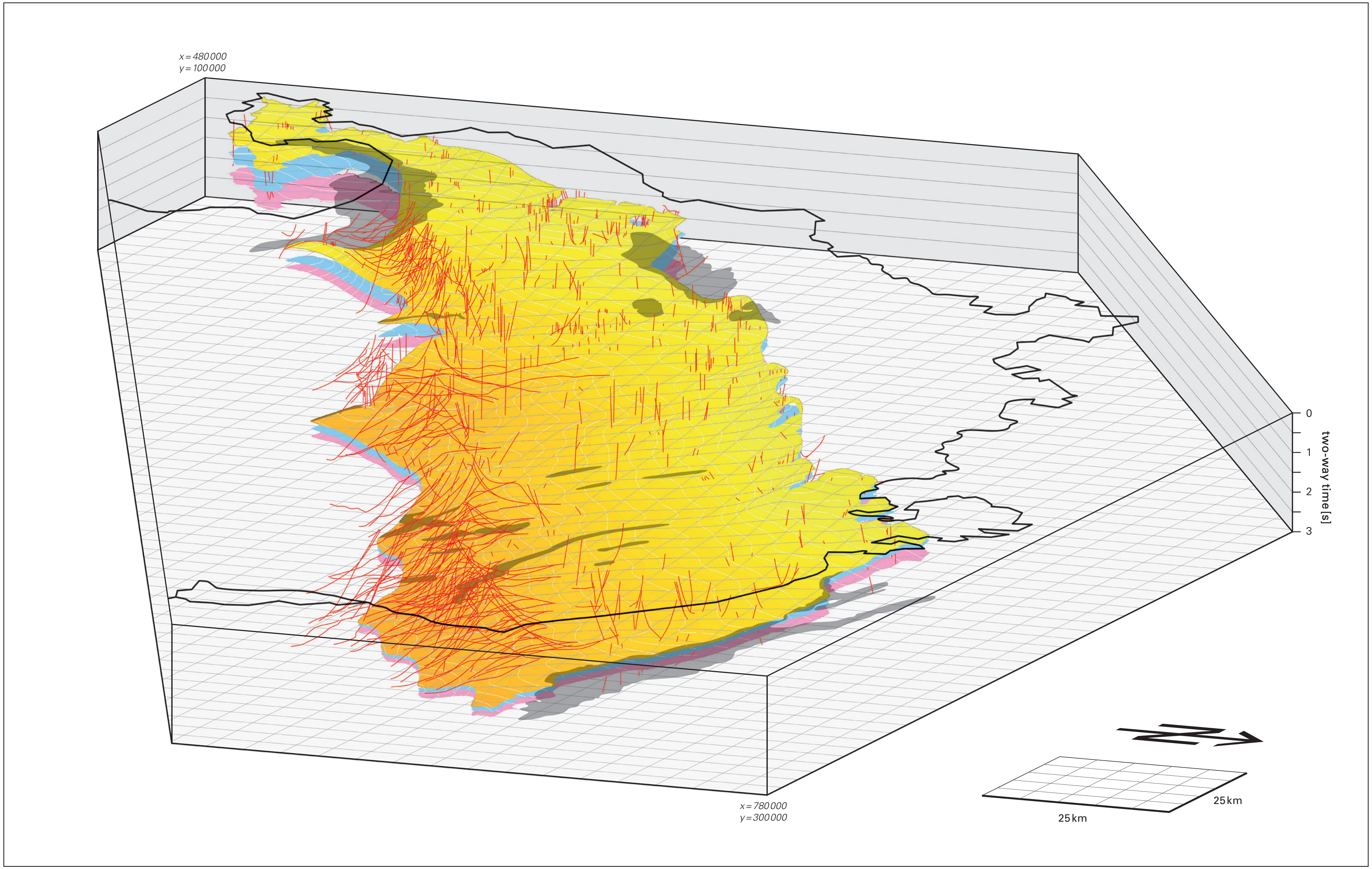

Fig. 5.5: Perspective views of three TWT seismic-horizon surfaces with seismically defined faults (same TWT maps as shown in Enclosure 17). The horizons are: Near Base Tertiary (yellow), Near Top Dogger (blue) and Near Base Mesozoic (purple). Faults are shown as red line segments (see text and Figure 3.3 for explanations). Vertical scale is from 0 s (= 500 m) to 3 s; vertical exaggeration is approximately 5 x. Coordinates refer to the Swiss coordinate system. a) View from the southwest towards the northeast. b) View from the northeast towards the southwest. A grid with cell size of 5 x 5 km is projected on the maps. Modified from an ArcScene (ArcGIS) image. Political borders of Switzerland are shown at zero elevation. Lakes are projected on the Near Base Tertiary surface. Note that Figure 5.5a is on page 76 and Figure 5.5b is on page 77.

tral and eastern SMB. In Encloure 22, the depth-converted profiles have been aligned to the frontal end-deformation point where the roof thrust meets the sole thrust within the Tertiary unit (BOYER & ELIOT 1982).

5.3.2 Structures within the Mesozoic unit

The thickness of the Mesozoic strata diminishes by a factor of four from Lake Geneva to Lake Constance. We observe a decreasing Mesozoic thickness from NW to SE (e.g. along Transects 07 and 04). The main feature in the Mesozoic strata is the absence of Cretaceous layers in the central and eastern part of the Swiss Molasse Basin. Early–Middle Triassic sediments thin from west to east and essentially east of an axis linking the Pfaffnau-1 and Entlebuch-1 wells. The Malm unit is deeply eroded as observed in Canton Aargau (e.g. Transect 09) and further to the east.

Throughout the Swiss Molasse Basin there is no large-scale doubling of Mesozoic carbonate units. Structures within the Mesozoic unit to the west of the Basin appear more complex than to the east. Lateral thickness variations have consequences on the rheological behaviour of the strata (tectonic style). To the east (Transects 09–13), the Mesozoic strata appear as monoclines, and small structures are located under the Folded and the Subalpine Molasse. Folds are related to reverse faults. Small-scale synthetic and antithetic normal faults affect the entire Mesozoic cover and even the pre-Mesozoic unit at the east the end of the Jura fold-and-thrust belt (Transects 11, 12, 13 and 15).

To the west of the Swiss Molasse Basin, low-amplitude, long-wavelength deformation is observed in association with evaporite-cored detachment folds (Transects 03, 05, 06). In some cases, thrust or reverse faults are also associated with the folds. Partial doubling of Mesozoic strata is observed in a few places within the basin over distance as short as a few hundred metres (well Cuarny-1). The presence of these anticlines above the smooth Near Base Mesozoic horizon implies a décollement zone in between. This zone is located in the Early–Middle Triassic evaporates, and it is indicated as a conceptual décollement zone from Transects 01 to 10.

Tear fault zones cut the Mesozoic and Tertiary layers in the west SMB, and they extend into the Jura Mountains (e.g. Pontarlier–Vallorbe–Aubonne or St-Cergue–Nyon tear faults, see Figure 4.5). Such structures were not observed to the east of the Swiss Molass Basin.

East of the Lägeren, the last Jura fold, the SMB is in contact to the north with the undeformed Tabular Jura. From there to the east, no major décollement zone is present within the Triassic evaporites, meaning no main deformation within the Mesozoic layers. According to AFFOLTER & GRATIER (2004), thin-skinned shortening in the Jura fold-and-thrust belt increases from about 1–2 km close to Transect 10 (Lägeren) to 7 km close to Transect 09, to 13 km close to Transect 07 and to 25–30 km further to the west. East of Lägeren, this shortening is transferred into the Subalpine Molasse (BURKHARD 1988 and 1990).

5.3.3 Pre-Mesozoic features

Permo-Carboniferous sediments were tentatively interpreted either along the northern (Transects 10 and 11) and the south edges of the SMB (Transects 03 and 08) as well as in the Geneva area (Transect 01). Direction and extension of the Paleozoic sediments are not proposed in this Atlas because no map correlation of this unit was carried out due to insufficient data quality below the Mesozoic strata. No major argument in favour of inversion of Permo-Carboniferous troughs was found in the seismic profiles, except to the south end of Transect 03 and under well Entlebuch-1 on Transect 08.

To summarize, slight changes of dip at the base of the Mesozoic unit are observed from west to east along distinct NS-oriented zones. The monoclinal dip of pre-Mesozoic basement remains smooth with increasing steepening to the south. Furthermore, the western part of the SMB differs stratigraphically and structurally from the eastern part. A transition occurs in Canton Bern along an axis running from Lake Biel to Lake Thun to the east of the Fribourg fault zone. Across this axis, from SW to NE, Cretaceous layers disappear, the dip direction of the interpreted seismic horizons changes, and a triangle zone in the Tertiary unit appears.

6 General conclusions and outlook

We present the first 3D seismic Atlas and geological model of the entire Swiss Molasse Basin (SMB). The seismic Atlas is a significant step towards a better understanding of the SMB at a basin scale. Our model is represented by a regional grid of 1284 km of profiles displayed in 15 transects. The seismic interpretation of these transects follows a specifically designed procedure that includes quantitative assessment of data uncertainty. In total, we interpreted 4357 km of 2D reflection seismic profiles calibrated with more than 30 deep wells. This Atlas includes supplementary maps that helped us to define the 3D model: interpreted seismic horizons, unit velocities, and unit thickness between the horizons. In addition, we have compiled the available data from deep wells drilled into the SMB.

The main features we interpret are:

- geometry of the Tertiary Molasse infill, the subalpine thrust faults, and the triangle zone within the Tertiary layers,
- stratigraphy and structure of the Mesozoic units and
- possible presence of Permo-Carboniferous sediments above the crystalline basement.

In the Tertiary Molasse unit: three structural domains are observed: Plateau Molasse, Folded Molasse and Subalpine Molasse. We document thickening of the Plateau Molasse from NW to SE, and imply a décollement at its base. The Folded Molasse and the Subalpine Molasse are highly deformed tectonic units. In the Subalpine Molasse, NW-verging thrusts are observed in the western part of the basin, whereas in the central and eastern parts of the basin, thrusts in opposed directions define a triangle zone.

In the Mesozoic unit: layer thickness varies laterally, decreasing from west to east. The Cretaceous beds are present only in the western part of the SMB, and the whole Mesozoic unit is more tectonized to the west than in the central and eastern parts. A décollement level is implied at the base of the Mesozoic strata except in the easternmost part of the SMB.

In the pre-Mesozoic unit: geometry of possible accumulations of Permo-Carboniferous sediments is indicated by seismically reflective zones beneath the Mesozoic unit above the crystalline basement. We find no major argument in favour of inversion of Permo-Carboniferous troughs in the seismic profiles.

This Atlas provides foundation for many applications. Here we name only a few:

- Establishing seismic hazard maps in the densely urbanized Swiss Plateau: the Atlas shows that fault density varies from region to region and indicates the length and possible extension of observed faults.
- Assessing fault distribution and fault patterns from seismic data: the results presented in this Atlas can now be combined with surface geology and tectonic maps to build a new tectonic model of the SMB, and they provide building blocks for further research.
- Locating and characterizing potential geothermal energy resources: the Atlas provides hints on depth of possible target layers and deformation in the crystalline basement.
- Locating and characterizing potential areas suitable for CO_2 sequestration: favourable stratigraphic and tectonic settings can be inferred from the Atlas that enables numerical estimates at regional scale.

Our work also indicates areas where further research could be done:

- Zones of seismic reflectivity and their boundaries in pre-Mesozoic units identified on the transects of this Atlas should be investigated further for thermal anomalies. This would also include building isopach and facies maps of the coal-bearing Permo-Carboniferous series.
- Gravity back-stripping using the new Tertiary and Mesozoic unit thickness maps could be used to map variations in the lithological composition of the basement and to confirm the presence of Permo-Carboniferous grabens.
- Creation and application of a basin-wide strain model to aid future interpretations.
- The problem of linking faults observed on separate seismic sections remains, and should be investigated further taking into account existing profiles that were not available for interpretation or calibrating against existing 3D sets (Benken, St. Gallen). Any more detailed interpretation requires not only incorporating all existing seismic profiles but the addition of more modern, high-quality seismic data.

In summary, the Atlas is an important first step towards making some of Swiss seismic and well data publicly available. As a result of this work, a number of deep seismic profiles and well data are now easily accessible to the interested public. We compiled a new location map of all 2D seismic profiles and deep wells in the SMB that allows a quick assessment of data density in a specific area. To benefit future projects, additional seismic profiles need to be integrated into a public Swiss database. In today's digital world, the goal should be to build a national digital database that comprises all existing deep seismic profiles including recently acquired or reprocessed lines.

Acknowledgements

We are grateful to the following companies or institutions that gave us access to their data:

- Büro für angewandte Geologie (Frauenfeld)
- Canton Bern, Bergregalarchiv, BVE Direktion
- Canton Fribourg, Direction de l'aménagement, de l'environnement et des constructions
- Canton Geneva, Service Cantonal de Géologie
- Canton Vaud, Musée cantonal de géologie (Lausanne)
- CELTIC Ltd (London)
- FREAG, Freiburg Erdöl AG (Fribourg)
- GEOFORM (Villeneuve)
- Lundin Petroleum (Geneva)
- Nagra, Nationale Genossenschaft für die Lagerung Radioaktiver Abfälle (Wettingen)
- PROSEIS-INTEROIL (Zürich)
- SEAG, Aktiengesellschaft für schweizerisches Erdöl (Langnau am Albis)
- SHELL (Den Haag)
- SIG, Services Industriels de Genève (Geneva)
- swisstopo, Geological Information Center (Wabern)
- University of Basel,
- University of Fribourg, Département des Géosciences
- University of Geneva, Département de Géologie et Paléontologie
- University of Neuchâtel, Institut de Géologie

The SEAG company (Patrick Lahusen, Conrad Frey) deserves special thanks for providing the majority of seismic and well data without which this project would have been impossible (contract SEAG-010205). Werner Leu helped us in many aspects of the SEAG data; his contribution is gratefully acknowledged. He also provided a copy of his report on the interpretation of public seismic data in Switzerland. Frau Kissling-Näf, at the time Secretary General of the Swiss Academy of Sciences, is acknowledged for her help in conveying to us the legal guarantee of the Academy by signing a data contract with SEAG.

Several scientists provided input through interesting discussions that benefited the Atlas. We thank in particular: Jean-Pierre Berger † (University of Fribourg), Philip Birkhäuser (Nagra), Peter Blümling † (Nagra), Luigi Burlini † (ETHZ), Gilles Borel (Musée cantonal de géologie, Lausanne), Martin Burkhard † (University of Neuchatel), Walter Frei, (GeoExpert AG), Pierre Gex (University of Lausanne), Georges Gorin (University of Geneva), René Graf (Interoil), Oliver Kempf (swisstopo), Emile Klingele (Zürich), Werner Leu (Geoform), Robin Marchant (Musée cantonal de géologie, Lausanne), Beat Meier (Interoil), Jon Mosar (University of Fribourg), Heinrich Naef (Büro für angewandte Geologie), Sabrina Paolacci (University of Geneva), Adrian Pfiffner (University of Bern), Chris Pullan (Celtic), Philippe Roth (Interoil), Stefan Schmid (University of Basel), Michael Schnellmann (Nagra), Kamil Ustaszewski (University of Basel), Marc Weidmann (Jogny), David Williams (Celtic), Peter Ziegler (Basel).

Dr. Robin Engler was instrumental in all computing aspects of the project. He showed much ingenuity at performing numerous tasks to be carried out with the GIS database such as minimizing mis-ties between seismic profiles or computing 3D surface grids from the digitized seismic horizons. We also relied on him for maintaining the GIS database and for extracting maps and other information. His essential contribution is gratefully acknowledged.

Drafting was a major task that involved not only professional and technical ability but also patience, ingenuity, and a good aesthetic sense. In that respect, we are indebted to Andreas Baumeler (GRENZEN – Digitale Kartografie, Zurich) who drafted the enclosures and the text figures to their final state. He also did the final text layout. Drafting earlier versions of the enclosures was carried out with talent by Denise Bussien and Bastien Delacou. Catherine Aviolat-Nigg drafted the majority of the text figures with great care. Martinus Abdenego helped drafting of the ARCScene figures. Francis Perret drafted the very first seismic transect.

At a very early stage of the work, Pierre François Erard and Milan Beres helped gather digital seismic data on tapes and seismic location maps. Claire Odello reprocessed the seismic data; she had to wrestle hard to get the most out of old, often incomplete data files. Thomas Czáka initiated the GIS database, and Baptiste Dafflon geo-referenced most of the seismic location maps. Bertrand Dumont digitized the numerous interpreted seismic sections (some of them several times), and he also helped in other technical aspects such as superimposing the well data on the interpreted seismic scans. Roland Baumberger converted seismic horizons from the transects (in Adobe Illustrator format) into digitally readable files. David Dupuy and Dieb Hammami facilitated the implementation of interpreted seismic horizons on the Kingdom Suite software. Philippe Logean efficiently took care of all aspects of computer hardware and was responsible for assuring file backups. Sabrina Damiani was instrumental in establishing work contracts for the many coworkers employed for the project at the Institute of Geophysics. Her help in other aspects is acknowledged including formatting the Atlas text.

The Atlas greatly benefitted from comments and suggestions by Philip Birkhäuser and his team and by Luigi Burlini † on an earlier version. We also thank René Graf, Philip Birkhäuser and Micheal Schnellmann for a second review of the text. We also acknowledge comments on a previous version of the transects and some other enclosures by Georges Gorin, Werner Leu, Jon Mosar, Heinrich Naef, Marc Weidmann, and Peter Ziegler. Roy Freemann corrected the English with dedication, and we thank him for his knowledgeable input.

The Atlas could not have been published without the support from many people at swisstopo: Roland Baumberger, Milan Beres, Stefan Dall'Agnolo, Laurent Jemelin, Andreas Möri, Nils Oesterling and Remo Trüssel. Andreas Kühni as a representative of the Swiss Geological Survey (swisstopo) at the Swiss Geophysical Commission always supported the project with his authorities. Andreas Möri supervised the final steps of the Atlas production.

This work was financially supported mainly by the Swiss Geophysical Commission. We thank all the members of this commission and its presidents Emile Klingelé and Eduard Kissling for their continuous support and encouragement. A significant financial and logistic contribution was also provided by the University of Lausanne, and more specifically through the Institut de Géophysique (directors Raymond Olivier and Klaus Holliger) and the Dean's Office of the Faculté des Géosciences et de l'Environnement of the University of Lausanne. We are grateful to the University of Fribourg (Département des Géosciences) and the ISSKA (Institut Suisse de Spéléologie et de Karstologie) which provided access to their infrastructures to Anna and Urs respectively during the last year of this project.

We thank the Swiss Geological Survey (swisstopo), in particular Laurent Jemelin, for their help with the design of the Enclosures and for printing the Atlas. The rigorous swisstopo drafting guidelines produced beautiful results.

We acknowledge the help of Martin Burkhard †, former Professor at University of Neuchâtel, through whom Anna Sommaruga and Urs Eichenberger first met and who was instrumental at getting them involved in this project.

Last but not least, we acknowledge the help of Prof. Eduard Kissling and sincerely thank him for his many contributions and steadfast support. With time he became more and more involved in the project, not only as an editor, but also in many other aspects of the project such as providing management support, scientific counselling, help in legal negotiations with SEAG, overseeing the drafting progress with Andreas Baumeler on a daily basis in Zürich, and ensuring close contact with swisstopo.

References

AFFOLTER, T. & GRATIER, J. P. (2004): Map view retrodeformation of an acur ate fold-and-thrust belt: The Jura case. – J. Geophys. Res. *109*/ B03404, doi:10.1029 / 2002JB002270.

ALLEN, P. A., HOMEWOOD, P. & WILLIAMS, G. D. (1986): Foreland basins: an introduction. In: ALLEN, P. A. & HOMEWOOD, P. (Ed.): Foreland basins, *8* (p. 3–12). – Spec. Publ. int. assoc. sediment.

ALTHAUS, H. E. & RICKENBACH, E. (1947): Erdölgeologische Untersuchungen in der Schweiz, I. Teil. – Beitr. Geol. Schweiz, geotech. Ser. *26*/ 1, 88 p.

ARNEMANN, A. (1978): Bericht über die seismische Geschwindigkeitsmessung in der Tiefbohrung Romanens-1 (Schweiz). Bericht Nr. 773665, Hannover. Unpublished report.

AUBERT, D. (1941): Feuille 1221 Vallée de Joux [Le Sentiers]. – Atlas géol. Suisse 1: 25 000, Notice expl. *17.*

– (1959): Le décrochement de Pontarlier et l'orogénèse du Jura. – Mém. soc. vaudoise sci. nat. *12*/ 4, 93–152.

– (1977): Géomorphologie de la source de l'Orbe. – Stalactite *27*, 27–42.

BACHMANN, G. H. & MÜLLER, M. (1992): Sedimentary and structural evolution of the German Molasse Basin. – Eclogae geol. Helv. *85*/3, 519–530.

BACHMANN, G. H., DOHR, G. & MÜLLER, M. (1982): Exploration in a classic thrust belt and its foreland: Bavarian Alps, Germany. – Am. Ass. Petroleum Geologists Bull. *66*, 2529–2542.

BACHMANN, G. H., MÜLLER, M. & WEGGEN, K. (1987): Evolution of the Molasse Basin (Germany, Switzerland). – Tectonophysics *137*, 77–92.

BAUJARD, C., SIGNORELLI, S. & KOHL, T. (2007): Atlas des ressources géothermiques de la Suisse Occidentale – Domaine Sud-Ouest du Plateau Suisse. – Matér. Carte géol. Suisse, Sér. géotech. *40.*

BERGER, J.-P. (1992): Correlative chart of the European Oligocene and Miocene: Application to the Swiss Molasse Basin. – Eclogae geol. Helv. *85*/3, 573–609.

– (2011): Du Bassin molassique au fossé rhénan: évolution des paléoenvironnements dans un avant pays dynamique. – Géochronique *117*, 47–49.

BERGER, J.-P., REICHENBACHER, B., BECKER, D., GRIMM, M., GRIMM, K., PICOT, L., STORNI, A., PIRKENSEER, C. & SCHAEFER, A. (2005): Eocene – Pliocene time scale and stratigraphy of the Upper Rhine Graben (URG) and the Swiss Molasse Basin (SMB). – Int. J. Earth Sci. *94*/ 4, 711–731.

BERGER, J.-P., REICHENBACHER, B., BECKER, D., GRIMM, M., GRIMM, K., PICOT, L., STORNI, A., PIRKENSEER, C., DERER, C. & SCHAEFER, A. (2005): Paleogeography of the Upper Rhine Graben (URG) and the Swiss Molasse Basin (SMB) from Eocene to Pliocene. – Int. J. Earth Sci. *94*/ 4, 697–710.

BERSIER, A. (1958): Forage Chapelle-1. Rapport de contrôle géologique. Lausanne. Département des Travaux Publics, Service des Routes. Unpublished report.

– (1976): Rapport d'interprétation, Jura Vaudois Petrole SA. CGG 140.36.30, Shell Switzerland. Unpublished report.

BIRKHÄUSER, P., ROTH, P., MEIER, B. & NAEF, H. (2001): 3D-Seismik: Räumliche Erkundung der mesozoischen Sedimentschichten im Zürcher Weinland. Nagra Techn. Ber., NTB 00-03, Wettingen.

BODMER, P. & GUNZENHAUSER, B. (1992): TGK Hydrocarbon Exploration in Central Switzerland: Experience with Alpine Reflection Seismics. – Bull. Assoc. suisse Géol. Ing. pétrole *59*/ 135, 15–22.

BONNET, C., MALAVIEILLE, J. & MOSAR, J. (2007): Interactions between Tectonics, erosion and sedimentation during the recent evolution of the Alpine orogen – Analogue modeling insights. – Tectonics *26*/ TC6016, doi:10.1029 / 2006TC002048.

BOYER, S. E. & ELLIOTT, D. (1982): Thrust systems. – Am. Ass. Petroleum Geologists Bull. *66*/ 9, 1196–1230.

BÜCHI U. P. (1988): Die schweizerische Erdöl- und Erdgasfrage 1987. – Bull. Assoc. suisse Géol. Ing. pétrole *54*, 31–38.

BÜCHI, U. P. & SCHLANKE, S. (1977): Zur Paläogeographie der Schweizerischen Molasse. – Erdöl-Erdgas-Zeitschrift *93*, 57–69.

BÜCHI, U. P. & BODMER, P. (1983): Der Tiefenverlauf der seismischen Geschwindigkeiten in den Molassesedimenten des schweizerischen Mittellandes. – Bull. Assoc. suisse Géol. Ing. pétrole *49*/ 116, 3–13.

BÜCHI, U. P., LEMCKE, K., WIENER, G. & ZIMDARS, J. (1965 a): Geologische Ergebnisse der Erdölexploration auf das Mesozoikum im Untergrund des schweizerischen Molassebeckens. – Bull. Assoc. suisse Géol. Ing. pétrole *32*/ 82, 7–38.

BÜCHI, U. P., WIENER, G. & HOFMANN, F. (1965 b): Neue Erkenntnisse im Molassebecken auf Grund von Erdöltiefbohrungen in der Zentral- und Ostschweiz. – Eclogae geol. Helv. *58*, 87–108.

BURKHARD, M. (1988): L'Helvétique de la bordure occidentale du massif de l'Aar (évolution tectonique et métamorphique). – Eclogae geol. Helv. *81*/ 1, 63–114.

– (1990): Aspects of the large scale Miocene deformation in the most external part of the Swiss Alps (Subalpine Molasse to Jura fold belt). – Eclogae geol. Helv. *83*/ 3, 559–583.

BURKHARD, M. & SOMMARUGA, A. (1998): Evolution of the Swiss Molasse basin: structural relations with the Alps and the Jura belt. In: MASCLE, A., PUIGDEFFABREGAS, C., LUTERBACHER, H. & FERNANDEZ, M. (Ed.): Cenozoic Foreland Basins of Western Europe, *134* (p. 279–298). – Geol. Soc. Spec. Publ., London.

BURKHARD, M. & GRUNTHAL, G. (2009): Seismic source zone characterization for the seismic hazard assessment project PEGASOS by the Expert Group 2 (EG1b). – Swiss J. Geosciences *102*/ 1, 149–188.

BUXTORF, A. (1907): Zur Tektonik des Kettenjura. – Ber. Vers. oberrh. geol. Vers. *30*/ *40*/ Vers. 1906 / 7, 79–111.

CHAROLLAIS, J., WEIDMANN, M., BERGER, J. P., ENGESSER, B., HOTELLIER, J. F., GORIN, G., REICHENBACHERI, B. & SCHÄFER, P. (2007): The Molasse in the Greater Geneva area and its substratum. – Archives des Sciences, Société de Physique et d'Histoire Naturelle de Genève *60*/ 2–3, 59–173.

CHEVALIER, G., DIAMOND, L. W. & LEU, W. (2010): Potential for deep geological sequestration of CO_2 in Switzerland: a first appraisal. – Swiss J. Geosciences *103*/ 3, 427–455.

CHOIGNARD, J. (1989): Bilan de 21 ans d'exploration petrolière sur les permis de Berne et Fribourg sud. ELF aquitaine international, à partir de documents de J. P. Boeldieu, M. Couhier et J. Micholet. Unpublished report.

DIEBOLD, P. (1987): Résultats géologiques des analyses de sismique-réflexion de la Cédra dans le nord de la Suisse. – Cédra informe *1–2*, 23–33.

DIEBOLD, P. & NAEF, H. (1990): Der Nordschweizer Permokarbontrog. – Nagra informiert *2*, 29–36.

DIEBOLD, P. & NOACK, T. (1997): Late Paleozoic troughs and Tertiary structures in the eastern folded Jura. In: PFIFFNER, O. A., LEHNER, P., HEITZMAN, P. Z., MUELLER, S. & STECK, A. (Ed.): Deep structure of the Swiss Alps – Results from NRP 20, (p. 59–63). – Birkhäuser, Basel.

DIEBOLD, P., NAEF, H. & AMMAN, M. (1991): Zur Tektonik der Zentralen Nordschweiz. Nagra Tech. Ber., NTB 90-04, Baden.

DIEBOLD, P., BITTERLI-BRUNNER, P. & NAEF, H. (2006): Blatt 1069 / 1049 Frick – Laufenburg. – Geol. Atlas Schweiz 1: 25 000, Erläut. *110.*

DUFLOT, R. (1989): Rapport final du sondage de Thoune-1. EAI, DIFEX, Unpublished report.

ENGESSER, B., MAYO, N.-A. & WEIDMANN, M. (1984): Nouveaux gisements de mammifères dans la molasse subalpine vaudoise et fribourgeoise. – Mém. suisses Paléont. *107*, 1–39.

ERARD, P.-F. (1999): Traitement et interprétation de cinq lignes sismique réflexion à travers la Plateau molassique et les Préalpes suisses, de Bienne à Lenk. – Université de Lausanne. Institut de Géophysique, 107 p. Thèse de doctorat.

FASEL, J. M. (1984): Paléohydraulique dans l'épandage fluviatile du Mt-Pèlerin Oligocène suisse. 5th Reg. Mtg. int. Assoc. Sedi., Marseille. Abstract. (163).

FISCHER, H. & LUTERBACHER, H. (1963): Das Mesozoikum der Bohrungen Courtion-1 (Kt. Fribourg) und Altishofen-1 (Kt. Luzern). – Matér. Carte géol. Suisse *115*, 40.

FRAME, P., CEBDON, C., ELLIOTT, C. J., SIMMONS, M. D. & STRANK, A. R. E. (1987): Biostratigraphy of the well Courtion-1: Results of micropalaeontological analysis of additional core samples. Report STR / 105 /86, Unpublished report.

FORNAGE, P. (1983): Rapport géologique final du sondage Hermrigen 1D (Her 1D). Elf Aquitaine Exploration Production SA. Unpublished report.

FROMMHOLZ, R. & LENK, G. (1960): Bericht über die seismische Geschwindigkeitsmessung in der Tiefbohrung Küsnacht-1. Rap. Ges. Brigitta Elverath, Hannover. Ber. Nr. 060158, Unpublished report.

GALLOWAY, W. E. (1989): Genetic stratigraphic sequences in basin analysis – part 1: sequence architecure and genesis of flooding-surface bounded depositional units. – AAPG Bull. *73*, 115–142.

GORIN, G. (1989): Interprétation géologique de la Campagne sismique GG87 dans le canton de Genève. Genève. Département de l'Intérieur et de l'Agriculture, service cantonal de géologie, Genève. Unpublished report.

– (1992): Rapport sur l'interprétation de la campagne de sismique de réflexion 1990 dans le Canton de Genève (Perimètre Vernier – Onex – Sezegnin – Avully – Vernier). Genève. Rapport pour les Services Industrielles de Genève, Service du Gaz. Unpublished report.

GORIN, G., PLANCHEREL, R. & WEIDMANN, M. (1995): Preliminary geological observations derived from reflection seismic profiles in the Fribourg area. Swiss Tectonic Studies Group, Fribourg, Poster.

GORIN, G., MOREND, D. & PUGIN, A. (2003): Bedrock, Quaternary sediments and recent fault activity in central Lake Neuchatel, as derived from high-resolution reflection seismics. – Eclogae geol. Helv. *96* / Supplement 1, 3–10.

GORIN, G., SIGNER, C. & AMBERGER, G. (1993): Structural configuration of the western Swiss Molasse Basin as defined by reflection seismic data. – Eclogae geol. Helv. *86* / 3, 693–716.

GREBER, E., LEU, W. & SCHEGG, R. (2004): Hydrocarbon Habitat and Potential of Switzerland – An evaluation of the oil and gas potential of Switzerland based on public well data, seismic lines and basin modelling results. Unpublished Internal Report, Geoform Ltd.

GREBER, E., GRÜNENFELDER, T., KELLER, B. & WYSS, R. (1994): Die Geothermie-Bohrung Weggis Kanton Luzern. – Bull. Assoc. suisse Géol. Ing. pétrole *61* / 138, 17– 43.

GUELLEC, S., MUGNIER, J. L., TARDY, M. & ROURE, F. (1990): Neogene evolution of the western Alpine foreland in the light of ECORS data and balanced cross sections. In: ROURE, F., HEITZMANN, P. & POLINO, R. (Ed.): Deep structure of the Alps, *1* (p. 165–184). – Mém. Soc. géol. suisse, Zürich.

HABICHT, K. (1945): Geologische Untersuchungen im südlichen sanktgallisch – appenzellischen Molassegebiet. – Matér. Carte géol. Suisse *83*, 166 p.

HEIM, A. (1921): Geologie der Schweiz. Band I Molasseland und Juragebirge. – Molasseland und Juragebirge *1*, 704, Tauchniz, Leipzig.

HEIMBURG, P. & NEUMAN, Q. (1954): Seismische Geschwindigkeitsmessung in der Tiefbohrung Altishofen, Laufzeit- und Geschwindigkeits-Tiefendiagramm. Ber. Nr. 053168, Hannover. Unpublished report.

HERB, R. (1988): Eocaecene Palägeographie und Paläotektonik des Helvetikums. – Eclogae geol. Helv.*81* / 3, 611–657.

HINZE, W., JÄGGI, K., SCHENKER, F. & GEMAG AG (1989): Sondierbohrungen Böttstein, Weiach, Riniken, Schafisheim, Kaisten, Leuggern – Gasmessungen. Nagra Tech. Ber., NTB 86-11, Baden.

HIRSCH, B. (1992): Eclépens-1, Synthetische Seismogramme. Nr. 92534558, Unpublished report.

HOFMANN, F. (1955): Beziehungen zwischen Tektonik, Sedimentation und Vulkanismus im Schweizerischen Molassebecken. – Bull. Assoc. suisse Géol. Ing. pétrole *22* / 62, 5–18.

– (1956): Die OSM in der Ostschweiz und im Hegau. – Bull. Assoc. suisse Géol. Ing. pétrole *23* / 64, 23–35.

– (1957): Pliozäne Schotter und Sande auf dem Tannenberg NW St. Gallen. – Eclogae geol. Helv. *50*, 477– 482.

HOMEWOOD, P. (1974): Le flysch du Meilleret (Préalpes Romandes) et ses relations avec les unités de l'encadrant. – Eclogae geol. Helv. *67*, 349– 401.

– (1986): Geodynamics and paleogeography of the western Molasse basin: a review. – Giornale di Geologia, ser. 3a *48* / 1, 275–284.

HOMEWOOD, P., ALLEN, P. A. & WILLIAMS, G. D. (1986): Dynamics of the Molasse Basin of western Switzerland. Giornale di Geologia, ser. 3a *48*, 199–217.

HOMEWOOD, P., RIGASSI, D. & WEIDMANN, M. (1989): Le bassin molassique Suisse. In: ASSOC. SÉDIM. FRANÇAISE (Ed.): Dynamique et méthodes d'étude des bassins sédimentaires, (p. 299–314). – Technip, Paris.

HOUSSE, B. A. (1982): Forage Hermrigen-1, Informations intéressant la Géothermie recueillies au cours du forage et des essais. Office de l'Economie Hydraulique et Energétique du Canton de Berne. Deposited at Neuchâtel University. Unpublished report.

IBELE, T. (2011): Tectonics of the western Swiss Molasse Basin during Cenozoic times. – Geosciences Departement. University of Fribourg, Fribourg. PhD Thesis.

ISLER, A., PASQUIER, F. & HUBER, M. (1984): Geologische Karte der zentralen Nordschweiz, 1:100 000. Geologische Spezialkarte Nr. 121. Nationalen Genossenschaft für die Lagerung Radioaktiver Abfälle (Nagra) und Schweizerischen Geologischen Kommission.

JENNY, J., BURRI, J.-P., MURALT, R., PUGIN, A., SCHEGG, R., UNGEMACH, P., VUATAZ, F.-D. & WERNLI, R. (1995): Le forage géothermique de Thônex (Canton de Genève): Aspects stratigraphiques, tectoniques, diagénétiques, géophysiques et hydrogéologiques. – Eclogae geol. Helv. *88* / 2, 365–396.

JORDAN, P. (1994): Evaporite als Abscherhorizonte. Eine gefügekundlich-strukturgeologische Untersuchung am Beispiel der Nordschweizer Trias. – Matér. Carte Géol. Suisse *164*, 79.

JORDI, H. A. (1990): Tektonisch-strukturelle Übersicht Westschweizerisches Molassebecken. – Bull. Assoc. suisse Géol. Ing. pétrole *56* / 130, 1–11.

– (1993): Tectonique du bassin molassique et de son substratum Jurassique-Crétacé dans la région Orbe – Yverdon – Grandson. – Bull. soc. vaudoise sci. nat. *82* / 3, 279–299.

KELLER, B. (1990): Wirkung von Wellen und Gezeiten bei der Ablagerung der Oberen Meeresmolasse. – Mitt. Naturf. Ges. Luzern *31*, 245–271.

KEMPF, O. (1998): Magnetostratigraphy and facies evolution of the Lower Freshwater Molasse (USM) of eastern Switzerland. – Geological Department, University of Bern. Bern. PhD Thesis.

KEMPF, O. & PFIFFNER, O. A. (2004): Early Tertiary evolution of the north Alpine Foreland Basin of the Swiss Alps and adjoining areas. – Basin Research *16*, 549–567.

KERN, G. (1982): Interprétation de la Campagne sismique 1981, Permis de Berne, Berne Sud et Fribourg Sud. Bau-, Verkehrs- und Energiedirektion, Amt für Wasser und Abfall, Bergregal-Geologisches Archiv, Erdöl für Kanton Bern.

LAHUSEN, P. H. (1992): Hydrocarbon exploration in the Swiss Molasse Basin. – Eclogae geol. Helv. *85* / 3, 707–714.

LAHUSEN, P. & WYSS, R. (1995): Erdöl- und Erdgasexploration in der Schweiz: Ein Rückblick. – Bull. Assoc. suisse Géol. Ing. pétrole *62* / 141, 43–72.

LAUBSCHER, H. (1961): Die Fernschubhypothese der Jurafaltung. – Eclogae geol. Helv. 54, 221–280.

– (1965): Ein kinematisches Modell der Jurafaltung. – Eclogae geol. Helv. *58* / 2, 232–318.

– (1986): The eastern Jura: Relations between thin-skinned and basement tectonics, local and regional. – Geol. Rundschau *75*/3, 535–553.

– (1992): Jura kinematics and the Molasse basin. – Eclogae geol. Helv. *85*/3, 653–676.

– (2008): The Grenchenberg conundrum in the Swiss Jura: a case for the centenary of the thin-skin décollement nappe model (Buxtorf 1907). – Swiss J. Geosciences *101*, 41–60.

Lemcke, K. (1959): Das Profil der Bohrung Chapelle-1. – Bull. Assoc. suisse Géol. Ing. pétrole *26*/70, 25–29.

– (1963): Die Ergebnisse der Bohrung Savigny-1 bei Lausanne. – Bull. Assoc. suisse Géol. Ing. pétrole *30*/78, 4–11.

– (1970): Schichtenverzeichnis der Aufschlussbohrung Boswil-1. München. Unpublished report.

Lemcke, K., Büchi, U. P. & Wiener, G. (1968): Einige Ergebnisse der Erdölexploration auf die mittelländische Molasse der Zentralschweiz. – Bull. Assoc. suisse Géol. Ing. pétrole *35*/87, 15–34.

Leu, W. (2008): Permokarbon-Kartenskizze (Rohstoffe) – Kompilation eines GIS-Datensatzes auf der Basis von bestehenden Unterlagen (Bereich Schweizer Mittelland). Nagra Arbeits Ber., NAB 08-49, Wettingen. Unpublished report.

Louis, L. (1960): Carottage de vitesses continu et carottage sismique. Courtion-1. British Petroleum Company, Limited. Unpublished report deposited at the University of Fribourg.

Loup, B. (1992): Mesozoic subsidence and streching models of the lithosphere in Switzerland (Jura, Swiss Plateau and Helvetic realm). – Eclogae geol. Helv. *85*/3, 541–572.

Lüschen, E., Lammerer, B., Gebrande, H., Millahn, K. & Nicolich, R. (2004): Orogenic structure of the Eastern Alps, Europe, from TRANSALP deep seismic reflection profiling. – Tectonophysics *388*, 85–102.

Lutze, A, Zettel, W. & Ruprecht, L. (1958): Seismische Geschwindigkeitsmessung in der Tiefbohrung Chapelle-1, Laufzeit- und Geschwindigkeits-Tiefendiagramm. Ber. Nr. 058158, Unpublished report.

Marchant, D., Ringgenberg, Y., Stampfli, G., Birkhäuser, P., Roth, P. & Meier, B. (2005): Paleotectonic evolution of the Zürcher Weinland (northern Switzerland), based on 2D and 3D seismic data. – Eclogae geol. Helv. *98*/3, 345–362.

Matter, A. (1987): Faciesanalyse und Ablagerungsmilieus des Permokarbons im Nordschweizer Trog. Eclogae geol. Helv. *80*/2, 345-367.

Matter, A., Peters, T., Isenschmid, C., Bläsi, H.-R. & Ziegler, H.-J. (1987): Sondierbohrung Riniken – Geologie. Nagra Tech. Ber., NTB 86-02, Baden.

Matter, A., Peters, T., Bläsi, H.-R., Meyer, J., Ischi, H. & Meyer, C. (1988a): Sondierbohrung Weiach – Geologie. Nagra Tech. Ber., NTB 90-04, Baden.

Matter, A., Peters, T., Bläsi, H.-R., Schenker, F. & Weiss, H.-P. (1988b): Sondierbohrung Schafisheim – Geologie. Nagra Tech. Ber., NTB 86-03, Baden.

Matter, A., Homewood, P., Caron, C., Rigassi, D., Van Stujivenberg, J., Weidmann, M. & Winkler, W. (1980): Flysch and Molasse of western and central Switzerland. In: Trümpy, R. (Ed.): Geology of Switzerland, a guide book, part II, (p. 261–293). – Wepf and Co., Bern.

Matzenauer, E. (2007): Spannunganalysen der Mittelland Molasse des Kantons Freiburg anhand von Deformationserscheinungen an Geröllen und Bruchbildung. – Department of Geosciences. Fribourg Univeristy. Fribourg, 102 p. Master Thesis.

Maurer, H. (1983a): Sedimentpetrographische Analysen an Molasseabfolgen der Westschweiz. – Jb. Geol. B. A. *126*/1, 23–69.

– (1983b): Sedimentpetrographische Ergebnisse der Bohrung Fendringen-1 (Kt. Fribourg). – Bull. Assoc. suisse Géol. Ing. pétrole *49*/117, 61–68.

Maurer, H. & Nabholz, W. (1980): Sedimentpetrographie in der Molasse-Abfolge der Bohrung Romanens-1 und in der benachbarten subalpinen Molasse (Kt. Fribourg). – Eclogae geol. Helv. *73*/1, 205–222.

Meia, J. (1969): Géologie du Mont Aubert et de l'anticlinal Soliat–Montagne de Boudry au Nord du lac de Neuchâtel (Jura vaudois sud-oriental et Jura neuchâtelois méridional, Suisse). – Institut de Géologie, University of Neuchâtel. Neuchâtel. PhD Thesis.

Meier, B. (1994a): Untere Süsswassermolasse des westlichen Mittellandes: Regionale Interpretation bestehender Seismik und petrophysikalische Analyse von Fremdbohrungen. Nagra unpublished internal report.

Meier, B. (1994b): Untere Süsswassermolasse des zentralen und östlichen Mittellandes: Regionale Interpretation bestehender Seismik und petrophysikalische Analyse von Fremd- und Eigenbohrungen. Nagra unpublished internal report.

– (2010): Ergänzende Interpretation reflectionsseismischer Linie zwischen dem östlichen und westlichen Molassebecken. Nagra unpublished internal report.

Micholet, J. (1992): Le puits de Thoune – Forage d'exploration pétrolière en Suisse, Consortium Pétrolier Fribourgeois et Bernois. – Bull. Assoc. suisse Géol. Ing. pétrole *58*/133, 23–32.

Mitchum, R. M. & Vail, P. R. (1977): Seismic stratigraphic interpretation procedure. In: Payton, C. E. (Ed.): Seismic stratigraphy – applications to hydrocarbon exploration, Am. Ass. Petroleum Geologists Memoir *26*,135–144.

Mitchum, R. M., Vail, P. R. & Thompson, S. (1977): Seismic stratigraphy and global changes of sea level, Part 2: the depositional sequence as a basic unit for stratigraphic analysis. In: Payton, C. E. (Ed.): Seismic stratigraphy – application to hydrocarbon exploration, Am. Ass. Petroleum Geologists Memoir *26*, 53–62.

Mosar, J., Ibele, T. & Matzenauer, E. (2008): Tectonics of the Molasse Basin of Western Switzerland: An Overview. Nagra Arbeitsber. NAB 08-07, Wettingen. Unpublished report.

Mosar, J., Abednego, M., Ibele, T., Matzenauer, E., Meier, B., Sommaruga, A., Sprecher, C. & Vouillamoz, N. (2011): Du Jura central aux Préalpes romandes – Une tectonique active dans l'avant-pays des Alpes. – Géochronique *117*, 52–55.

Müller, M., Nieberding, F. & Wanninger, A. (1988): Tectonic style and pressure distribution at the northern margin of the Alps between Lake Constance and the River Inn. – Geol. Rundschau *77*/3, 787–796.

Müller, W. H., Naef, H. & Graf, H. R. (2002): Geologische Entwicklung der Nordschweiz, Neotektonik und Langzeitszenarien Zürcher Weinland. Nagra Tech. Ber. NTB 99-08, Wettingen.

Mugnier, J. L. & Ménard, G. (1986): Le développement du bassin molassique suisse et l'évolution des Alpes externes: un modèle cinématique. – Bull. Centres Recherche et Exploration-Production d'Elf-Aquitaine *10*/1, 167–180.

Muralt, R., Vuataz, F. D., Schönborn, G., Sommaruga, A. & Jenny, J. (1997): Intégration des méthodes hydrochimiques, géologiques et géophysiques pour la prospection d'une nouvelle ressource en eau thermale. Cas d'Yverdon les Bains, pied du Jura. – Eclogae geol. Helv. *90*, 179–197.

Naef, H. (1999): Erläuterungen zur geologischen Übersichtskarte des Kantons Thurgau. In: Schläfli, H. (Ed.): Mitt. Naturforsch Ges. Thurgau, *55*.

Naef, H. & Diebold, P. (1990): Interprétation géologique de la sismique réflexion. – Cédra informe *2*, 16–28.

Naef, H. & Birkhäuser, P. (1996): Refelxionsseismik zur Erkundung des Opalinustons in der Nordschweiz. – Bull. angew. Geol. *1*/2, 11–134.

Naef, H., Birkhäuser, P. & Roth, P. (1995): Interpretation der Reflexionsseismik im Gebiet nördlich Lägeren – Zürcher Weinland. Nagra Tech. Ber., NTB 94-14, Baden.

Nagra (1989): Sondierbohrung Weiach – Untersuchungsbericht. Nagra Tech. Ber., NTB 88-08, Baden.

– (1992): Sondierbohrung Siblingen – Untersuchungsbericht. Nagra Tech. Ber., NTB 90-34, Baden.

– (2001): Sondierbohrung Benken: Untersuchungsbericht. Nagra Tech. Ber., NTB 00-01, Wettingen.

– (2008): Vorschlag geologischer Standortgebiete für das SMA- und das HAA-Lager «Geologische Grundlagen». Nagra Tech. Ber., NTB 08-04, Wettingen.

NICKEL, H., STEINMANN, W. & WIERCZEYKO, E. (1964): Bericht über die seismische Geschwindigkeitsmessung in der Tiefbohrung Pfaffnau-Süd-1 (Schweiz), Rap. Ges. Brigitta Elverath. Ber. Nr. 064223, Hannover. Unpublished report.

OCEN (1994): Forage géothermique de Thônex. Rapport final. Volume *1*, Unpublished report.

ODELLO, C. (2004): Etude sismique du bassin molassique du Plateau suisse. Dorigny. Institut de Géophysique, Université de Lausanne. Unpublished report deposited at the Institute of geophysics.

OTTO, S. (1994): Bresse–Valence Basin & Jura foldbelt. Petroconsultants, Geneva. Petroconsultants.

PAOLACCI, S. & GORIN, G. (2001): Structural configuration of the westernmost part of the Swiss Molasse basin, as derived from petroleum reflection seismic. Tectonic Studies Group meeting, Neuchâtel. 18th volume, 42–43.

PASQUIER, J. B. (2004): Feuille 1225 Gruyères. – Atlas géol. Suisse 1: 25 000, Notice expl. 115.

PAVONI, N. (1961): Faltung durch Horizontalverschiebung. – Eclogae geol. Helv. *54*/2, 515–534.

PERRY, J. T. O. B. (1961): Well summary report of Sorens-1, Switzerland. British Petrleum. Fribourg. Unpublished report deposited at Fribourg Universiy.

PERSOZ, F. (1982): Inventaire minéralogique, diagenèse des argiles et minéralostratigraphie des séries jurassiques et crétacées inférieures du Plateau suisse et de la bordure Sud-Est du Jura entre les lacs d'Annecy et de Constance. – Matér. Carte géol. Suisse *155*.

PETERS, T., MATTER, A., BLÄSI, H. R., ISENSCHMID, C., KLEBOTH, P., MEYER, C. & MEYER, J. (1989): Sondierbohrung Leuggern: Geologie. Nagra Technischer Berich, NTB 86-05, Baden.

PFIFFNER, O. A. (1986): Evolution of the north Alpine foreland basin in the Central Alps. – Spec. Publ. int. Ass. sedimentologists *8*, 219–228.
— (2006): Thick-skinned and thin-skinned styles of continental contraction. – GSA Special papers *414*, 153–177.
— (2009): Geologie der Alpen. – (359 p.). – Haupt Verlag, Bern.

PFIFFNER, O. A., ERARD, P. F. & STÄUBLE, M. (1997): Two cross-sections through the Swiss Molasse Basin (line E4-E6, W1, W7/W10). In: PFIFFNER, A. O., LEHNER, P., HEITZMANN, P., MÜLLER, S. & STECK, A. (Ed.): Deep structure of the Swiss Alps, results from NFP / PNR 20. – Birkhäuser, Basel.

RAHN, M. K. & SELBEKK, R. (2007): Absolute dating of the youngest sediments of the Swiss Molasse basin by apatite fission track analysis. – Swiss J. Geosciences *100*, 137–381.

REMANE, J., ADATTE, T., BERGER, J. P., BURKHALTER, R., DALL'AGNOLO, S., DECROUEZ, D., FISCHER, H., FUNK, H.-P., FURRER, H., GRAF, H. R., GOUFFON, Y., HECKENDORN, W., & WINKLER, W. (2005): Guidelines for stratigraphic nomenclature. – Eclogae geol. Helv. *98*/3, 385–405.

RESUN (2008): Ersatz Kernkraftwerk Mühleberg. Sicherheitsbericht, Resun. Unpublished report.

RIGASSI, D. A. (1977): Genèse tectonique du Jura: une nouvelle hypothèse. – Paleolab News *2*, 1–27.

ROTH, P., NAEF, H. & SCHNELLMANN, M. (2008): Kompilation und Interpretation der Reflexionsseismik im Tafeljura und Molassebecken der Zentral- und Nordostschweiz. Nagra Intern. Ber., Wettingen. Unpublished report.

S.N.P.A (1973): Rapport forage Linden-1 (Suisse): Diagraphies de vitesses, films synthétiques, corrélations, Profils sismiques BS 10 et BS 14. Pl. 8. Unpublished report.

SCHEGG, R., LEU, W., CORNFORD, C. & ALLEN, P. A. (1997): New coalification profiles in the Molasse Basin of Western Switzerland: Implications for the thermal and geodynamic evolution of the Alpine Foreland. – Eclogae geol. Helv. *90*/1, 79–96.

SCHLANKE, S., HAUBER, L. & BÜCHI, U. (1978): Lithostratigraphie und Sedimentpetrographie der Molasse in den Bohrungen Tschugg-1 und Ruppoldsried-1 (Berner Seeland). – Eclogae geol. Helv. *71*/2, 409–425.

SCHLUNEGGER, F. & MOSAR, J. (2010): The last erosional stage of the Molasse Basin and the Alps – Int. J. Earth Sci. DOI 10.1007/s00531-010-0607-1.

SCHLUNEGGER, F., MATTER, A. & MANGE, M. A. (1993): Alluvial fan sedimentation and structure of the southern Molasse Basin margin, Lake Thun area, Switzerland. – Eclogae geol. Helv. *86*/3, 717–750.

SCHLUNEGGER, F., RAMSEYER, K. & RIEKE-ZAPP, D. (2007): Possible environmental effects on the evolution of the Alps-Molasse Basin system. – Swiss J. Geosciences *100*, 383–406.

SCHMID, S. M. & SLEJKO, D. (2009): Seismic source characterization of the Alpine foreland in the context of a probabilistic seismic hazard analysis by PEGASOS Expert Group 1 (EG1a). – Swiss J. Geosciences *102*/1, 121–148.

SCHNEGG, P.-A. (1992): Testing a new multichannel controlled-source audio magnetotelluric method (CSAMT) on a borehole. – Eclogae geol. Helv. *85*/2, 459–470.

SCHUERMANN, W. (1980): Seismische Geschwindigkeitsmessung in der Tiefbohrung Entlebuch-1, Laufzeit- und Geschwindigkeits-Tiefendiagramm. Bericht Nr. 803630, Hannover. Unpublished report.

SCHUERMANN, W, & WIERCZEYCKO, E. (1977): Bericht über die seismische Geschwindigkeitsmessung in der Tiefbohrung Ruppoldsried-1 (Schweiz). Bericht Nr. 773619, Prakla GmbH Hannover. Unpublished report.

SHELL (1974): Répartition des vitesses, Courtion-1, corrélation secondes / mètres (Encl. 25). Rapport d'interprétation, Campagne vibrosismique 1972, 1973, 1974 par J.-P. Loriol. Unpublished report.
— (1978): Well report of Treycovagnes-1. Shell-Switzerland. Unpublished report.

SIGNER, C. (1992): Interprétation sismique structurale et sismostratigraphique entre Jura et front alpin dans la région genevoise. – Genève. Diplôme.

SIGNER, C. & GORIN, G. E. (1995): New geological observations between the Jura and the Alps in the Geneva area, as derived from reflection seismic data. – Eclogae geol. Helv. *88*/2, 235–265.

SINCLAIR, H. D., COAKLEY, B. J., ALLAN, P. A. & WATTS, A. B. (1991): Simulation of foreland basin stratigraphy using a diffusion model of mountain belt uplift and erosion: an example from the Central Alps, Switzerland. – Tectonics *10*/3, 599–620.

SOMMARUGA, A. (1997): Geology of the Central Jura and the Molasse Basin: new insight into an evaporite-based foreland fold and thrust belt. – Mém. soc. neuchâteloise sci. nat. *12*, 176.
— (1999): Décollement tectonics in the Jura foreland fold-and-thrust belt. – Marine and Petroleum Geology *16*, 111–134.

SOMMARUGA, A., EICHENBERGER, U. & MARILLIER, F. (2011): Vision 3D du Bassin molassique en Suisse à partir de la sismique réflexion. – Géochronique *117*, 44–47, 73.

SPORLEDER, G. (1965): Seismische Geschwindigkeitsmessung in der Tiefbohrung Hünenberg-1, Laufzeit- und Geschwindigkeits-Tiefendiagramm. Prakla G.m.b.H, Ber. Nr. 065163, Hannover.

SPORLEDER, G. & FROMMHOLZ, R. (1960): Bericht über die seismische Geschwindigkeitsmessung in der Tiefbohrung Savigny-1 (Schweiz). Rap. Ges. Brigitta Elverath. Ber. Nr. 064223, Hannover. Unpublished report.

SPRECHER, C. & MÜLLER, W. (1986): Geophysikalisches Untersuchungsprogramm Nordschweiz: reflectionsseismische Messungen 82. Nagra Techn. Ber., NTB 84-15, Baden.

STAMPFLI, G. M., MOSAR, J., MARCHANT, R., MARQUER, D., BAUDIN, T. & BOREL, G. (1998): Subduction and obduction processes in the Swiss Alps. – Tectonophysics *296*, 159–204.

STÄUBLE, M. & PFIFFNER, O. A. (1991): Processing, interpretation and modeling of seismic reflection data in the Molasse basin of Eastern Switzerland. – Eclogae geol. Helv. *84*/1, 151–175.

STEINMANN, W. (1964): Bericht über die seismische Geschwindigkeitsmessung in der Tiefbohrung Lindau-1. Ber. Nr. 064083, Hannover. Unpublished report.
— (1965): Seismische Geschwindigkeitsmessung in der Tiefbohrung Boswil-1, Laufzeit- und Geschwindigkeits-Tiefendiagramm. Ber. Nr. 065214, Hannover. Unpublished report.

STEINMANN, W. & WIERCZEYKO, E. (1964): Bericht über die seismische Geschwindigkeitsmessung in der Tiefbohrung Pfaffnau-1 (Schweiz), Rap. Ges. Brigitta Elverath. Ber. Nr. 063188, Prakla G.m.b.H, Hannover. Unpublished report.

STRUNCK, P. (2001): The Molasse of Western Switzerland. – Geologisches Institut. Universität Bern. Bern, PhD Thesis.

STRUNCK, P. & MATTER, A. (2002): Depositional evolution of the western Swiss Molasse. – Eclogae geol. Helv. *95*, 197–222.

SWISSPETROL (1992): Seismic Lageplan Schweiz. – Bull. Assoc. suisse Géol. Ing. pétrole *59*/ 134, Plate.

SWISSTOPO (2005a): Geologische Karte der Schweiz. Karte 1: 500 000. – Bundesamt für Landestopografie swisstopo, Wabern.

— (2005b): Tektonische Karte der Schweiz. Karte 1: 500 000. – Bundesamt für Landestopografie swisstopo, Wabern.

THOMAS, O. J. (1961): Report on a well velocity survey of Sorens-1 in the Canton of Fribourg, Switzerland. British Petroleum, No. OC2357, Unpublished report.

THURY, M. & DIEBOLD, P. (1987): Survey of the geological research-program carried out by Nagra (National Cooperative for the storage of Radioactive Waste) in Northern Switzerland. – Eclogae geol. Helv. *80*/ 2, 271–286.

TOWNSEND, P. J. (1983): Geological Completion Report Fendringen-1, Switzerland Report Nr. DOS 20981, Unpublished report.

TRÜMPY, R. (1980): Geology of Switzerland: a guide-book. – Wepf and Co., Bern.

TURRINI, C., DUPS, K. & PULLAN, C. (2009): 2D and 3D structural modelling in the Swiss-French Jura Mountains. – first break *27*, 65–71.

USTASZEWSKI, K. & SCHMID, S. H. (2007): Latest Pliocene to recent thick-skinned tectonics at the Upper Rhine Graben – Jura Mountains junction. – Eclogae geol. Helv. *100*, 293–312.

USTASZEWSKI, K. M. (2004): Reactivation of pre-existing crustal continuities: the southern Upper Rhine Graben and the northern Jura Mountains – a natural laboratory. – Geologisch-Paläontolosches Institut. University of Basel. Basel, 145 p. PhD.

VANN, I. R., GRAHAM, R. H. & HAYWARD, A. B. (1986): The structure of mountain fronts. – J. Structural Geology *8*, 215–227.

VOLLMAYR, T. (1983): Temperaturmessungen in Erdölbohrungen der Schweiz. – Bull. Assoc. suisse Géol. Ing. pétrole *49*/ 116, 15–27.

— (1992): Strukturelle Ergebnisse der Kohlenwasserstoffexploration im Gebiet von Thun, Schweiz. – Eclogae geol. Helv. *85*/ 3, 531–539.

VOLLMAYR, T. & WENDT, A. (1987): Die Erdgasbohrung Entlebuch-1, ein Tiefenaufschluss am Alpennordrand. – Bull. Assoc. suisse Géol. Ing. pétrole *53*/ 125, 67–79.

WAGNER, J.-J., GONG, G., SARTORI, M. & JORDI, S. (1999): A catalogue of physical properties of rocks from the Swiss Alps and nearby areas. – Matér. Géol. Suisse, Sér. Géophys. *33*, 1–80.

WEBER, H. P., SATTEL, G. & SPRECHER, C. (1986): Sondierbohrungen Weiach, Riniken, Schafisheim, Kaisten, Leuggern – Geophysikalische Daten, Texband. Baden. Nagra Techn. Ber., NTB 85-50, Baden.

WEGMANN, E. (1963): Le Jura plissé dans la perspective des études sur le comportement des socles. In: FRANCE, S. G. (Ed.): Livre Mém. Prof. P. Fallot, Mém. hors-série *1* (p. 99–104). – Paris.

WEIDMANN, M. (1988): Feuille 1243 Lausanne. – Atlas géol. Suisse 1: 25 000, Notice expl. *85*.

WIERCZEYKO, E. (1962): Bericht über die seismische Geschwindigkeitsmessung in der Tiefbohrung Kreuzlingen 1. Rap. Ges. Brigitta Elverath. Ber. Nr. 062149, Hannover.

WILDI, W., BLONDEL, T., CHAROLLAIS, J., JAQUET, J. & WERNLI, R. (1991): Tectonique en rampe latérale à la terminaison occidentale de la Haute Chaîne du Jura. – Eclogae geol. Helv. *84*/ 1, 265–277.

WILLETT, S. D. & SCHLUNEGGER, F. (2010): The last phase of deposition in the Swiss Molasse Basin: from foredeep to negative-alpha basin. – Basin Research *22*/ 5, 623–639.

ZIEGLER, P. A. (1982): Geological Atlas of Western and Central Europe (130 p.). – Shell Internationale Petroleum Maatschappij B.V., The Hague.

— (1992): Swiss Molasse Basin-Geodynamics, resources, hazards – an introduction. – Eclogae geol. Helv. *85*/ 3, 511–517.

ZIEGLER, P. A. & DÈZES, P. (2007): Cenozoic uplift of Variscan Massifs in the Alpine foreland: Timing and controlling mechanisms. – Global and Planetary Change *58*, 237–269.

ZIEGLER, P. A. & FRAEFEL, M. (2009): Response of drainage systems to Neogene evolution of the Jura fold-thrust beld and Upper Rhein Graben. – Swiss J. Geosciences *102*, 57–75.

ZORASTER, S. (2003): A Surface Modeling Algorithm Designed for Speed and Ease of Use With All Petroleum Industry Data. – Computers & Geosciences *29*/ 9, 1175–1182.